

Electronic Thesis and Dissertation Repository

8-29-2016 12:00 AM

Estimation of Wind Hazard over Canada and Reliability-based Assignment of Design Wind Load

Qian Tang, *The University of Western Ontario*

Supervisor: Hanping Hong, *The University of Western Ontario*

A thesis submitted in partial fulfillment of the requirements for the Master of Engineering Science degree in Civil and Environmental Engineering

© Qian Tang 2016

Follow this and additional works at: <https://ir.lib.uwo.ca/etd>



Part of the [Civil and Environmental Engineering Commons](#)

Recommended Citation

Tang, Qian, "Estimation of Wind Hazard over Canada and Reliability-based Assignment of Design Wind Load" (2016). *Electronic Thesis and Dissertation Repository*. 4092.

<https://ir.lib.uwo.ca/etd/4092>

This Dissertation/Thesis is brought to you for free and open access by Scholarship@Western. It has been accepted for inclusion in Electronic Thesis and Dissertation Repository by an authorized administrator of Scholarship@Western. For more information, please contact wlsadmin@uwo.ca.

Abstract

The current National Building Code of Canada (NBCC) recommends a wind load factor of 1.4 and the nominal wind velocity pressure corresponding to a 50-year return period value of the annual maximum hourly-mean wind speed, V_{AH} . This study is focused on mapping wind hazard for Canada and on calibrating the required design wind load to improve reliability consistency of designed structures.

Extreme value analysis of V_{AH} was carried out by considering surface wind observations from approximately 1300 stations. The results indicate that the spatial trends of the estimated mean of V_{AH} are similar whether the data from stations with at least 20 or 10 years' useable wind observations are considered, but the small sample size affects the spatial variations of the coefficient of variation (cov) of V_{AH} . The estimated 50-year return period values of V_{AH} based on the at-site analysis differ from those inferred from two previous versions of the NBCC, and the differences persist if the estimates were obtained by using the region of influence approach. Potential reasons for the discrepancy were elaborated.

It was shown that an improved reliability consistency can be achieved if a wind load factor of 1.0 is employed and the nominal wind velocity pressure is assigned using the 500-year return period value of V_{AH} . It is also shown that a further improvement of the reliability consistency can be achieved if a variable return period as a function of cov of V_{AH} is used to assign the nominal wind velocity pressure.

Keywords: Annual maximum wind speed, Code calibration, Design code, Design wind velocity pressure, Extreme value analysis, Reliability analysis, Target reliability index, Wind hazard mapping

Acknowledgements

First and foremost, I would like to express my sincere gratitude to my supervisor, Dr. Hanping Hong for his advice on my thesis work. This thesis could not be completed without his guidance. His attitude towards research is contagious and inspiring.

I want to thank my colleagues, Shucheng Yang, Qian Huang, Jiyang Gu and Chao Feng for providing suggestion and comments on my thesis and my graduate studies. Special thanks to Drs. Sihan Li and Wei Ye for teaching and helping me with data process and data mapping tasks. Collaboration from Mr. P. Hong for Chapter 3 is appreciated and acknowledged.

Many thanks go to Dr. Newson, Dr. Wang, and Dr. Zhou for reading my thesis and providing constructive comments and suggestions.

Lastly, I am deeply and forever indebted to my parents for their love, support and encouragement.

Table of Contents

Abstract	i
Acknowledgements	ii
List of Tables	v
List of Figures	vi
List of Symbols and Abbreviations.....	x
Chapter 1 Introduction	1
1.1 Introduction and background	1
1.2 Research objectives and thesis outline.....	5
Reference	6
Chapter 2 At-site Analysis and Regional of Influence	8
2.1 Introduction.....	8
2.2 Surface wind observations	12
2.3 Extreme value analysis approach: at-site and regional approaches	15
2.4 Wind hazard estimation and mapping.....	21
2.4.1 Wind hazard mapping based on extreme wind speed inferred from the NBCC.....	21
2.4.2 Comparison of the spatial varying wind hazard using data with $n_A \geq 20$ and ≥ 10 ...	22
2.4.3 Estimated wind hazard using the ROI approach.....	28
2.5 Effect of additional considerations on spatially interpolated wind hazard maps.....	32
2.6 Summary and conclusions	37
References.....	39

Chapter 3 Codification of Wind Load for Improved Reliability Consistency over Canadian Sites	42
.....	42
3.1 Introduction.....	42
3.2 Probabilistic models adopted for the calibration	44
3.3 Calibrating design wind load for spatially varying extreme wind characteristics	48
3.3.1 Limit state function and analysis procedure	48
3.3.2 Calibration results and wind speed contour map for reliability consistent design	49
3.4 Conclusions.....	53
References.....	54
Chapter 4 Conclusions and Recommendations for future work.....	56
4.1 Summary and conclusions	56
4.2 Recommendations for future work	58
Appendix A. Spatially Interpolated Statistics of Annual Maximum Wind Based on Ordinary Kriging with Nugget Equal to Zero	59
Appendix B. Interpolated 50-year Return Period Values for Specified Locations in NBCC Based on At-site Analysis and ROI.....	64
Curriculum Vitae	82

List of Tables

Chapter 2

Table 2-1. Methods for estimating the model parameters and quantiles based on the Gumbel model (for n samples, with sample mean m and sample standard deviation s).....	17
Table 2-2. Methods for estimating the model parameters and quantiles based on the generalized extreme value distribution.....	18
Table 2-3. Equations used to calculate L-moment ratios \bar{t}^i and \bar{t}_3^i for R_i . (Burn 1990).	20

Appendix B

Table B1. Comparison of NBCC-2005, NBCC-2010 and interpolated 50-year return period values (km/h) based on at-site analysis and ROI.....	64
---	----

List of Figures

Chapter 2

Figure 2-1. Locations of the meteorological stations where wind speed records are available in EC HLY01 digital archive, and empirical cumulative distribution of the length of wind measurement period at each station: a) Spatial distribution of the stations, b) Empirical cumulative distribution of length of wind measurement period. 13

Figure 2-2. Locations of 583 stations with useable data used in this study. 15

Figure 2-3. Wind hazard maps inferred from the reference velocity wind pressures given in the NBCC-2005 and NBCC-2010. 22

Figure 2-4. Mean and coefficient of variation of V_{AH} for the case with $n_A \geq 20$ 23

Figure 2-5. Mean and coefficient of variation of V_{AH} for the case with $n_A \geq 10$ 23

Figure 2-6. Empirical distribution of $\xi_{V_{AH}}$ 25

Figure 2-7. Comparison of the estimated v_{AH-50} by different fitting methods and considering V_{AH} is Gumbel distributed: a) using the MOM vs using the GLM; b) using the MML vs using the GLM; c) using the MLM vs using the GLM. 25

Figure 2-8. Estimated v_{AH-50} using the GLM for the selected meteorological stations shown in Figure 2-2: a) Contour map of v_{AH-50} for the case with $n_A \geq 20$, b) Contour map of v_{AH-50} for the case with $n_A \geq 10$ 26

Figure 2-9. Empirical distribution of $R_{C05/E10}$ and $R_{C10/E10}$ 27

Figure 2-10. Comparison of the estimated v_{AH-50} by different distribution types: a) using MOM, b) using the MML, and c) using MLM. 28

Figure 2-11. Wind hazard maps developed based on the ROI approach: a) Gumbel distribution and $n_A \geq 20$, b) Gumbel distribution and $n_A \geq 10$, c) GEVD and $n_A \geq 20$, d) GEVD and $n_A \geq 10$ 30

Figure 2-12. Wind hazard maps developed based on the ROI approach and considering the Gumbel model: a) v_{AH-100} for $n_A \geq 20$, b) v_{AH-100} for $n_A \geq 10$, c) v_{AH-500} for $n_A \geq 20$, and d) v_{AH-500} for $n_A \geq 10$ 31

Figure 2-13. Trends of the 50-year return period values based on the adopted criteria and applying the ordinary kriging technique without/with nugget equal to zero for the case with $n_A \geq 20$ 34

Figure 2-14. Trends of the 50-year return period values based on the adopted criteria and applying the ordinary kriging technique without/with nugget equal to zero for the case with $n_A \geq 10$ 35

Figure 2-15. Statistics of the estimated ratio the 50-year wind speed by considering the values inferred from the codes and the estimated values shown in Figure 2-13c and 2-14c: a) For the case with $n_A \geq 20$, b) For the case with $n_A \geq 10$, c) For the case with $n_A \geq 20$ & satisfy Criterion 1, and d) For the case with $n_A \geq 10$ & satisfy Criterion 1..... 37

Chapter 3

Figure 3-1. Coefficient of variation of the annual maximum hourly-mean wind speed: a) for the case with $n_A \geq 20$ and b) for the case with $n_A \geq 10$ 46

Figure 3-2. Voronoi polygon associated with each station for the estimation of area-weighted mean of COV of V_{AH} : a) for the case with $n_A \geq 20$ and b) for the case with $n_A \geq 10$ 46

Figure 3-3. Mean and coefficient of variation of the annual maximum hourly-mean wind speed: a) Mean of V_{AH} (km/hr), and b) cov of V_{AH} (inferred from the analysis results obtained from the ROI approach, see Chapter 2). 47

Figure 3-4. Estimated β_{50} and P_f for $\alpha_W = 1.40$ and using $T = 50$ years to assigning the reference wind velocity pressure: a) Estimated β_{50} and b) Estimated P_f 50

Figure 3-5. Estimated β_{50} and P_f for $\alpha_W = 1.0$ and using $T = 500$ years to assigning the reference wind velocity pressure: a) Estimated β_{50} and b) Estimated P_f 50

Figure 3-6. Estimated β_{50} and P_f for $\alpha_W = 1.0$ and using the return period given in Eq. (3.5) to assign v_T : a) Estimated β_{50} and b) Estimated P_f 51

Figure 3-7. Suggested design wind speed considering the return period shown in Eq. (3.5). 52

Figure 3-8. Ratio of factored design wind load to the suggested factored design wind load 53

Appendix A

Figure A1. Wind hazard maps inferred from the reference velocity wind pressures given in the NBCC-2005 and NBCC-2010. 59

Figure A2. Mean and coefficient of variation of V_{AH} for the case with $n_A \geq 20$ 60

Figure A3. Mean and coefficient of variation of V_{AH} for the case with $n_A \geq 10$ 60

Figure A4. Estimated v_{AH-50} using the GLM for the selected meteorological stations shown in Figure 2-2: a) Contour map of v_{AH-50} for the case with $n_A \geq 20$, b) Contour map of v_{AH-50} for the case with $n_A \geq 10$ 61

Figure A5. Wind hazard maps developed based on the ROI approach: a) Gumbel distribution and $n_A \geq 20$, b) Gumbel distribution and $n_A \geq 10$, c) GEVD and $n_A \geq 20$, d) GEVD and $n_A \geq 10$ 62

Figure A6. Wind hazard maps developed based on the ROI approach and considering the

Gumbel model: a) v_{AH-100} for $n_A \geq 20$, b) v_{AH-100} for $n_A \geq 10$, c) v_{AH-500} for $n_A \geq 20$, and d) v_{AH-500} for $n_A \geq 10$ 63

List of Symbols and Abbreviations

v_{AH-50} :	50-year return period value of annual maximum (hourly-mean) wind speed
n_A :	the number of years of useable wind measurements at a station
V_{AH} :	the annual maximum moving average (AMMA) of the hourly-mean wind speed
v_X :	coefficient of variation of X
D_{ij} :	a distance to measure the closeness of the i -th and j -th stations in ROI
ξ_{VAH} :	coefficient of variation of V_{AH}
$R_{C05/E10}$:	the ratio of v_{AH-50} inferred from the NBCC-2005 to the estimated v_{AH-50} for the case with $n_A \geq 10$
$R_{C10/E10}$:	the ratio of v_{AH-50} inferred from the NBCC-2010 to the estimated v_{AH-50} for the case with $n_A \geq 10$
v_{LB} :	a lower bound of 77.55 km/h which is used in the NBCC-2010
β_{50} :	reliability index for a service period of 50 years.
P_f :	the probability of failure
v_v :	coefficient of variation of V_{AH}
v_T :	the T -year return period value of V_{AH}
W :	the ratio of the wind load effect to the nominal wind load effect
W_n :	the reference (or nominal) wind load effect on the structural member calculated according to the design code
α_W :	the wind load factor
α_D :	the dead load factor
γ_R :	the resistance factor

$R_{W/D}$:	the ratio of the factored design wind load $\alpha_W W_n$ to the factored design dead load $\alpha_D D_n$
R_n :	the nominal resistance
D_n :	the nominal dead load
NBCC:	National Building Code of Canada
AIC:	Akaike Information Criterion
ROI:	the region of influence
COV:	coefficient of variation
RMSE:	the root-mean-square-error
GEVD:	the generalized extreme value distribution
GPD:	the generalized Pareto distribution
MOM:	the method of moments
MML:	the method of the maximum likelihood
MLM:	the method of L-moments
GLM:	the generalized least-squares method

Chapter 1 Introduction

1.1 Introduction and background

The results of wind hazard assessment are used as the basis to assign wind load for design new structures and assessing existing structures and infrastructure systems. Return period values of the annual maximum hourly-mean wind speed, V_{AH} , are employed to assign reference wind velocity pressure in the National Building Code of Canada (NBCC). The T -year return period value of V_{AH} is defined as the value of V_{AH} such that its corresponding probability of exceedance equals $1/T$. The wind velocity pressure is used to evaluate the design wind load according to

$$p = I_w q C_e C_g C_p \quad (1.1)$$

here p is the specified external pressure caused by wind acted in a direction normal to the surface of the structure (as a pressure directed towards or as a suction directed away from the surface), I_w is the importance factor for wind load, q is the reference velocity pressure, C_e is the exposure factor, C_g is the gust effect factor and C_p is the external pressure coefficient averaged over the area of the surface considered.

The current NBCC recommends a wind load factor of 1.4 and the nominal wind velocity pressure corresponding to 50-year return period value of V_{AH} .

Some relevant information on the evaluation of the return period value of the annual maximum wind speed can be found in Yip and Auld (1993), Yip et al. (1995), Morris (2009), and Hong et al. (2014). Yip and Auld (1993) and Yip et al. (1995) described the update to the reference wind pressures implemented in the NBCC-1995 (NRCC 1995). The Gumbel distribution was used to fit the annual maximum wind speed by using the method of moments (MOM). More specifically,

they used wind records from 233 stations each with at least 10 years of data to estimate the 30-year return period value of the annual maximum wind speed by adopting the Gumbel model fitted using the MOM. A wind hazard map was plotted based on the 30-year return period value of the annual maximum wind speed estimated using the at-site statistics of the wind. The wind speeds at locations tabulated in the NBCC were extracted from the map. To estimate extreme wind speed for return period T other than 30 years, they introduced a ratio of the standard deviation to the 30-year return period value of the annual maximum wind speed, and assumed that the ratio can be approximated by a constant for all stations considered. The error caused by using 30-year return period values of the annual maximum wind speed and this constant ratio to estimate the return period value other than 30 years (e.g., 10 and 100 years) depends on T and the actual statistics of the annual maximum wind speed at a considered site (Hong et al. 2014).

Companion-action load combinations were adopted in the NBCC-2005 and the 50-year return period value of the wind velocity pressure coupled with a wind load factor of 1.4 was recommended in the NBCC-2005 (Bartlett et al. 2003a, b). The 50-year return period values of the wind velocity pressure were calculated based on their corresponding 30-year values recommended in the NBCC-1995 and by considering that the annual maximum wind speed is a Gumbel variate. The reference wind velocity pressures were updated for the NBCC-2010 by fitting the Gumbel distribution to the annual extreme wind speed using the MOM. For the updating, it was assumed that a constant cov of the annual maximum wind speed equal to 0.124 could be adequate for all the meteorological stations considered (Morris 2009). A comparison of the 50-year return period value of annual maximum (hourly-mean) wind speed, v_{AH-50} , inferred from the NBCC-2010 and NBCC-2005 (Hong et al. 2014) indicated that there are significant changes in v_{AH-50} for some locations common in these two editions of the code. The largest

decrease in the NBCC-2010 as compared to the NBCC-2005 is about 30%; the largest increase is less than 10%; the majority of changes are within 10%; two relatively high wind regions in the Northwest Territories and Nunavut in the NBCC-2005 are eliminated in the NBCC-2010; a series of continuous “consistent” wind speed regions from east to west of the country shown in the wind map inferred from the NBCC-2010 was not present in the map inferred from the NBCC-2005. It was considered that these differences are partly due to the use of a constant cov to develop v_{AH-50} for the NBCC-2010.

A wind hazard mapping for Canada was carried out based on the annual maximum wind speed from more than 230 stations, where at least 20 years of useable data are available from each station (Hong et al. 2014). They also applied the Akaike Information Criterion (AIC) (Akaike 1974) and concluded that the Gumbel distribution is preferable than the generalized extreme value distribution (GEVD) for more than 70% of cases. The consideration of at least 20 years of useable data was aimed at reducing the statistical uncertainty in the estimated wind hazard due to small sample size, although it is inconsistent with the attitude taken in develop wind hazard for previous versions of the code. The wind hazard maps in Hong et al. (2014) were developed based on the at-site analysis results (i.e., results from the extreme value analysis of the annual maximum wind speed at each meteorological station with suitable surface wind observations). It was shown that there are discrepancies between their estimated v_{AH-50} and those inferred from the NBCC-2005 and NBCC-2010. In an attempt to further investigate the wind hazard at Canadian sites and to further reduce the effect of small sample size to estimate return period values of the annual maximum wind speed, the use of regional frequency analysis (Hosking and Wallis 1997) for wind hazard mapping was presented by Hong and Ye (2014). Comparison of the v_{AH-50} values estimated based on the regional frequency analysis to those obtained from the at-site analysis indicated that they

are in good agreement, especially if the Gumbel model is used. One of the major disadvantages of using the wind records from a station with at least 20 years of useable data is that the valuable information from a station with less than 20 years of useable data is neglected for wind hazard mapping. Therefore, the density of the spatial distribution of the potentially available meteorological stations with valuable wind records is reduced for wind hazard mapping. In addition, it is unknown if the consideration of the stations, each with less than 20 years of useable data, could affect the estimated return period value of the annual maximum wind speed in the regional frequency analysis and wind hazard mapping.

It must be emphasized that the recommended wind load factor of 1.4 and the nominal wind velocity pressure corresponding to 50-year return period value of the annual maximum hourly-mean wind speed, V_{AH} , in the NBCC (NRCC 2005, 2010) are calibrated based on a typical coefficient of variation (COV) of V_{AH} for a (50-year) target reliability index of 3.0 (i.e., failure probability of 1.35×10^{-3}) (Bartlett et al. 2003a, b). However, the COV of V_{AH} is geographically varying and ranges from 0.05 to 0.3; the reliability indices of the structures designed according to the current code is sensitive to the COV of V_{AH} at the construction site (Hong et al. 2016). This is partly because the wind load is proportional to the square of V_{AH} , resulting in that the COV of the wind load equals about twice of the COV of V_{AH} if all other variables involved in evaluating the wind force are treated deterministically. Moreover, although the use of a specified return period value of the wind velocity pressure and a calibrated wind load factor given a COV of V_{AH} can lead to a target reliability, such a set of specified values and wind load factors is not unique. In fact, if the resulting factored design wind loads for different sets of specified values and wind load factors are the same, the same target reliability can be achieved. In addition, it is noted that the ASCE-7-10 adopts a wind load factor of 1.0 with the design wind speed estimated using a return period, T ,

of 700 years for the strength design of Category II structures (Vickery et al. 2010; Cook et al. 2011).

The above background information raises questions as to whether the design wind load requirements could be modified to improve the reliability consistency of codified design under wind load.

1.2 Research objectives and thesis outline

There are two main objectives for the proposed study which are listed below:

- 1) Evaluate and map wind hazard for Canada using surface wind observations.
- 2) Calibrate required factored design wind load considering the geographically varying wind climate (i.e., geographically varying coefficient of variation of the annual maximum hourly-mean wind speed).

For the evaluation and mapping of wind hazard, surface wind observations from Environment Canada for approximately 1300 stations are processed and adjusted by exposure and height. Data from stations, each with at least 10 years of usable data are employed. The wind hazard assessment was carried out using the at-site analysis and region of influence approach. For the analysis, only the winds due to synoptic winds are considered; the winds caused by high intensity wind events such as downbursts and tornados are excluded from the analysis. This is justified since the winds due high intensity wind events are not considered in the current National Building Code of Canada.

For the calibration, the commonly employed first-order reliability method (Madsen et al. 2006) is employed, and a selected target reliability index consistent with that used to develop current design code is considered. The selected target reliability index is based on that employed to calibrate the current design code (Bartlett et al. 2003a, b). The original contributions presented in

this thesis are 1) developed Canadian wind hazard map based on at-site analysis and regional of influence approach, and 2) calibrated the required design wind load that can be easily implemented in the design code to achieve improved reliability consistency.

The tasks carried out to achieve the first objective are presented in Chapter 2, and those to achieve the second objective are described in Chapter 3. Finally, a summary of concluding remarks is presented in Chapter 4. Also, some potential future studies are suggested.

Chapter 2 contains part of a manuscript (co-authored by H.P. Hong) to be submitted for possible publication; Chapter 3 contains part of a manuscript (co-authored by P. Hong and H.P. Hong) to be submitted for possible publication.

Reference

- Akaike, H. 1974. A new look at the statistical model identification. *IEEE Transactions on Automatic Control*, 19 (6), 716–723.
- Bartlett, F.M., Hong, H.P. and Zhou, W. 2003. Load factor calibration for the proposed 2005 edition of the National Building Code of Canada: Companion-action load combinations, *Canadian Journal of Civil Engineering*, 30 (2) 440-448.
- Bartlett, F.M., Hong, H.P. and Zhou, W. 2003. Load factor calibration for the proposed 2005 edition of the National Building Code of Canada: Statistics of loads and load effects, *Canadian Journal of Civil Engineering*, 30 (2) 429-439
- Cook R., Griffis L., Vickery P. and Stafford E. 2011. ASCE 7-10 wind loads. In *Proceedings of the 2011 Structures Congress*, ASCE, Las Vegas, NV.
- Hong H.P., Mara T.G., Morris R., Li S.H. and Ye, W. 2014. Basis for recommending an update of wind velocity pressures in the 2010 National Building Code of Canada, *Canadian Journal of Civil Engineering*, March, Vol. 41, No.3: 206-221.
- Hong, H. P. and Ye, W. 2014. Estimating extreme wind speed based on regional frequency analysis. *Structural Safety*, 47, 67-77.
- Hong, H. P., Ye, W. and Li, S. H. (2016). Sample size effect on the reliability and calibration of design wind load. *Structure and Infrastructure Engineering*, 12(6), 752-764.
- Hosking, J.R.M. and Wallis, J.R. (1997). *Regional frequency analysis: an approach based on L-moments*, Cambridge University Press, Cambridge, UK.
- Madsen H.O., Krenk S. and Lind N.C. 2006. *Methods of structural safety*. Courier Corporation.

- Morris, R. 2009. Wind interim report on the updating of the design winds speeds in the National Building Code of Canada for the task Group on climatic loads, National Research Council of Canada, Ottawa, Canada.
- NBCC. 1995. National Building Code of Canada 1995. Institute for Research in Construction, National Research Council of Canada, Ottawa, Ont.
- NRCC. 2005. National Building Code of Canada. Institute for Research in Construction, (NRCC) National Research Council of Canada, Ottawa, Ontario.
- NRCC. 2010. National Building Code of Canada. Institute for Research in Construction, National Research Council of Canada, Ottawa, Ontario.
- Vickery P.J., Wadhera D. Galsworthy J., Peterka, J.A., Irwin, P.A. and Griffis, L.A. 2010. Ultimate wind load design gust wind speeds in the United States for use in ASCE-7. *Journal of Structural Engineering*, ASCE, 136(5), 613-625.
- Yip, T. and Auld, H. 1993. Updating the 1995 National building code of Canada wind pressures. In *Proceedings of the Electricity '93 Engineering and Operating Division Conference*. Canadian Electrical Association, Montréal, Canada.
- Yip, T., Auld, H. and Dnes, W. 1995. Recommendations for updating the 1995 National building code of Canada wind pressures. In *Proceedings of the 9th International Conference on Wind Engineering*. International Association for Wind Engineering, New Delhi, India.

Chapter 2 At-site Analysis and Regional of Influence

2.1 Introduction

Wind loads recommended in the structural design codes are often developed using extreme value analysis results from the surface wind observations. In particular, the reference wind velocity pressures implemented in the National Building Code of Canada (NBCC) prior to, and including, 1990 can be found in NRCC (1990). Estimates of the 10-, 30- and 100-year return period values of the annual maximum wind velocity pressures were provided; these return period values were calculated based on the return period values of the annual maximum wind speed. It was further indicated that the Gumbel probability distribution fitted by the least-squares method was used for the annual maximum wind speed.

Yip and Auld (1993) and Yip et al. (1995) described the update to the reference wind pressures implemented in the NBCC-1995 (NRCC 1995). Again, the Gumbel distribution was used to fit the annual maximum wind speed but using the method of moments (MOM). More specifically, they used wind records from 233 stations each with at least 10 years of data to estimate the 30-year return period value of the annual maximum wind speed by adopting the Gumbel model fitted using the MOM. A wind hazard map was plotted based on the 30-year return period value of the annual maximum wind speed estimated using the at-site statistics of the wind. The wind speeds at locations tabulated in the NBCC were extracted from the map. To estimate extreme wind speed for return periods T other than 30 years, they introduced a ratio of the standard deviation to the 30-year return period value of the annual maximum wind speed, and assumed that the ratio can be approximated by a constant for all stations considered. The error caused by using a 30-year return period value of the annual maximum wind speed and this constant ratio to estimate the return

period value other than 30 years (e.g., 10 and 100 years) depends on T and the actual statistics of the annual maximum wind speed at a considered site (Hong et al. 2014).

The companion-action load combinations were adopted in the NBCC-2005, and the 50-year return period value of the wind velocity pressure coupled with a wind load factor of 1.4 was recommended in the NBCC-2005 (Bartlett et al. 2003). The 50-year return period values of the wind velocity pressure were calculated based on their corresponding 30-year values recommended in the NBCC-1995 and by considering that the annual maximum wind speed is a Gumbel variate. The reference wind velocity pressures were updated for the NBCC-2010 by fitting the Gumbel distribution to the annual extreme wind speed using the MOM. For the updating, it was assumed that a constant cov of the annual maximum wind speed equal to 0.124 would be adequate for all of the meteorological stations considered (Morris 2009). A comparison of the 50-year return period value of annual maximum (hourly-mean) wind speed, v_{AH-50} , inferred from the NBCC-2010 and NBCC-2005 (Hong et al. 2014) indicated that there are significant changes in v_{AH-50} for some locations common in these two editions of the code. The largest decrease in the NBCC-2010 as compared to the NBCC-2005 is about 30%; the largest increase is less than 10%; the majority of changes are within 10%; two relatively high wind regions in the Northwest Territories and Nunavut in the NBCC-2005 are eliminated in the NBCC-2010; a series of continuous “consistent” wind speed regions from east to west of the country shown in the wind map inferred from the NBCC-2010 was not present in that inferred from the NBCC-2005. It was shown that these differences are partly due to the use of a constant cov to develop v_{AH-50} for the NBCC-2010.

For the extreme wind hazard assessment, the Gumbel distribution, and the generalized extreme value distribution (GEVD) and the generalized Pareto distribution (GPD) are the most widely used probabilistic models (Peterka and Shahid 1998; Frank 2001; Sacre 2002; Holmes and Moriarty

1999; Kasperski 2002; Miller 2003; Hong et al. 2014; Mo et al. 2015). If the Gumbel distribution is considered, the most often used distribution fitting methods include the MOM, the method of the maximum likelihood (MML), the method of L-moments (MLM) (Hosking 1990), the least-squares method, and the generalized least-squares method (GLM) (also known as Lieblein-BLUE) (Lloyd 1952; Lieblein 1974). The MOM, MLM and MML are also often used if the GEVD and GPD are considered. The Gumbel distribution and GEVD are frequently adopted to fit the annual maximum wind speed, while the GPD is applied to the wind speeds over a threshold.

For simplicity and to avoid the subjective selection of the threshold, a wind hazard mapping for Canada was recently carried out based on the annual maximum wind speed from more than 230 stations, where at least 20 years of useable data are available from each station (Hong et al. 2014). They also applied Akaike Information Criterion (AIC) (Akaike 1974) and concluded that the Gumbel distribution is preferable than the GEVD for more than 70% of cases. The consideration of at least 20 years of useable data was aimed at reducing the statistical uncertainty in the estimated wind hazard due to small sample size, although it is inconsistent with the attitude taken in develop wind hazard for previous versions of the code. The wind hazard maps in Hong et al. (2014) were developed based on the at-site analysis results (i.e., results from the extreme value analysis of the annual maximum wind speed at each meteorological station with suitable surface wind observations). It was shown that there are discrepancies between their estimated v_{AH-50} and those inferred from the NBCC-2005 and NBCC-2010.

In an attempt to further investigate the wind hazard at Canadian sites and to further reduce the effect of small sample size to estimate return period value of the annual maximum wind speed, the use of the regional frequency analysis (Hosking and Wallis 1997) for wind hazard mapping was presented in Hong and Ye (2014). For their analysis, the same data set used in Hong et al. (2014)

was considered; the k-means, hierarchical and self-organizing map clustering (Kohonen 2001; Hastie et al. 2001; Lin and Chen 2006) were used to explore potential clusters or regions; and statistical tests were then applied to identify homogeneous regions for subsequent regional frequency analysis. It was concluded that the GEVD provides a better fit than the Gumbel distribution to the normalized data within a cluster, although the GEVD is associated with a low upper bound value that influences significantly the return period values with return period greater than 500 years. Comparison of the v_{AH-50} values estimated based on the regional frequency analysis to those obtained from the at-site analysis indicated that they are in good agreement, especially if the Gumbel model is used. It was noteworthy that the use of cluster analysis to identify the climatic zones for other countries was also considered by Fovell and Fovell (1993) and Kruger et al. (2012).

A major disadvantage of using the wind records from a station with at least 20 years of useable data is that the valuable information from a station with less than 20 years of useable data is neglected for wind hazard mapping. Therefore, the density of the spatial distribution of the potentially available meteorological stations with valuable wind records is reduced for wind hazard mapping. In addition, it is unknown if the consideration of the stations, each with less than 20 years of useable data, could affect the estimated return period value of the annual maximum wind speed in the regional frequency analysis and wind hazard mapping.

The main objectives of this study were to compare wind hazard estimations based on the at-site analysis and regional approaches, to investigate the influence of including small number of annual maximum wind speed data from stations on the wind hazard mapping for Canada, and to assess the differences between the current wind hazard estimates to those inferred from the NBCC-2005 and NBCC-2010. For the analysis, information from approximately 1300 stations were considered, and the data from stations, each with at least 10 years of useable wind records, were

processed and analyzed. The consideration of 10 years of useable data was consistent with an earlier code development (Yip and Auld 1993, Yip et al. 1995). It increased the task of the data processing since the wind measurements must be adjusted for exposure and height for them to represent those for a standardized condition stipulated in design codes. The use of the cluster analysis together with the regional frequency analysis given in Hosking and Wallis (1997) as well as the region of influence analysis advocated by Burn (1990) was attempted. Wind hazard maps based on the return period values of the annual maximum wind speed estimated using the considered approaches were developed and compared. The comparison was extended to include the return period values of the annual maximum wind speed inferred from the NBCC-2005 and NBCC-2010. Since the developed wind hazard maps based on the estimated v_{AH-50} may not comply with the code imposed requirements (e.g., a minimum design wind speed of 77.55 km/h is implied in the NBCC-2010), maps by considering a set of practical criteria were also presented.

2.2 Surface wind observations

The characteristics of the anemometer types operated in Canada and the types of wind data recorded at meteorological stations were presented in Yip et al. (1993), Yip and Auld (1995), and Hong et al. (2014). The available wind speed records in Environment Canada (EC) HLY01 digital archive (see http://www.climate.weatheroffice.gc.ca/prods_servs/documentation_index_e.html#hly01) were considered in this study. The archive has been maintained by EC since January 1953, and only for some major Canadian airports the data tend to extend back to this date. The information on the anemometer site, including the history of anemometer height, location and instrumentation, was obtained from EC and used to assess the quality of wind data at each station (Morris 2013, private communication). The locations of 1224 stations (each with at least more

than one year's of data) where the wind records are available were shown in Figure 2-1a. The empirical cumulative distribution of the record length at a station based on the considered stations was shown in Figure 2-1b, indicating that there are approximately 63% and 32% of the stations where each station has a wind record length greater than 10 and 20 years, respectively. The maximum length of the wind record at a station is 58 years. The wind measurements for some stations were not suitable for the purpose of wind hazard assessment for the standardized condition due to a variety of reasons, including the anemometer location (e.g., on the roof of a building) and frequency of observation. In such cases, the wind measurements during the affected observation periods were removed from the dataset.

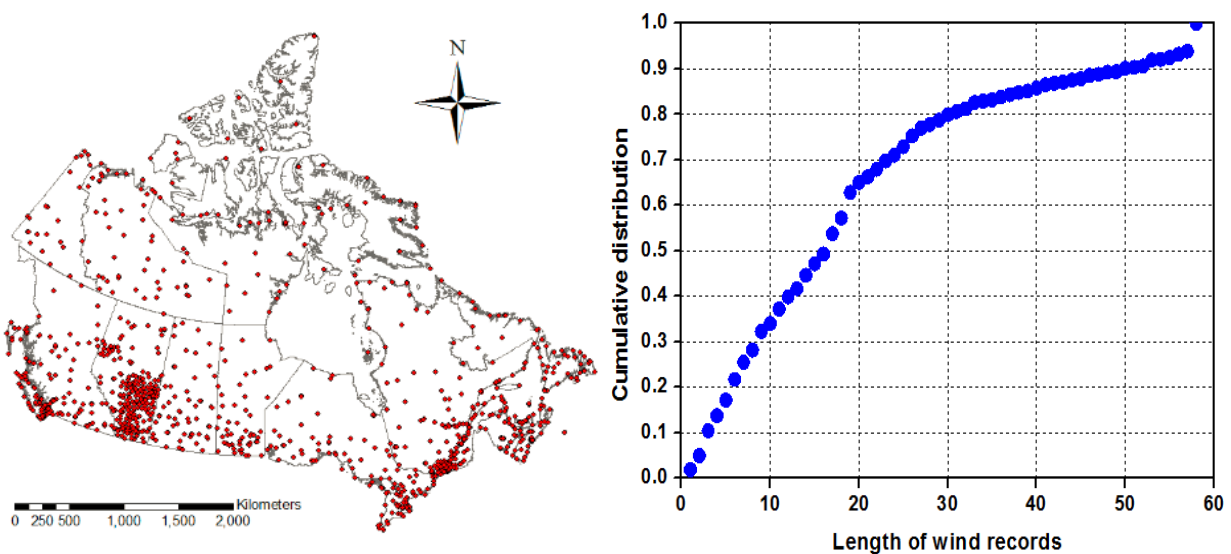


Figure 2-1. Locations of the meteorological stations where wind speed records are available in EC HLY01 digital archive, and empirical cumulative distribution of the length of wind measurement period at each station: a) Spatial distribution of the stations, b) Empirical cumulative distribution of length of wind measurement period.

Let n_A denote the number of years of useable wind measurements at a station. By considering that $n_A \geq 10$ or $n_A \geq 20$ was needed for a station to be included for the extreme value analysis of

the annual maximum wind speed, the number of identified stations were 620 and 236, respectively. As indicated in Hong et al. (2014), the wind records from 4 out of the 236 stations, each with $n_A \geq 20$, are not reliable because they are affected significantly by local topographic conditions. For improved spatial resolution they included three additional stations, each with at least 17 years of usable data, to improve the spatial resolution. To facilitate the comparison of the results with those given in Hong et al. (2014) and for simplicity of reference, data from these 235 stations (i.e., 232+3) are referred to as the case with $n_A \geq 20$, even though n_A is less than 20 for three of the stations. Also, an analysis showed that the wind records from 36 out of the 384 stations with wind record length within 10 to 19 are not reliable because they are affected significantly by local topographic conditions or appear to report erroneously wind speeds as compared with those from nearby stations. These resulted in the consideration of 583 stations identified in Figure 2-2 for this study.

The adjustment of wind speed measurements at a station with $n_A \geq 20$ for anemometer height and for exposure was already carried out in Hong et al. (2014). The adjusted for anemometer height was carried out using a power law with an exponent of 1/7 (NRCC 2010, Wan et al. 2010). The exposure adjustment was carried out based on the method recommended in ESDU (2002) and by following the steps given in Mara et al. (2013). As an integral part of exposure adjustment analysis, satellite photos for each of the considered stations were scrutinized; numerous transitions in roughness length over varying fetches were considered; the exposure adjustment factor less than unity was considered for over exposed (open water) stations – an exposure condition that is not considered in the NBCC-2010. This approach for the adjustment was adopted in this study to process the wind measurements from stations where n_A is greater than or equal to 10 but less than 20.

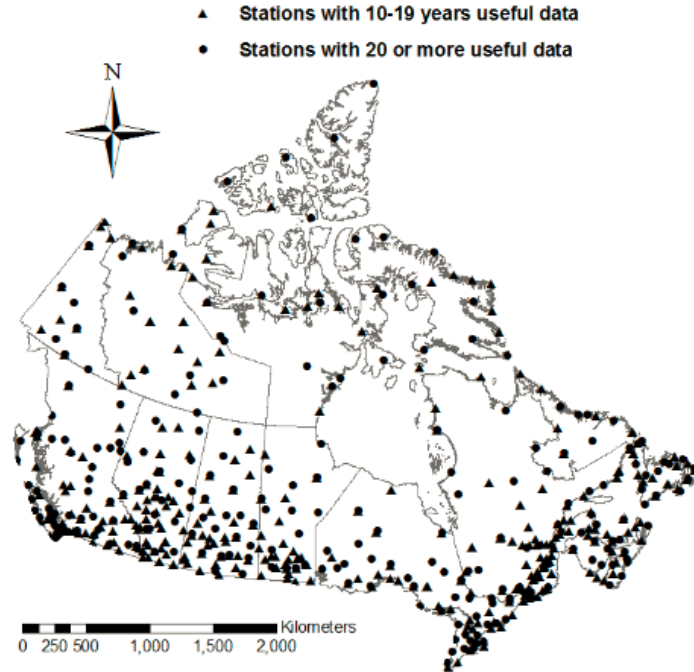


Figure 2-2. Locations of 583 stations with useable data used in this study.

In all cases, no distinction was made for thunderstorm days and non-thunderstorm days in processing the wind speed data; data quality control was carried out; the annual maximum wind speed was extracted from the adjusted wind speed measurements; and the extracted value was considered to be representative of the annual maximum moving average (AMMA) of the hourly-mean wind speed V_{AH} . Detailed justification for these was already given in Hong et al. (2014).

2.3 Extreme value analysis approach: at-site and regional approaches

Two approaches were employed to estimate the T -year return period value of V_{AH} , V_{AH-T} . The first one was the often used at-site analysis and the second one was a regional approach (Hosking and Wallis 1997, Burn 1990). The application of the at-site analysis is directly focused on fitting samples of V_{AH} from each meteorological station using a selected probabilistic model (Castillo

1988, Coles 2001). This approach is adequate for a relatively large samples size. The regional approach makes additional assumptions to allow the incorporating of data from other stations to estimate statistics for a site of interest. In other words, it attempts to increase the sample size for the site of interest by borrowing data from other stations so the extreme value analysis can be carried out with a reduced or negligible statistical uncertainty caused by small sample size.

As mentioned in the introduction, two of the most commonly used probability distributions for V_{AH} are the Gumbel distribution and the GEVD.

The Gumbel distribution is given by (Castillo 1988, Cole 2001),

$$F_{GU}(x) = \exp(-\exp(-(x-u)/a)), \quad (2.1)$$

where $F_{GU}(x)$ denotes the cumulative distribution function, x denotes the value of the random variable X (representing V_{AH}), and a and u are the scale and location parameters. The mean μ_X and the standard deviation σ_X of a Gumbel variate X , are equal to $u + 0.5772a$ and $a\pi/\sqrt{6}$, respectively. The cov of X , v_x , by definition, equals σ_X/μ_X . For the distribution fitting, the MOM, MML, MLM and GLM could be considered (Castillo 1988, Hosking and Wallis 1997, Hong et al. 2013).

The estimators of a and u , denoted by \hat{a} and \hat{u} , for the selected methods was listed in Table 2-1. The estimated T -year return period value of X , \hat{x}_T , (representing V_{AH-T}) can be estimated using,

$$\hat{x}_T = \hat{u} - \hat{a} \ln(-\ln(1-1/T)) \quad (2.2)$$

Table 2-1. Methods for estimating the model parameters and quantiles based on the Gumbel model (for n samples, with sample mean m and sample standard deviation s).

Method	Equations for estimating model parameters \hat{a} and \hat{u}
MOM	$\hat{a} = s\sqrt{6}/\pi$, and $\hat{u} = m - \gamma s\sqrt{6}/\pi$
MML	Maximizing: $\mathcal{L} = -n \ln a - \sum y_i - \sum \exp(-y_i)$, Or solving, $-n - \sum y_i - \sum y_i \exp(-y_i) = 0$, and $-n - \sum \exp(-y_i) = 0$ where $y_i = (x_i - u)/a$
MLM	$\hat{a} = (2b_1 - b_0)/\ln 2$, and $\hat{u} = b_0 - \gamma\hat{a}$
GLM	$\hat{a} = \sum c_{a,i} x_{n,i}$, $\hat{u} = \sum c_{u,i} x_{n,i}$ where $c_{a,i}$ and $c_{u,i}$ are known as the coefficients of the best linear unbiased estimators (Lieblein 1974), and $x_{j:n}$ denotes the j -th ordered sample (in ascending order) of a set of random samples of size n . (See the tabulated constant in Hong et al. 2013)

Simulation analysis results indicate that the GLM is the preferred method for estimating \hat{x}_T , especially if the sample size is not large; this preference is followed by the MML, MLM and MOM in descending order (Hong et al. 2013). These methods are considered for distribution fitting in the following sections.

The GEVD $F_{GE}(x)$ is expressed as (Castillo 1988, Coles 2001),

$$F_{GE}(x) = \exp\left(-\left(1 - k(x - u)/a\right)^{1/k}\right), \text{ for } k \neq 0 \quad (2.3)$$

where u , a and k are the model parameters. This distribution turns to the Gumbel distribution shown in Eq. (2.1) if k tends to 0. The \hat{x}_T in this case is given by,

$$\hat{x}_T = \hat{u} + \frac{\hat{a}}{\hat{k}} \left(1 - (-\ln F_G(x))^{\hat{k}}\right), \quad (2.4)$$

where \hat{a} , \hat{u} and \hat{k} are the estimators of a , u and k shown in Eq. (2.3), and can be obtained using the MOM, MLM and MML (see Table 2-2). Hosking (1985) showed that the estimated x_T is biased

if the MLM is used, but preferable to the MML because the use of MML leads to greater scatter in estimated x_T if the sample size is small. Martin and Stedinger (2000) indicated that the performance of the MOM, MLM and MML depends on the sample size, the distribution upper tail behaviour, the criteria such as the minimum bias and root-mean-square-error of \hat{x}_T . Both of these studies indicated that the MML could give unrealistic predictions if the sample size is small. The MOM, MLM, and MML are used to fit the GEVD for the numerical analysis.

Table 2-2. Methods for estimating the model parameters and quantiles based on the generalized extreme value distribution.

Method	Equations for estimating model parameter \hat{a} , \hat{u} and \hat{k} .
MOM	Solving: $m = u + a(1 - \Gamma(1+k))/k$, $s = a(\Gamma(1+2k) - \Gamma^2(1+k))^{1/2} / (\text{sign}(k)k)$, and $\gamma_3 = \text{sign}(k)(-\Gamma(1+3k) + 3\Gamma(1+k)\Gamma(1+2k) - 2\Gamma^3(1+k)) / (\Gamma(1+2k) - \Gamma^2(1+k))^{3/2}$ where γ_3 is the sample skewness.
MML	Maximizing: $\mathcal{L} = -n \ln a - (1-k) \sum y_i - \sum \exp(-y_i)$ where $y_i = -k^{-1} \ln(1 - k(x_i - u)/a)$.
MLM	Solving: $b_0 = u + a(1 - \Gamma(1+k))/k$, $2b_1 - b_0 = a\Gamma(1+k)(1 - 2^{-k})/k$, and $(3b_2 - b_0)/(2b_1 - b_0) = (1 - 3^{-k})/(1 - 2^{-k})$

The application of the regional frequency analysis (Hosking and Wallis 1997) to assess wind hazard for Canada was presented in Hong and Ye (2014) by considering the same data set used in Hong et al. (2014). The application required, firstly, the identification of the potential homogeneous regions. A preliminary analysis by using this approach and considering data from stations each with $n_A \geq 10$ was carried out in this study. Three clustering analysis methods, namely the k-means clustering, hierarchical clustering and self-organizing map (Hastie et al. 2001;

Kohonen 2001), were used to explore possible homogeneous regions. Unfortunately, the number of the stations within some of the identified regions are very small and the test of homogeneity (Hosking and Wallis 1997) carried out indicated that many of the identified regions are definitely heterogeneous. Therefore, application of this approach was not considered further, and an alternative regional approach – the region of influence (ROI) approach proposed by Burn (1990), was considered. The ROI was developed to assess flood frequency; it was also applied to assess snow hazards (Mo et al. 2015). The approach uses a distance D_{ij} to measure the closeness of the i -th and j -th stations, where D_{ij} is defined by,

$$D_{ij} = \left(\sum_{m=1}^M w_m (A_m^i - A_m^j)^2 \right)^{1/2} \quad (2.5)$$

where M is the number of attributes used to measure the similarity of the stations, w_m is the weight of the m -th attribute, and A_m^i is the value of attribute m for station i . The statistics of V_{AH} from the j -th station are weighted and used to estimate the T -year return period value of V for the i -th station if D_{ij} is within a threshold. It is noted that for assessing other types of climate data (Mo et al. 2015), the normalized latitude, longitude and L-coefficient of variation (L-cv) of V_{AH} associated with the stations were used as attributes for the ROI approach, where the normalization was carried out by dividing the variable value by its corresponding range for all stations, and equal weight is assigned to each attribute. The threshold θ_i used to accept the j -th station to form the i -th ROI, R_i , if $D_{ij} \leq \theta_i$, that was suggested by Burn (1990) is,

$$\theta_i = \begin{cases} \theta_L, & N_{Li} \geq N_D \\ \theta_L + (\theta_U - \theta_L) \times \frac{N_D - N_{Li}}{N_D}, & N_{Li} < N_D \end{cases} \quad (2.6)$$

where θ_L is a lower threshold value to include stations into R_i ; N_{Li} is the number of stations included in R_i if the threshold value is set at θ_L ; N_D is the desired number of stations for R_i ; and θ_U is an

upper threshold value for sites with $N_{Li} < N_D$.

The L-moment ratios $(1, \bar{t}^i, \bar{t}_3^i)$ for R_i , are calculated using the equations shown in Table 2-3.

The Gumbel distribution and GEV distribution are employed to fit the calculated $(1, \bar{t}^i)$ and $(1, \bar{t}^i, \bar{t}_3^i)$, respectively, in the ROI approach, and the quantile of nonexceedance probability $F = 1 - 1/T$ at the i -th station, $Q_i(F)$ is given by,

$$Q_i(F) = \mu_i q(F), \quad (2.7)$$

where μ_i is the mean value of V_{AH} at the i -th station, and $q(F)$ is the regional quantile function determined based on the fitted distribution in the ROI approach.

Following the suggestions given in Burn (1990), for the numerical analysis in the following sections, N_D was taken equal to 50, and θ_L and θ_U were set to the 15th and 30th percentile of the ascendingly sorted, non-zero D_{ij} , respectively, for the case with $n_A \geq 20$. These values are set equal to the 25th and 50th percentile of D_{ij} for the case with $n_A \geq 10$.

Table 2-3. Equations used to calculate L-moment ratios \bar{t}^i and \bar{t}_3^i for R_i . (Burn 1990).

Equation for estimating L-moment ratios	Notes
$\bar{t}^i = \frac{\sum_{j=1}^{N_i} n_j \eta_{ij} t_j}{\sum_{j=1}^{N_i} n_j \eta_{ij}}$	N_i is the number of stations in R_i ; for the j -th station, $t_j = (l_2/l_1)$ is the L-coefficient of variation (L-CV), $t_{3,j} = (l_3/l_2)$ is L-skewness, and $(l_1, l_2, l_3)_j$ are the estimated first three L-moments, and n_j is the sample size; and η_{ij} is the weighting function given by Burn (1990)
$\bar{t}_3^i = \frac{\sum_{j=1}^{N_i} n_j \eta_{ij} t_{3,j}}{\sum_{j=1}^{N_i} n_j \eta_{ij}}$	
$\eta_{ij} = 1 - (D_{ij}/W)^n$	The parameters n and W are taken equal to 2.5 and the 50 th percentile of D_{ij} , respectively

2.4 Wind hazard estimation and mapping

2.4.1 Wind hazard mapping based on extreme wind speed inferred from the NBCC

The reference velocity wind pressure for specified locations in Appendix C of the NBCC-2005 and NBCC-2010 was developed based on extreme value analysis results, expert subjective opinion and judgement, and consideration of some practical criteria for code making. The velocity wind pressures in the NBCC-2005 and NBCC-2010 were considered to correspond to $50-v_{AH-50}$ and an average air density of 1.2929 kg/m^3 was considered to be adequate (Boyd 1967). Using the tabulated location-specific reference velocity wind pressures in the NBCC-2005 and NBCC-2010, v_{AH-50} was calculated and used for wind hazard mapping in Hong et al. (2014). They showed that there are changes to v_{AH-50} from the NBCC-2005 to NBCC-2010; most changes are within 10%; the largest decrease is about 30%; and the largest increase is less than 10%. Some of the changes were likely caused by the assumption of constant cov of V_{AH} made for updating the NBCC-2010. The spatial interpolation needed to map the wind hazard was carried out using the ordinary kriging implemented in ArcGIS (version 10.2) (ESRI 2011) (Johnston et al. 2003). The use of the ordinary kriging was justified since a comparison showed that it is the preferred spatial interpolation technique for the wind speed (Ye et al. 2015). These hazard maps were replotted in Figure 2-3 to facilitate the comparison in the following sections. Moreover, throughout this study, unless otherwise indicated, the ordinary kriging with nugget not equal to zero implemented in the ArcGIS were used for wind hazard mapping. However, for completeness, some of the corresponding maps interpolated with nugget equal to zero were included in Appendix A.

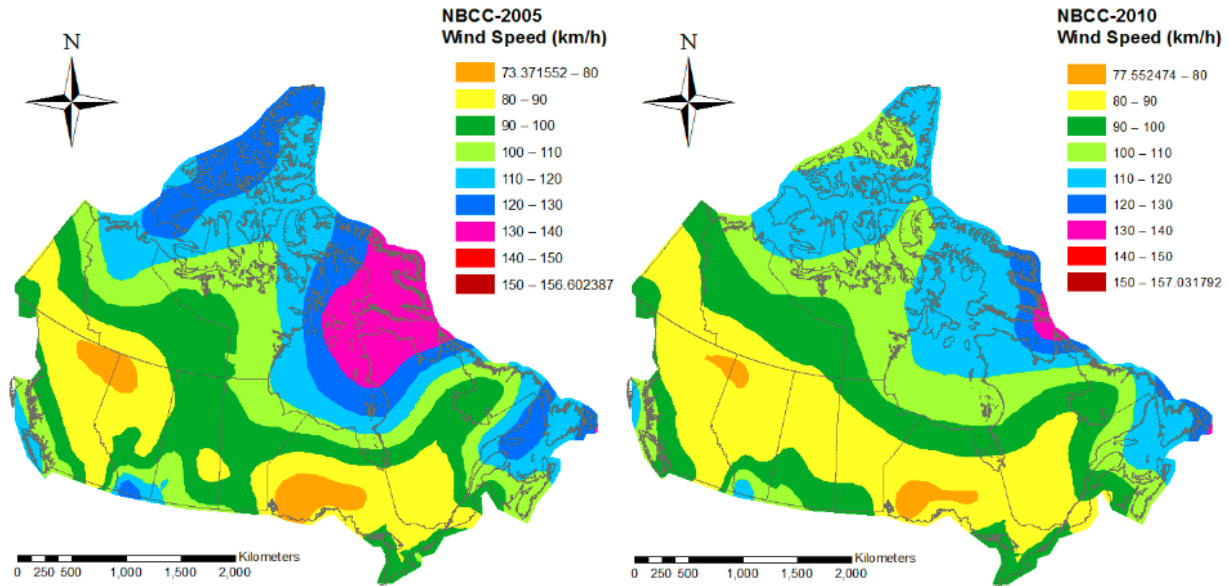


Figure 2-3. Wind hazard maps inferred from the reference velocity wind pressures given in the NBCC-2005 and NBCC-2010.

2.4.2 Comparison of the spatial varying wind hazard using data with $n_A \geq 20$ and ≥ 10

Using samples of V_{AH} for each of the stations shown in Figure 2-2, the mean and cov at each station were calculated. The calculated values were shown in Figure 2-4 for the case with $n_A \geq 20$, and in Figure 2-5 for the case with $n_A \geq 10$. Comparison of the plots shown in Figures 2-4 and 2-5 indicated that the spatial trends of the means for the two cases are similar except there are three patches of low mean values within the region where the mean is less than 50 km/h. There are differences in the spatial trends of the cov values for the two cases. For example, there are several patches in Figure 2-5b with large cov values. Inspection of the data from stations within these patches indicated that these large cov values are associated with stations where n_A is within 10 and 16. The decreasing spatial trend of the cov value from east towards west or northwest shown in Figure 2-4b is not apparent in Figure 2-5b. These indicated that while the spatial trends of the mean of V_{AH} are relatively stable by decreasing n_A from 20 to 10, the small sample size effect is

significant for the estimated cov.

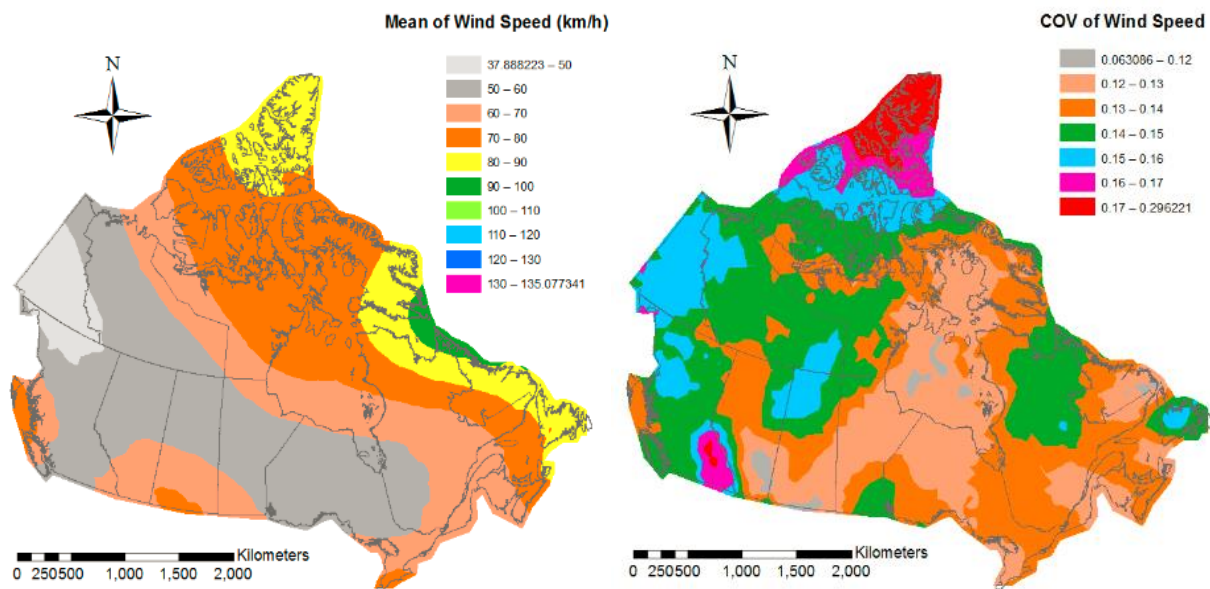


Figure 2-4. Mean and coefficient of variation of V_{AH} for the case with $n_A \geq 20$.

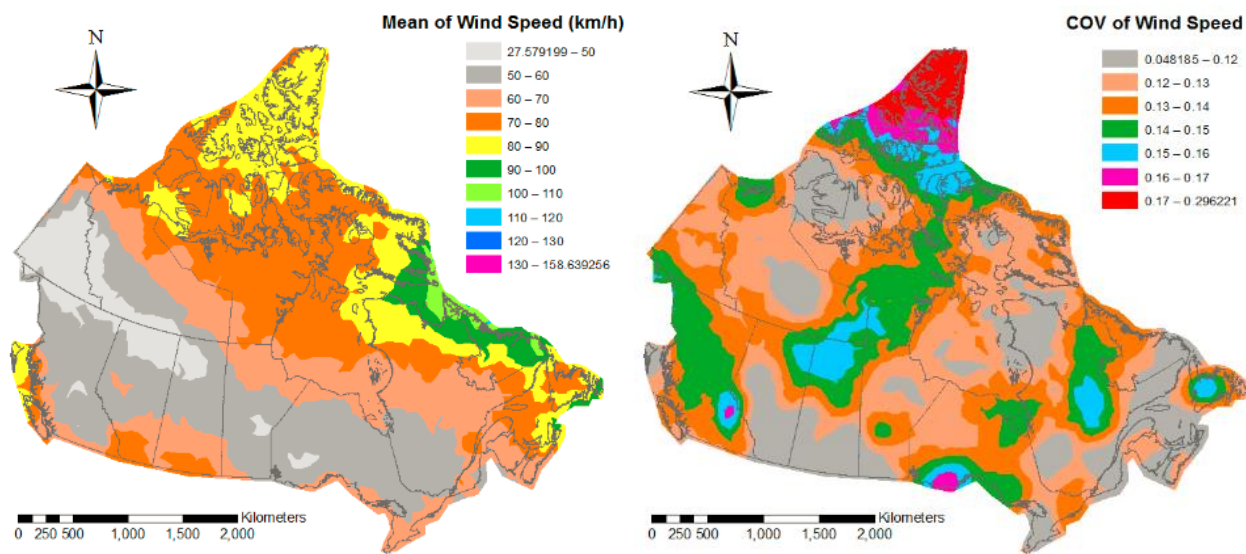


Figure 2-5. Mean and coefficient of variation of V_{AH} for the case with $n_A \geq 10$.

For the case with $n_A \geq 20$ which was already reported in Hong et al. (2014), the mean ranges approximately from 38 to 135 km/h, and the cov varies from 0.05 to 0.3 with an average of 0.138.

For the case with $n_A \geq 10$, the mean of V_{AH} ranges approximately from 28 to 159 km/h, and the cov of V_{AH} varies from 0.05 to 0.3 with an average of 0.125. This showed that the range of cov of V_{AH} for the case with $n_A \geq 10$ is similar to that for the case with $n_A \geq 20$. The smaller mean of cov value for the former is attributed to that there are many more stations with smaller cov values for the former than for the latter.

To inspect distribution of the cov of V_{AH} , ξ_{VAH} , for the considered cases, empirical cumulative distributions of ξ_{VAH} were presented in Figure 2-6, indicating that for the case with $n_A \geq 10$, the 0.1 and 0.9-quantiles of the ξ_{VAH} are 0.081 and 0.171, and the 0.2 and 0.8-quantiles of the ξ_{VAH} are 0.094 and 0.151. The values become 0.103 and 0.173, and 0.113 and 0.162 for the case with $n_A \geq 20$. Comparison of these ranges indicates that for wind measurements from majority of stations, the estimated cov ranges for the cases with $n_A \geq 10$ and $n_A \geq 20$ are consistent. However, there are large differences in the estimated cov values for cov values in the lower (or upper tail) region for the cases with $n_A \geq 10$ and $n_A \geq 20$. These are partly attributed to small sample size effect and to the spatial locations of stations.

By considering that V_{AH} was Gumbel distributed (see Eq. (2.1)), distribution fitting for the case with $n_A \geq 10$ was carried out using the MOM, MML, MLM and GLM, and v_{AH-50} was estimated using Eq. (2.2). Comparison of v_{AH-50} estimated by different fitting methods was depicted in Figure 2-7. The overall impression was that the differences between v_{AH-50} estimated by using different fitting methods are greater than those observed for the case with $n_A \geq 20$ (Hong et al. 2014), especially for the plots shown in Figure 2-7a and 2-7c. For reference purpose, the calculated V_{AH-50} by using the Gumbel distribution and the GLM are shown in Appendix B.

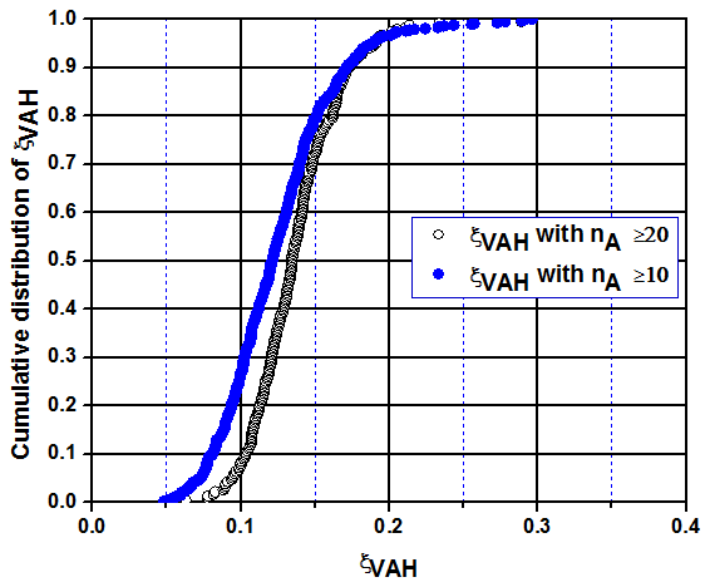


Figure 2-6. Empirical distribution of ξ_{VAH}

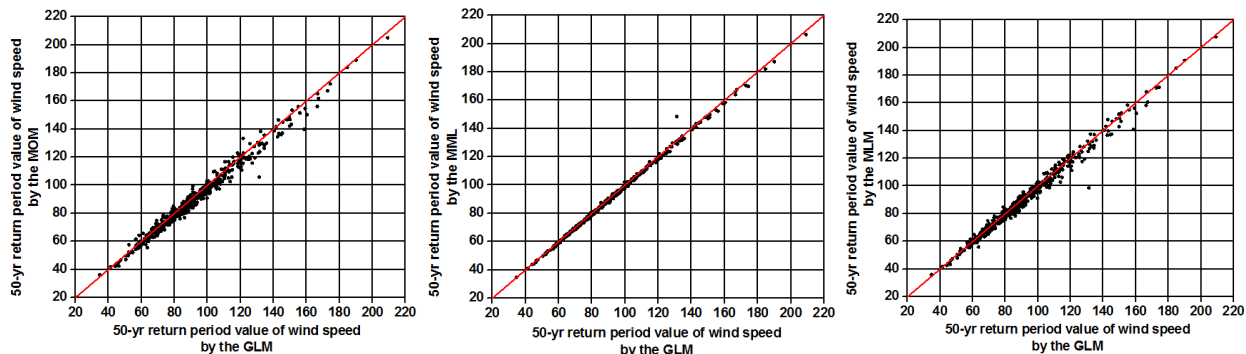


Figure 2-7. Comparison of the estimated v_{AH-50} by different fitting methods and considering V_{AH} is Gumbel distributed: a) using the MOM vs using the GLM; b) using the MML vs using the GLM; c) using the MLM vs using the GLM.

Since GLM is the preferred distribution fitting method, the estimated v_{AH-50} by the GLM was illustrated in Figure 2-8 to show the spatial trends and to aid a possible modification to v_{AH-50} recommended in the NBCC-2010. For the plotting, the results for the case with $n_A \geq 20$ and the

case with $n_A \geq 10$ were presented for comparison purpose, even though the results for the case with $n_A \geq 20$ were already given in Hong et al. (2014).

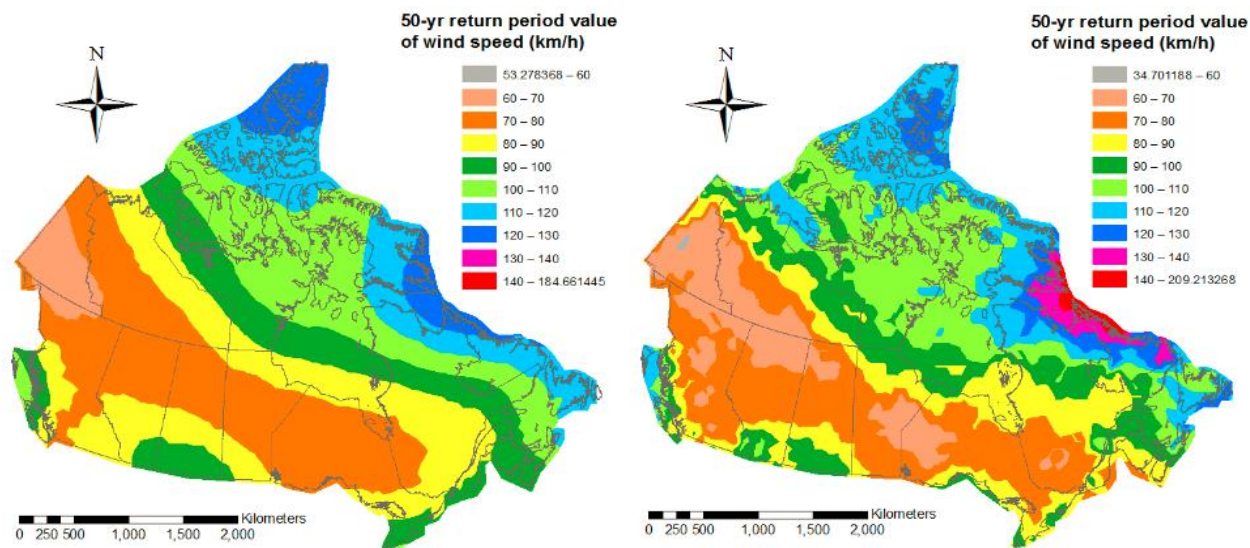


Figure 2-8. Estimated v_{AH-50} using the GLM for the selected meteorological stations shown in Figure 2-2: a) Contour map of v_{AH-50} for the case with $n_A \geq 20$, b) Contour map of v_{AH-50} for the case with $n_A \geq 10$.

Comparison of the results shown in Figure 2-8 indicated that the contour lines for the case with $n_A \geq 10$ are rougher than those for the case with $n_A \geq 20$, and the overall spatial trends in Figures 2-8a and 2-8b are similar, except that there are three visible patches of low wind speeds in Figure 2-8b (within the region where v_{AH-50} ranges from 70 to 80 km/h) that are consistent with those shown in Figure 2-5a for the mean value of V_{AH} . Visual inspection of the results presented in Figures 2-3 and 2-8 indicated that the wind hazard maps shown in Figure 2-8 differ from those shown in Figure 2-3. However, there are some resemblance as well, especially if the regions with v_{AH-50} less than the minimum design wind speed of 77.55 km/h were replaced by $v_{AH-50} = 77.55$ km/h. The resemblance included that some of the smoothness of the wind speed across the country

from east to west shown in Figure 2-3b are retained in Figure 2-8 and, the localized wind speed features shown in Figures 2-3a and 2-3b in the northern and coastal regions are maintained.

To quantify the differences, the ratio of v_{AH-50} inferred from the NBCC-2005 (or NBCC-2010) to the estimated v_{AH-50} for the case with $n_A \geq 10$, denoted as $R_{C05/E10}$ (or in $R_{C10/E10}$), was calculated for the locations where the tabulated reference wind velocity pressure is available. The empirical distributions of $R_{C05/E10}$ and $R_{C10/E10}$ were presented in Figure 2-9 by considering the values obtained for the locations where the inferred v_{AH-50} from the codes are greater than the lower bound value of 77.55 km/h mentioned earlier.

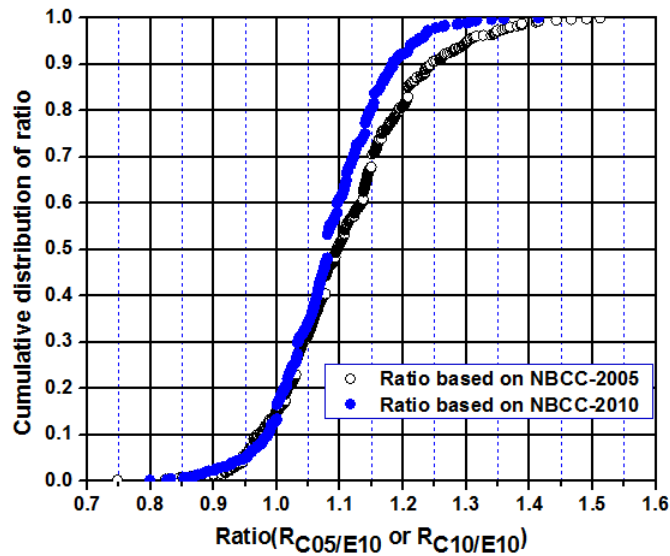


Figure 2-9. Empirical distribution of $R_{C05/E10}$ and $R_{C10/E10}$.

The empirical distributions presented in Figure 2-9, indicated that the ratios are within 0.95 to 1.05 for only 30% of the locations, and within 0.9 to 1.1 for 60% of the locations. This observation is consistent with that drawn from the results for the case with $n_A \geq 20$ (Hong et al. 2014).

The GEVD (see Eq. (2.4)) was also used to fit the data for the case with $n_A \geq 10$. For the fitting, the methods listed in Table 2-2 were employed and v_{AH-50} was estimated using Eq. (2.4) and the

fitted distribution parameters. A comparison of the estimated v_{AH-50} using the Gumbel distribution and the GEVD distribution but applying the same distribution fitting method was shown in Figure 2-10. The figure showed that the estimated v_{AH-50} by these two distributions are in relatively good agreement if the MOM and MML were used. This observation is consistent with that made by considering $n_A \geq 20$ (Hong et al. 2014). Moreover, by using the AIC, it was concluded that the use of the Gumbel distribution for V_{AH} is preferred for approximately 73% of stations for the case with $n_A \geq 10$. The percentage is slightly greater than the reported 70% for the case with $n_A \geq 20$. Therefore, for consistency and simplicity, the Gumbel distribution was recommended if the wind records from many stations are to be considered to develop wind hazard maps.

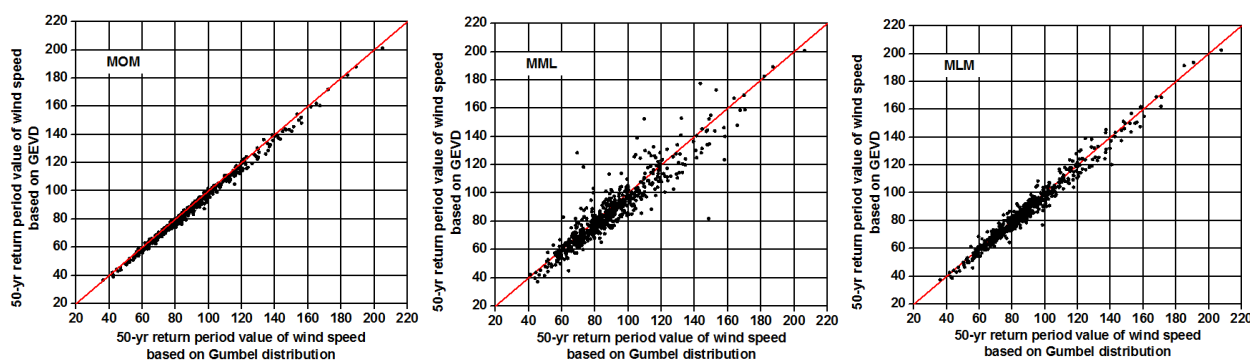


Figure 2-10. Comparison of the estimated v_{AH-50} by different distribution types: a) using MOM, b) using the MML, and c) using MLM

2.4.3 Estimated wind hazard using the ROI approach

By applying the ROI approach, values of v_{AH-50} at each of the stations shown in Figure 2-2 were estimated for the cases with $n_A \geq 20$ and $n_A \geq 10$. Inspection of the analysis results indicates that for the cases with $n_A \geq 20$ the number of stations included in a ROI for a station ranges from 4 to 100, and the average number of stations included in a ROI is 66. For the case with $n_A \geq 10$, the number of stations included in a ROI ranges from 2 to 173, and the average number of stations

included in a ROI is 93. The estimated values of v_{AH-50} were shown in Figure 2-11a and 2-11b by considering the Gumbel distribution, and in Figure 2-11c and 2-11d by considering the GEVD distribution. Comparison of maps obtained by using the ROI shown in the figure indicated that:

- a) In general, the spatial trends shown in Figures 2-11a and 2-11b are similar. There are more detailed local spatial variations of v_{AH-50} shown in Figure 2-11b for the case with $n_A \geq 10$ than those depicted in Figure 2-11b for the case with $n_A \geq 20$. This showed that even with the application of the ROI approach, the inclusion of stations with n_A within 10 to 19 still resulted sharper spatial changes. The differences between Figures 2-11a and 2-11b are similar to those between Figures 2-8a and 2-8b which are obtained based on the at-site analysis.
- b) For the case with $n_A \geq 20$, the maps of v_{AH-50} are not sensitive to whether the Gumbel distribution or the GEVD is employed, indicating that the fitted Gumbel distribution and GEVD are close for, at least, the nonexceedance probability of 0.98, and the estimated v_{AH-50} values are robust.
- c) The observed robustness in the estimated v_{AH-50} observed for the case with $n_A \geq 20$ is not applicable to the estimates for the case with $n_A \geq 10$, that are shown in Figures 2-11b and 2-11d.

Based on the above observations, and the fact that the results presented in Figure 2-8a, 2-11a and 2-11c are almost identical, it was suggested that maps shown in Figures 2-11a or 2-11b to be adopted to represent the wind hazard for Canada if v_{AH-50} is of interest. Again, for reference purpose, the calculated V_{AH-50} by using the Gumbel distribution and the ROI approach are shown in Appendix B.

Similarly, results based on v_{AH-100} and v_{AH-500} were calculated and shown in Figure 2-12 for completeness. The spatial trends observed from Figure 2-12 are similar to those shown in Figures 2-11a and 2-11b, except the magnitude of the estimated return period values for different T values

differs, which is expected. The are differences between the estimated V_{AH-T} for the cases with $n_A \geq 20$ and $n_A \geq 10$. The differences seem to increase slightly as T increases.

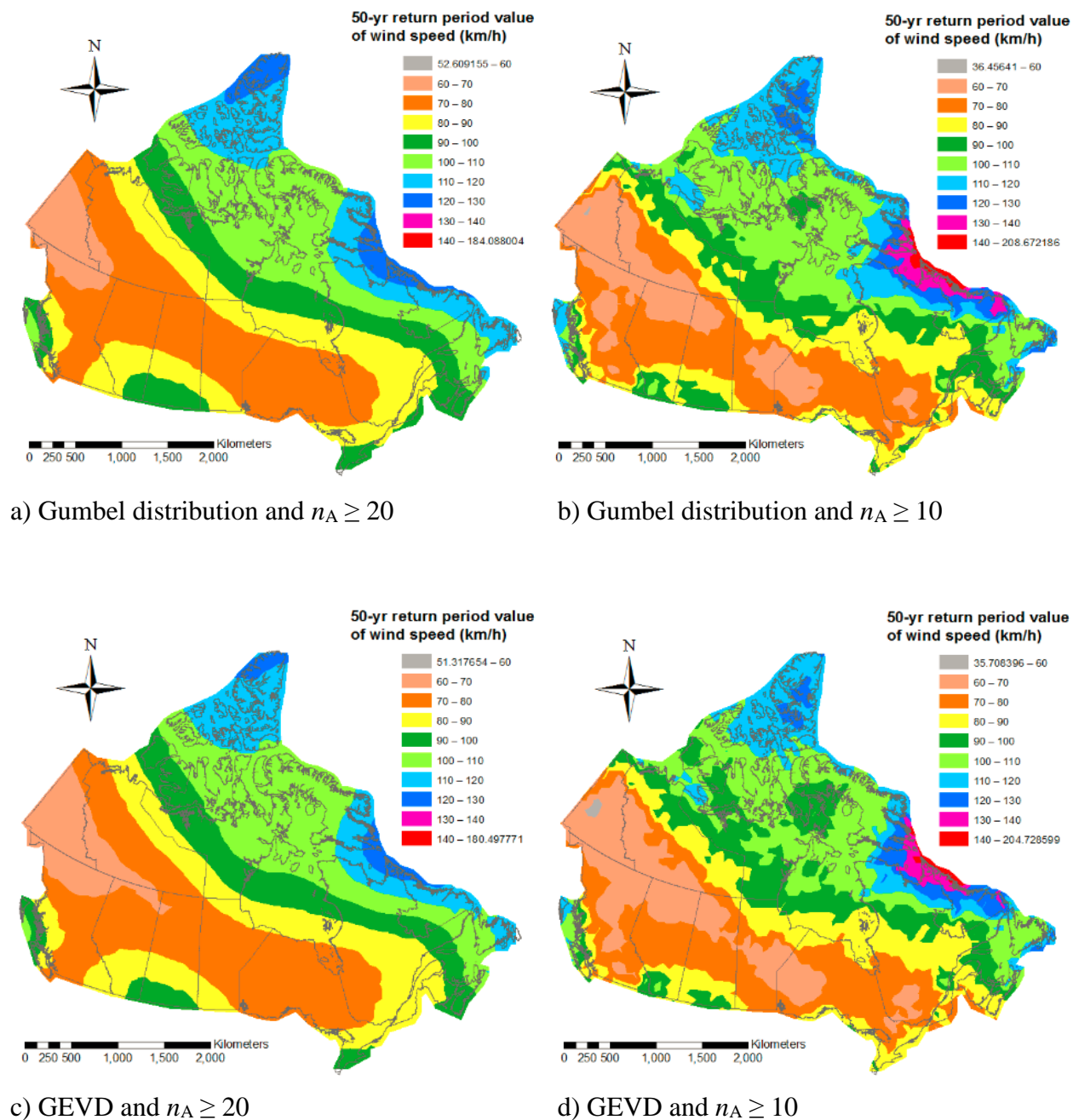
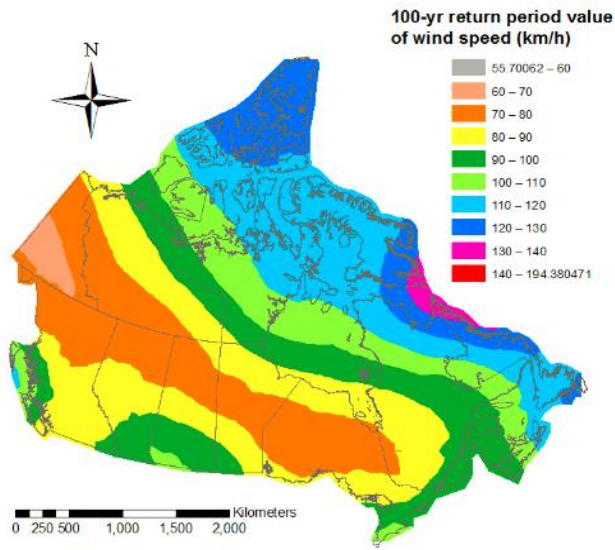
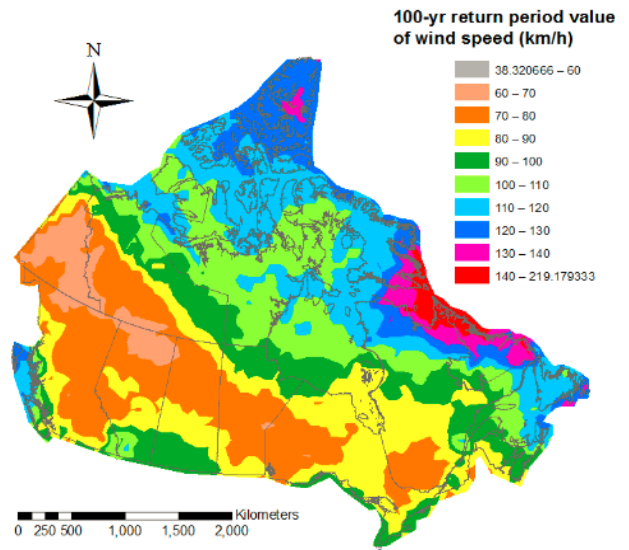


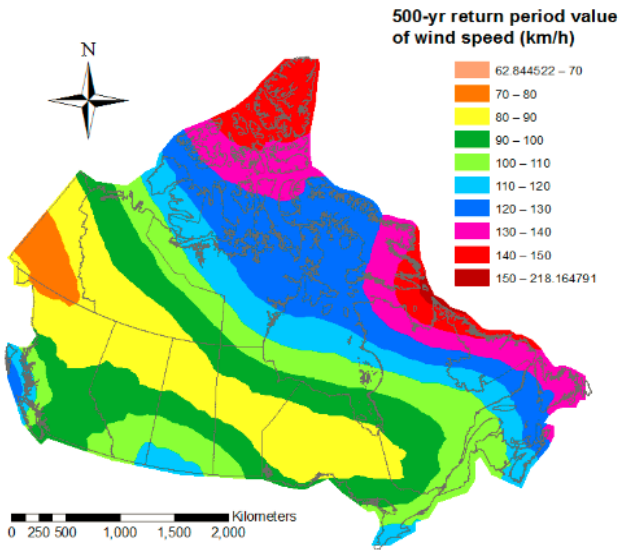
Figure 2-11. Wind hazard maps developed based on the ROI approach: a) Gumbel distribution and $n_A \geq 20$, b) Gumbel distribution and $n_A \geq 10$, c) GEVD and $n_A \geq 20$, d) GEVD and $n_A \geq 10$.



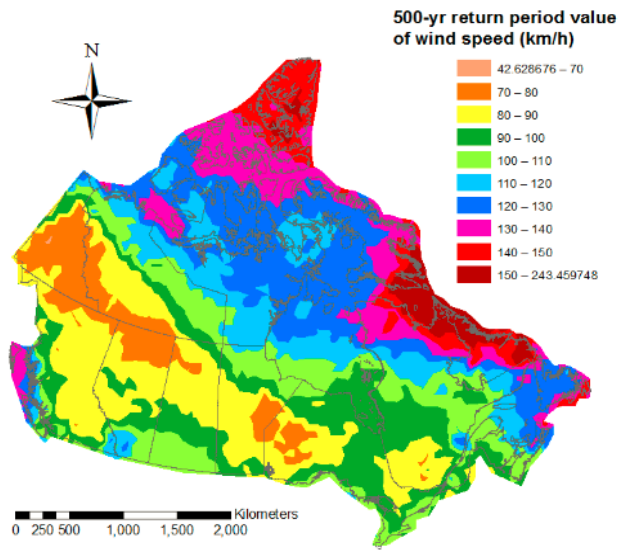
a) v_{AH-100} for $n_A \geq 20$



b) v_{AH-100} for $n_A \geq 10$



c) v_{AH-500} for $n_A \geq 20$



d) v_{AH-500} for $n_A \geq 10$

Figure 2-12. Wind hazard maps developed based on the ROI approach and considering the Gumbel model: a) v_{AH-100} for $n_A \geq 20$, b) v_{AH-100} for $n_A \geq 10$, c) v_{AH-500} for $n_A \geq 20$, and d) v_{AH-500} for $n_A \geq 10$.

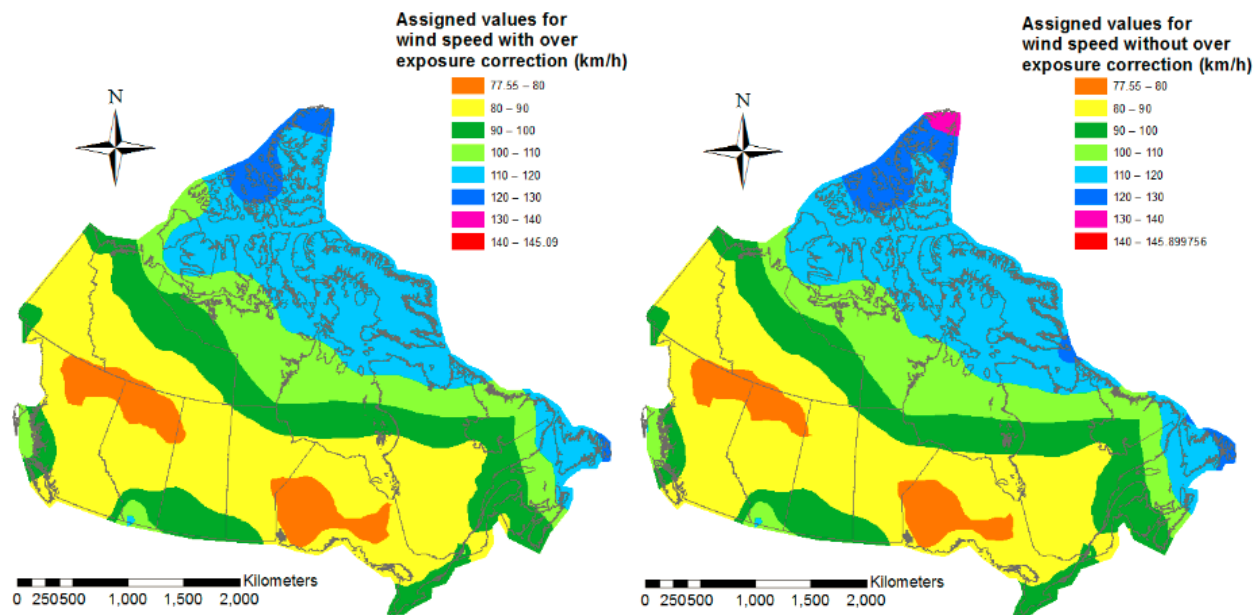
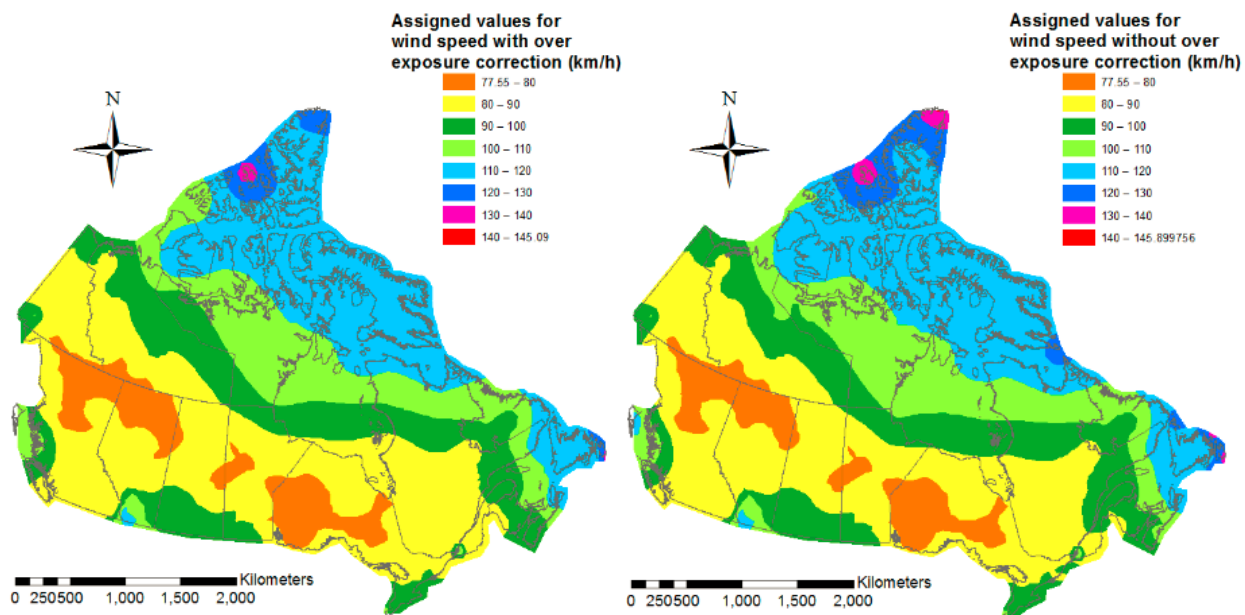
2.5 Effect of additional considerations on spatially interpolated wind hazard maps

If no additional constraints were to be considered, v_{AH-50} shown in Figures 2-11a or 2-11b could be adopted to represent the wind hazard and potentially used for code making. However, there were several additional considerations to assign the wind loads in the previous editions of NBCC. For example, the exposure correction factor can be less than unity due to over exposure (i.e., open water exposure at coastal regions); an open water exposure category is not currently considered in the NBCC-2010. If the open water exposure category is introduced in a future edition of NBCC, the results presented in the previous sections can be used directly. Otherwise, the exposure correction factor equal to one should be used for over exposed stations so the results to be consistent with the existing exposure categories specified in NBCC-2010. Also, a lower bound, v_{LB} , of 77.55 km/h which is used in the NBCC-2010. Therefore, using the value directly interpolating from v_{AH-50} obtained at the stations for locations specified in the NBCC-2010 may not be satisfactory. Also, the direct interpolation does not explicitly consider the proximity of a location to a meteorological station, and whether an exact or inexact interpolator is preferred. Although the exact interpolator leads to an estimated value to be the same as the observed value at a sample point, it may not be associated with the lowest root-mean-square-error (RMSE) obtained from the cross-validation analysis (Johnston et al. 2003; Ye et al. 2015). An inexact interpolator results in an estimated value differing from the known value at a sample point but could be associated with lowest RMSE obtained from the cross-validation analysis. The ordinary kriging can be an exact interpolator if the nugget equal to zero is used. Moreover, for a location tabulated in the NBCC table that is within a distance D from any meteorological stations, the use of v_{AH-50} for the station with the shortest distance to the location may be preferred if D is small.

Based on these considerations, maps are interpolated based on v_{AH-50} obtained using the ROI but considering the following additional criteria (Hong et al. 2014):

- 1) Use v_{AH-50} for the station with the shortest distance to the location if $D \leq 5$ km.
- 2) Use the maximum of the spatially interpolated value and the estimated v_{AH-50} for the station with the shortest distance to the location if $5 < D \leq 20$ km.
- 3) Use the interpolated value for the location if $20 < D \leq 50$ km,
- 4) The existing value shown in NBCC-2010 is adopted, if $D > 50$ km to a location,
- 5) v_{LB} is used if the estimate v_{AH-50} is less than v_{LB} .

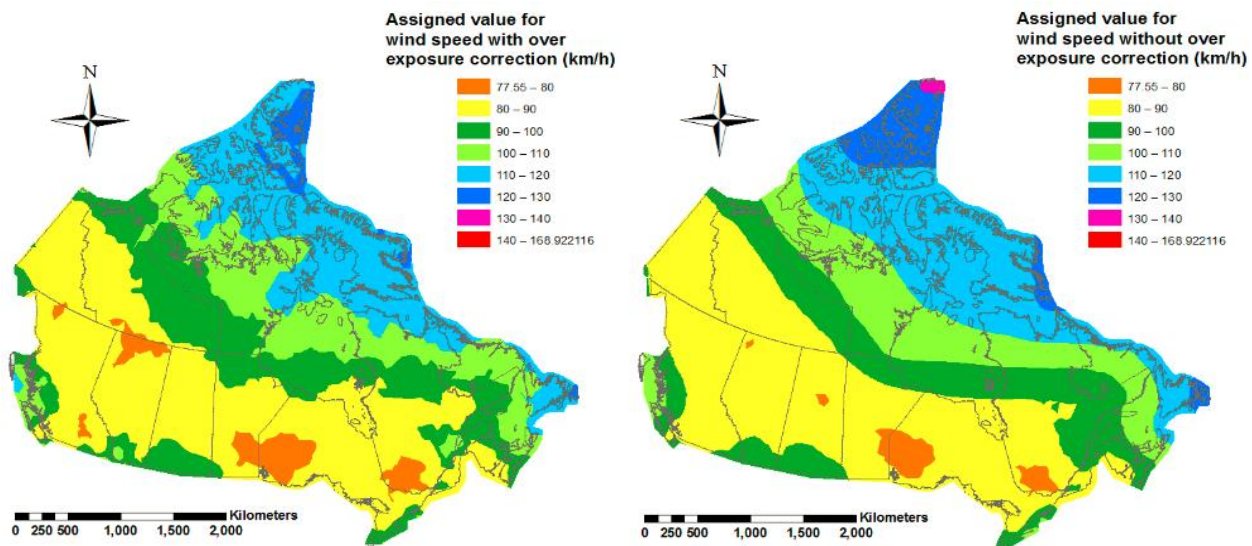
By considering the above requirements, sets of wind hazard maps are obtained and shown in Figure 2-13 for the case with $n_A \geq 20$ and Figure 2-14 for the case with $n_A \geq 10$. In all cases, the ROI approach was used with the Gumbel distribution. Comparison of the results shown in Figures 2-13a and 2-13b to those shown in Figures 2-13c and 2-13d, indicated that there are differences but not very large. This can be explained by noting that a degree of smoothing was already introduced in the estimated v_{AH-50} since they are estimated by using the ROI approach. Similar observations can be made by comparing the results shown in Figures 2-14a and 2-14b to those shown in Figure 2-14c and 2-14d.

a) With over exposure correction & nugget $\neq 0$.b) Without over exposure correction & nugget $\neq 0$.

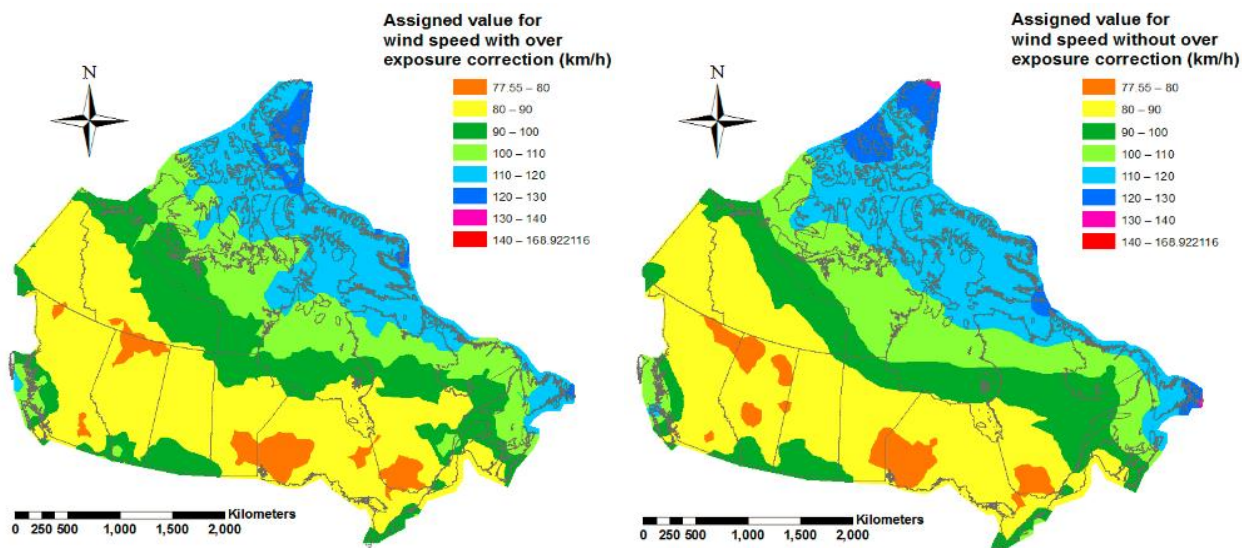
c) With over exposure correction & nugget = 0.

d) Without over exposure correction & nugget = 0.

Figure 2-13. Trends of the 50-year return period values based on the adopted criteria and applying the ordinary kriging technique without/with nugget equal to zero for the case with $n_A \geq 20$.



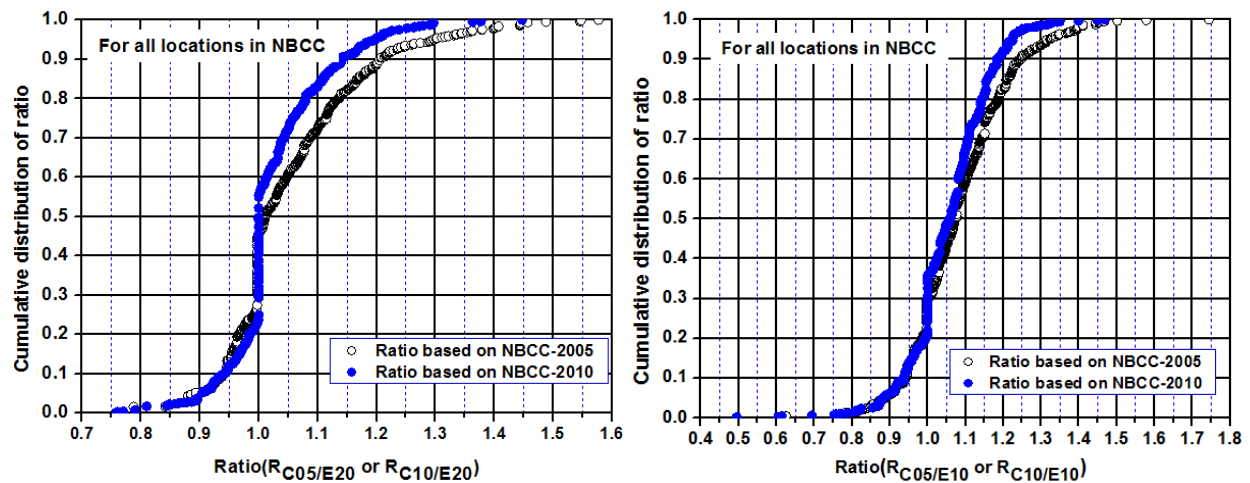
a) With over exposure correction & nugget $\neq 0$. b) Without over exposure correction & nugget $\neq 0$.



c) With over exposure correction & nugget = 0. d) Without over exposure correction & nugget = 0.

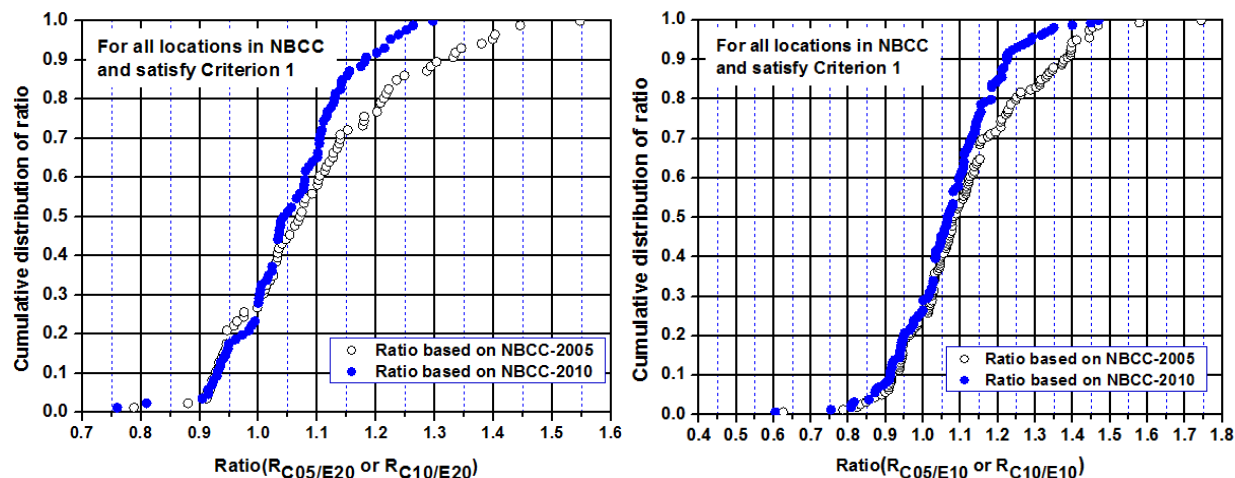
Figure 2-14. Trends of the 50-year return period values based on the adopted criteria and applying the ordinary kriging technique without/with nugget equal to zero for the case with $n_A \geq 10$.

To appreciate the differences between the estimated values shown in the plots presented in Figures 2-13 and 2-14 to those given in the NBCC-2005 and NBCC-2010, the ratio of the tabulated v_{AH-50} in the NBCC-2005 or NBCC-2010 to that inferred from Figure 2-13d or Figure 2-14d was calculated and shown in Figure 2-15. The symbol R with subscripts represents the ratio of the 50-year return period wind speed inferred from the code to that estimated in Figure 2-13d or 2-14d, where C05 and C10 indicate that the values are inferred from NBCC-2005 and NBCC-2010, respectively, and E10 and E20 indicate that the values are estimated for the case with $n_A \geq 10$ and the case with $n_A \geq 20$, respectively.



a) For the case with $n_A \geq 20$.

b) For the case with $n_A \geq 10$.



c) For the case with $n_A \geq 20$ & satisfy Criterion 1. d) For the case with $n_A \geq 10$ & satisfy Criterion 1.

Figure 2-15. Statistics of the estimated ratio the 50-year wind speed by considering the values inferred from the codes and the estimated values shown in Figure 2-13c and 2-14c: a) For the case with $n_A \geq 20$, b) For the case with $n_A \geq 10$, c) For the case with $n_A \geq 20$ & satisfy Criterion 1, and d) For the case with $n_A \geq 10$ & satisfy Criterion 1.

The figure showed that the ratio differs from unity for many locations. The concentration of $R_{C05/E10}$ and $R_{C10/E10}$ equal to one shown in Figures 2-15a and 2-15b is a direct consequence of Criterion 4. To better appreciate the ratios of $R_{C05/E10}$ and $R_{C10/E10}$ for locations that are within 5 km of a considered station, these values are plotted in Figures 2-15c and 2-15d, indicating that even locations that are within 5 km from any meteorological stations, the ratios differ from unity. This again suggest that the values tabulated in NBCC need to be scrutinized and updated.

2.6 Summary and conclusions

Wind records obtained from Environment Canada for approximately 1300 stations are processed. The processing includes the height and exposure adjustment so the processed wind records represent those for a standard height and exposure condition referred in the National

Building Code of Canada. It was identified that there are about 230 stations, each with more than 20 years of useable annual maximum wind speed (case with $n_A \geq 20$); and that there are about 580 stations, each with more than 10 years of useable annual maximum wind speed (case with $n_A \geq 10$).

The data are used to investigate the effect of small sample size on mapping the wind hazard for Canada and, the differences between the current wind hazard estimates to those inferred from the NBCC-2005 and NBCC-2010. For the investigation, both at-site analysis and the region of influence approach are employed, and the Gumbel as well as the generalized extreme value distributions are employed. It was concluded that:

- 1) The spatial trends of the estimated mean values of annual maximum wind speed, V_{AH} , for the two cases (i.e., $n_A \geq 20$ and $n_A \geq 10$) are similar except there are three patches of low mean values within the region where the mean is less than 50 km/h for the case with $n_A \geq 10$. There are differences in the spatial trends of the cov values for the two cases. This shows that the small sample size effect could be significant for the estimated cov, which is expected.
- 2) For the case with $n_A \geq 10$, the cov of V_{AH} varies from 0.05 to 0.30 with an average of 0.125. For the case with $n_A \geq 20$, the cov varies from 0.05 to 0.3 with an average of 0.138. This showed that the range of cov of V_{AH} for the case with $n_A \geq 10$ is similar to that for the case with $n_A \geq 20$. The smaller mean of cov value for the former is attributed to that there are many more stations with smaller cov values for the former than for the latter.
- 3) Based on the at-site analysis, the overall spatial trends of v_{AH} are similar for the cases with $n_A \geq 20$ and $n_A \geq 10$, except that the contours obtained for the case with $n_A \geq 20$ is smoother. However, the mapped wind hazard differs from those recommended in NBCC-2005 and NBCC-2010. This is partly attributed to the use of constant cov or constant ratio of the standard

deviation to the 30-year return period value of V_{AH} employed in developing the wind hazard in these editions of code.

- 4) Distribution fitting and the use of AIC criterion indicates that the Gumbel distribution for V_{AH} is preferable than the GEV distribution for approximately 70% of stations whether data from stations with $n_A \geq 10$ or $n_A \geq 20$ are considered. The estimated ratio of v_{AH-50} inferred from code to v_{AH-50} estimated based on the at-site analysis using the Gumbel distribution indicates that the ratio is within 0.95 to 1.05 for only 30% of the locations, and within 0.9 to 1.1 for 60% of the locations, quantifying the discrepancy.
- 5) The mapped wind hazard based on v_{AH-50} estimated using the ROI approach is not very sensitive to whether the Gumbel distribution or the GEVD distribution is employed, but is sensitive to whether the case with $n_A \geq 10$ or the case with $n_A \geq 20$ is considered. Therefore, to avoid possible small sample size effect, it is suggested the case with $n_A \geq 20$ to be employed for wind hazard mapping.

References

- Akaike, H. 1974. A new look at the statistical model identification. *IEEE Transactions on Automatic Control*, 19 (6), 716–723.
- Bartlett, F.M., Hong, H.P. and Zhou, W. 2003. Load factor calibration for the proposed 2005 edition of the National Building Code of Canada: Companion-action load combinations, *Canadian Journal of Civil Engineering*, 30 (2) 440-448.
- Boyd, D.W. 1967. Variations in air density over Canada. National Research Council of Canada, Division of Building Research, Technical Note No. 486.
- Burn, D.H. 1990. Evaluation of regional flood frequency analysis with a region of influence approach, *Water Resources Research*, 26(10): 2257-2265.
- Castillo, E. (1988). *Extreme Value Theory in Engineering*, Academic Press, New York.
- Coles, S. 2001. *An introduction to statistical modeling of extreme values*. Springer, London, UK.
- ESDU (2002). Computer program for wind speeds and turbulence properties: flat or hilly sites in terrain with roughness changes. Engineering Science Data Unit (ESDU) Data Item No. 01008.

- ESRI 2011. ArcGIS Desktop: Release 10. Redlands, CA: Environmental Systems Research Institute.
- Fovell, R.G. and Fovell, M.Y.C. 1993. Climate zones of the conterminous United States defined using cluster analysis. *Journal of Climate* 6, 2103–2135.
- Frank, H. 2001. Extreme winds over Denmark from the NCEP/NCAR reanalysis. Technical Report Risø-R-1238(EN), Risø National Laboratory.
- Hastie, T., Tibshirani, R. and Friedman, J.H. 2001. The elements of statistical learning: data mining, inference, and prediction, Springer New York.
- Holmes, J.D. and Moriarty, W.W. 1999. Application of the generalized Pareto distribution to extreme value analysis in wind engineering. *Journal of Wind Engineering and Industrial Aerodynamics*, **83**: 1-10.
- Hong, H.P. and Ye, W. 2014. An analysis of ground snow loads for Canada using snow depth records, *Natural Hazards*, September, Vol.73, No.2: 355–371.
- Hong, H.P., Li, S.H. and Mara, T.G. 2013. Performance of the generalized least-squares method for the Gumbel distribution and its application to annual maximum wind speeds. *Journal of Wind Engineering and Industrial Aerodynamics*, Vol.119: 121–132.
- Hong, H.P., Mara, T.G., Morris, R. Li, S.H. and Ye, W. 2014. Basis for recommending an update of wind velocity pressures in the 2010 National Building Code of Canada, *Canadian Journal of Civil Engineering*, 41(3): 206-221.
- Hosking, J. 1990. L-moments: Analysis and estimation of distributions using linear combinations of order statistics. *Journal of the Royal Statistical Society B*, **52**: 105–124.
- Hosking, J.R.M. and Wallis, J.R. (1997). *Regional frequency analysis: an approach based on L-moments*, Cambridge University Press, Cambridge, UK.
- Johnston, K., Ver Hoef J.M., Krivoruchko, K. and Lucas, N. (2003) ArcGIS 9, Using ArcGIS Geostatistical Analyst, Redlands, CA: Environmental Systems Research Institute.
- Kasperski, M. 2002. A new wind zone map of Germany. *Journal of Wind Engineering and Industrial Aerodynamics*, **90**: 1271–1287.
- Kohonen, T. (2001). *Self-Organizing Maps*. Berlin-Heidelberg, Springer.
- Kruger, A.C., Goliger, A.M., Retief, J.V. and Sekele, S.S. 2012. Clustering of extreme winds in the mixed climate of South Africa, *Wind and Structures*, Vol. 15: 87-109.
- Lieblein, J. 1974. Efficient methods of extreme-value methodology, report NBSIR 74-602, National Bureau of Standards, Washington.
- Lin, G.-F. and Chen L.-H. 2006. Identification of homogeneous regions for regional frequency analysis using the self-organizing map, *Journal of Hydrology* 324: 1–9.
- Lloyd, E.H., 1952. Least-squares estimation of location and scale parameters using order statistics. *Biometrika* 39, 88–95.
- Mara, T.G., Hong, H.P. and Morris, R.J. (2013) Effect of corrections to historical wind records on

- estimated extreme wind speeds, CSCE-2013 conference, Montreal, Canada.
- Martin, E.S. and Stedinger, J.R. 2000. Generalized maximum-likelihood generalized extreme-value quantile estimators for hydrologic data, *Water Resource Research*, **36**: 737-744.
- Miller, C.A. 2003. A once in 50-year wind speed map for Europe derived from mean sea level pressure measurements, *Journal of Wind Engineering and Industrial Aerodynamics*, 91, 1813-1826.
- Mo, H.M., Hong, H.P. and Fan, F. 2015. Estimating wind hazard for China using surface observations and reanalysis data, *J. of Wind Engineering & Aerodynamics Industry*, Vol.143:19-33.
- Morris, R. 2009. Wind interim report on the updating of the design winds speeds in the National Building Code of Canada for the task Group on climatic loads, National Research Council of Canada, Ottawa, Canada.
- NRCC. 2005. National Building Code of Canada. Institute for Research in Construction, (NRCC) National Research Council of Canada, Ottawa, Ontario.
- NRCC. 2010. National Building Code of Canada. Institute for Research in Construction, National Research Council of Canada, Ottawa, Ontario.
- Peterka, J. and Shahid, S. 1998. Design gust wind speeds in the United States. *Journal of Structural Engineering*, **124**: 207–214.
- Sacré, C. 2002. Extreme wind speed in France: the '99 storms and their consequences. *Journal of Wind Engineering and Industrial Aerodynamics*, **90**: 1163–1171.
- Wan, H., Wang, X.L. and Swail, V.R. 2010. Homogenization and trend analysis of Canadian near-surface wind speeds. *Journal of Climate*, 23: 1209-1225.
- Ye, W., Hong, H.P. and Wang, J.F. (2015) Comparison of spatial interpolation techniques for extreme wind speeds over Canada, *Journal of Computing Civil Engineering*, ASCE, Vol. 29(6), 04014095.
- Yip, T. and Auld, H. 1993. Updating the 1995 National building code of Canada wind pressures. In *Proceedings of the Electricity '93 Engineering and Operating Division Conference*. Canadian Electrical Association, Montréal, Canada.
- Yip, T., Auld, H. and Dnes, W. 1995. Recommendations for updating the 1995 National building code of Canada wind pressures. In *Proceedings of the 9th International Conference on Wind Engineering*. International Association for Wind Engineering, New Delhi, India.

Chapter 3 Codification of Wind Load for Improved Reliability Consistency over Canadian Sites

3.1 Introduction

The 2005 version of the National Building Code of Canada (NBCC) (NRCC 2005) adopts the 50-year return period value of the annual maximum hourly-mean wind speed to calculate the reference wind velocity pressure (i.e., nominal wind load) and a wind load factor of 1.4. These suggested factored design wind load is calibrated for a (50-year) target reliability index of 3.0 (i.e., failure probability of 1.35×10^{-3}) (Bartlett et al. 2003a, b). The reference wind velocity pressure and the wind load factor remained the same in the newer versions of the NBCC (NRCC 2010, 2015). For the calibration of the factored design wind load, commonly employed target reliability-based calibration procedure and the first order reliability method (Ellingwood et al. 1980; Madsen et al. 2006) are employed. The annual maximum hourly-mean wind speed, V_{AH} , is modeled as a Gumbel variate with a typical coefficient of variation (cov) of 0.134.

The consideration of Gumbel distribution for V_{AH} is justified and supported by several studies (Yip et al. 1995; Peterka and Shahid, 1998; Frank, 2001), although other probabilistic models are also considered in the literature. These include the generalized extreme value distribution (GEVD) (Jenkinson, 1955) and the generalized Pareto distribution (GPD) (Pickands 1975) (Holmes and Moriarty 1999; Kasperski 2002; Miller 2003; Hong and Ye 2014). Using the surface wind observations from Canadian sites, it was observed (Hong et al. 2014) that the Gumbel distribution is preferable to the generalized extreme value distribution (GEVD) for 70% of considered stations if the Akaike information criterion (AIC) (Akaike 1974) is adopted. In their analysis, V_{AH} values from 235 meteorological stations, each with 20 years of useable data (except 3 stations) are

considered. Their observation is also supported by the results shown in Chapter 2. The typical cov value of 0.134 is in agreement with the average cov value estimated using the recorded surface wind observations, although the cov value is geographically varying and ranges from 0.05 to 0.3 (Hong et al. 2014). The range of cov value is also confirmed in Chapter 2 by using surface wind observations from more than 500 stations, each with at least 10 years of useable data. The variation of the cov of V_{AH} can significantly impact the notional reliability of codified design that is governed by the wind load or its combination with other loads (Hong et al. 2016) partly because the wind load is proportional to the square of V_{AH} , resulting in that the cov of the wind load equals about twice of the cov of V_{AH} if all other variables involved in evaluating the wind force are treated deterministically. Moreover, although the use of a specified return period value of the wind velocity pressure and a calibrated wind load factor given a cov of V_{AH} can lead to a target reliability, such a set of the specified value and wind load factor is not unique. In fact, if the resulting factored design wind loads for different sets of specified value and wind load factor are the same, the same target reliability can be achieved. In addition, it is noted that the ASCE-7-10 adopts a wind load factor of 1.0 with the design wind speed estimated using a return period, T , of 700 years for the strength design of Category II structures (Vickery et al. 2010; Cook et al. 2011).

In this study, the differences in the implied notional reliability index for structures designed according to the current design code is examined by considering the spatially varying cov of V_{AH} . It is shown that the differences can be reduced if the geographically varying return period is used to assign the design wind velocity pressure and with wind load factor of 1.0. The reliability-based calibration takes into account the target reliability index implied by using the current design code for typical cov value. An equation to calculate the required return period as a function of cov of V_{AH} is developed based on the calibration results by considering ranges of combinations of

permanent, and wind loads. The required (factored) design wind velocity pressure map for Canada is also developed using the preferred probabilistic model of the annual maximum wind speed for Canadian sites.

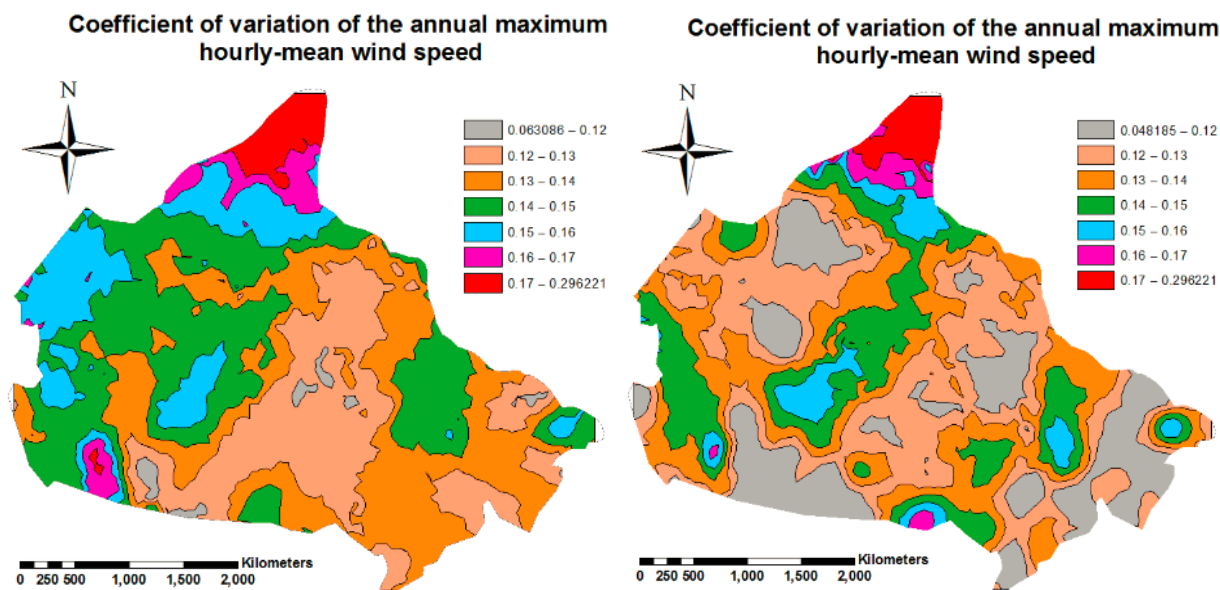
3.2 Probabilistic models adopted for the calibration

A review of previous studies focused on the reference wind pressure for earlier versions of NBCC carried out by Hong et al. (2014) indicate that V_{AH} is frequently considered as a Gumbel variate. They also obtained surface wind observations at 1224 locations from Environment Canada. After processing the data, and carrying out exposure and height adjustment, an extreme value analysis was carried out by considering surface wind observations at a station with the number of years of useable data, n_A , at least equal to 20 (except 3 stations). For the analysis, both the Gumbel distribution and GEVD are adopted and several commonly employed fitting methods are considered. From the at-site analysis, and the application of AIC, it was concluded that the Gumbel distribution is preferred at least in 69.5% of the cases. The use of data from stations with $n_A \geq 20$ is aimed at reducing the small sample size effect in estimating the return period value of V_{AH} . A disadvantage of treating the data in such a manner is that the valuable information from a station with $n_A < 20$ is neglected; the density of the spatial distribution of the potentially available stations with valuable wind records is reduced for wind hazard mapping.

To overcome this, the use of the at-site analysis and region of influence (Burn 1990) was considered in Chapter 2 by using data from a station with $n_A \geq 10$. Again, both the Gumbel distribution and the GEVD are considered. In this case, the use of the AIC indicates that that the Gumbel distribution for V_{AH} is preferred for approximately 73% of stations, which is slightly greater than 70% mentioned earlier for the case with $n_A \geq 20$. From the at-site analysis, it was

concluded that the spatial trends of the estimated mean values of V_{AH} for $n_A \geq 20$ and for $n_A \geq 10$ are similar except there are small patches of low mean values within the region where the mean is less than 50 km/h for the case with $n_A \geq 10$. There are some differences in the spatial trends of the cov values for the two cases, which are partly attributed to small sample size effects. For easy reference, the cov values are re-plotted in Figure 3-1. The ranges of the cov values in both plots are within 0.05 and 0.30. The estimated arithmetic mean of the cov for Figure 3-1a equals 0.138 which differs 0.125 that is obtained from Figure 3-1b. This large difference could be due to that there are many stations located in the sites with low cov value for the case with $n_A \geq 10$. To investigate this further and to have a better appreciation of the central tendency of cov of V_{AH} over Canada, an area-weighted mean of cov of V_{AH} is calculated, where the area associated with each station is defined using the Voronoi polygon (Aurenhammer,1991) as shown in Figure 3-2. The estimated area-weighted mean of cov of V_{AH} equals 0.141 for the case with $n_A \geq 20$, and 0.135 for the case with $n_A \geq 10$. Therefore, it seems appropriate to consider that the typical cov of V_{AH} equals 0.138.

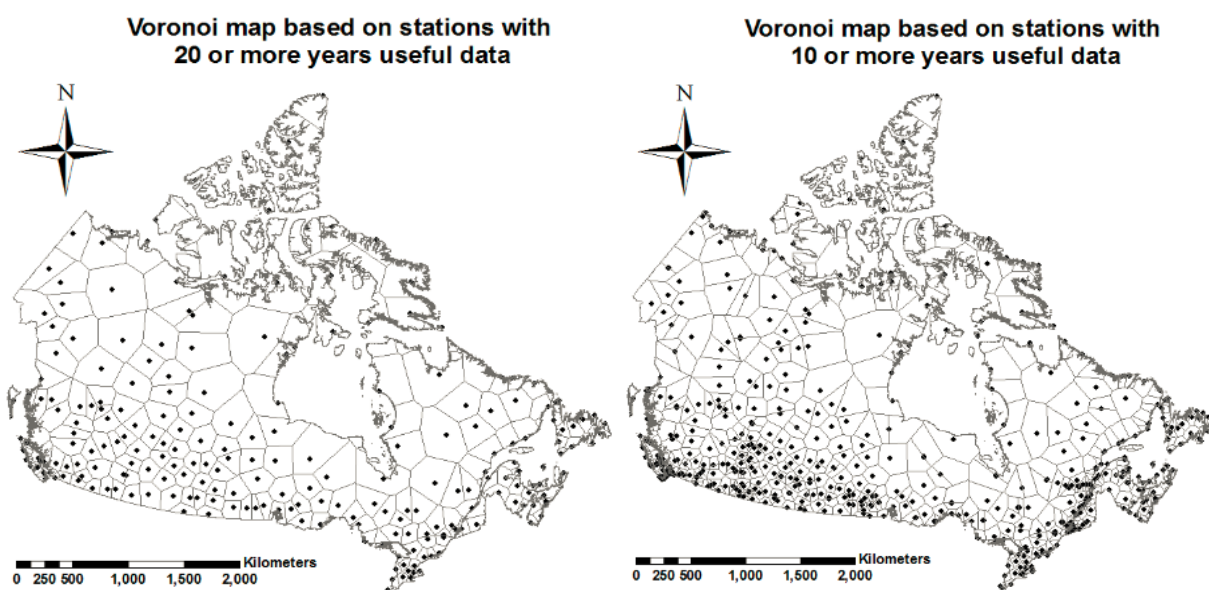
If the ROI approach is employed (see Chapter 2), the results indicates that the estimated return period value of V_{AH} is not very sensitive to whether the Gumbel distribution or the GEVD distribution is employed, but is sensitive to whether the case with $n_A \geq 10$ or the case with $n_A \geq 20$ is considered. To reduce small sample size effect, it was recommended that the data with $n_A \geq 20$ is to be considered for wind hazard mapping by using the ROI approach and the Gumbel distribution. The mean and cov of V_{AH} in this case is illustrated in Figure 3-3. Note that the mean of V_{AH} is not affected by whether the at-site analysis or ROI approaches are employed, while this is not the case for the cov. Based on the results shown in Figure 3-3b, the minimum, maximum and the area-weighted mean of cov of V_{AH} are 0.119, 0.285 and 0.141, respectively.



a) for the case with $n_A \geq 20$.

b) for the case with $n_A \geq 10$

Figure 3-1. Coefficient of variation of the annual maximum hourly-mean wind speed: a) for the case with $n_A \geq 20$ and b) for the case with $n_A \geq 10$.



a) for the case with $n_A \geq 20$.

b) for the case with $n_A \geq 10$

Figure 3-2. Voronoi polygon associated with each station for the estimation of area-weighted mean of cov of V_{AH} : a) for the case with $n_A \geq 20$ and b) for the case with $n_A \geq 10$.

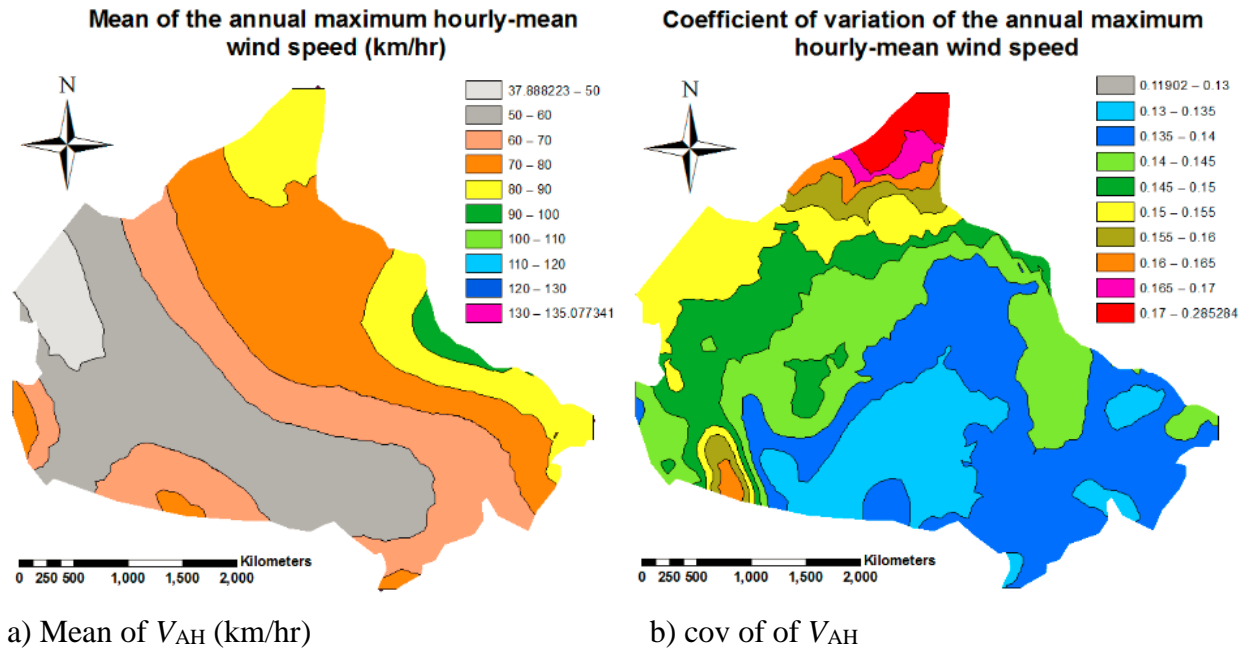


Figure 3-3. Mean and coefficient of variation of the annual maximum hourly-mean wind speed: a) Mean of V_{AH} (km/hr), and b) cov of of V_{AH} (inferred from the analysis results obtained from the ROI approach, see Chapter 2).

Besides of the probabilistic model for the annual maximum wind speed, it is considered that the ratio of the wind load effect to the nominal wind load effect on a structural member can be expressed as,

$$W = ZW_n \times (V_{AH} / v_T)^2 \quad (3.1)$$

where Z is an uncertain transformation factor that takes into account the uncertainty in the exposure coefficient, the external pressure coefficient, and the gust factor, and code specified values, W_n is the reference (or nominal) wind load effect on the structural member calculated according to the design code, and v_T denote the T -year return period value of V_{AH} . Z is considered to be a lognormal variate with mean of 0.68 and cov of 0.22 (Bartlett et al. 2003a, b).

Following previous calibration analysis, it is considered that the dead load effect can be modelled as normal variate with a typical mean to nominal ratio of 1.05 and a cov of 0.10, and that the member resistance for structural steel can be modelled as a lognormal variate with a typical mean to nominal ratio of 1.17 and a cov of 0.108.

3.3 Calibrating design wind load for spatially varying extreme wind characteristics

3.3.1 Limit state function and analysis procedure

The procedure for reliability-based design code calibration is frequently carried out for a selected target reliability index and structural member behaviour; it is well described in the literature (Ellingwood et al. 1980, Madsen et al. 2006). For designs that satisfy the minimum design strength requirement and are governed by dead load combined with the wind load, the limit state function $g(x_T)$, can be written as (Hong et al. 2016),

$$g(v_T) = \frac{1}{\gamma_R} X_R - \frac{1}{1 + R_{W/D}} \left(\frac{X_D}{\alpha_D} + R_{W/D} \frac{Z(V_{H50} / v_T)^2}{\alpha_W} \right) \quad (3.2)$$

where γ_R is the resistance factor; α_D is the dead load factor; α_W is the wind load factor; $R_{W/D}$ is the ratio of the factored design wind load $\alpha_W W_n$ to the factored design dead load $\alpha_D D_n$; $X_R = R/R_n$; R_n is the nominal resistance; $X_D = D/D_n$; D_n is the nominal dead load and V_{H50} is the 50-year maximum hourly-mean wind speed rather than the annual maximum hourly mean wind speed. According to the present applicant Canadian design codes, $\gamma_R = 0.9$ for structural steel, $\alpha_D = 1.25$, $\alpha_W = 1.40$ and $T = 50$ years (CSA S16 2001, NRCC 2010).

The failure probability for a service period of 50 years, denoted by P_f can be evaluated using the efficient first order reliability method (Madsen et al. 2006). In such a case,

$$P_f = \Phi(-\beta_{50}) \quad (3.3)$$

where $\Phi(\bullet)$ denotes the standard normal distribution function, and the reliability index of the design structural member for 50-year service period, β_{50} , is estimated by solving,

$$\left\{ \begin{array}{l} \beta_{50} = \min \left(\sum_{i=1}^4 y_i^2 \right)^{1/2} \\ \text{Subjected to:} \\ \frac{1}{\gamma_R} x_R - \frac{1}{1 + R_{W/D}} \left(\frac{x_D}{\gamma_D} + R_{W/D} \frac{z (v_{H50} / v_T)^2}{\gamma_W} \right) = 0 \end{array} \right. \quad (3.4)$$

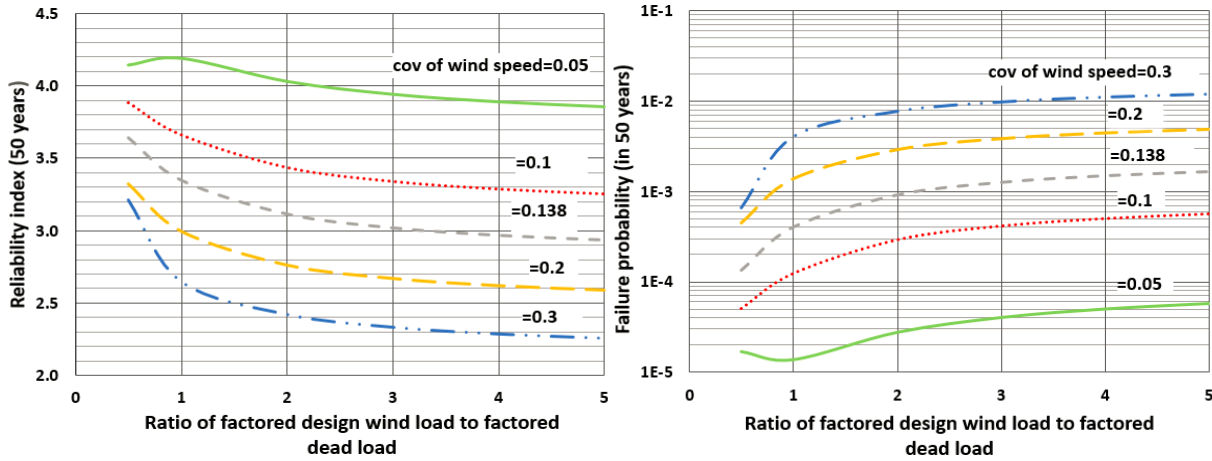
in which $(x_R, x_D, z, u) = (F_{X_R}^{-1}(\Phi(y_1)), F_{X_D}^{-1}(\Phi(y_2)), F_Z^{-1}(\Phi(y_3)), F_{V_{H50}}^{-1}(\Phi(y_4)))$; $F_{X_R}^{-1}(\bullet)$, $F_D^{-1}(\bullet)$, $F_Z^{-1}(\bullet)$ and $F_{V_{AH50}}^{-1}(\bullet)$ denote the inverse probability distributions of X_R , X_D , Z and V_{H50} respectively; and y_i , $i = 1, \dots, 4$, are values of independent standard normal variates Y_i .

3.3.2 Calibration results and wind speed contour map for reliability consistent design

Based on the formulation and analysis procedure presented in the previous section, reliability analysis is carried out for a range of cov values. The estimated β_{50} values for a range of cov values are shown in Figure 3-4a with corresponding P_f presented in Figure 3-4b.

Note that for the cov of V_{AH} , v_v , equal to the typical value of 0.138, the use of $T = 50$ years and $\alpha_W = 1.40$ is equivalent to the use of $T = 500$ years and $\alpha_W = 1.0$; and that the use of higher return period with $\alpha_W = 1.0$ is preferred to improve reliability consistency (Hong et al. 2016).

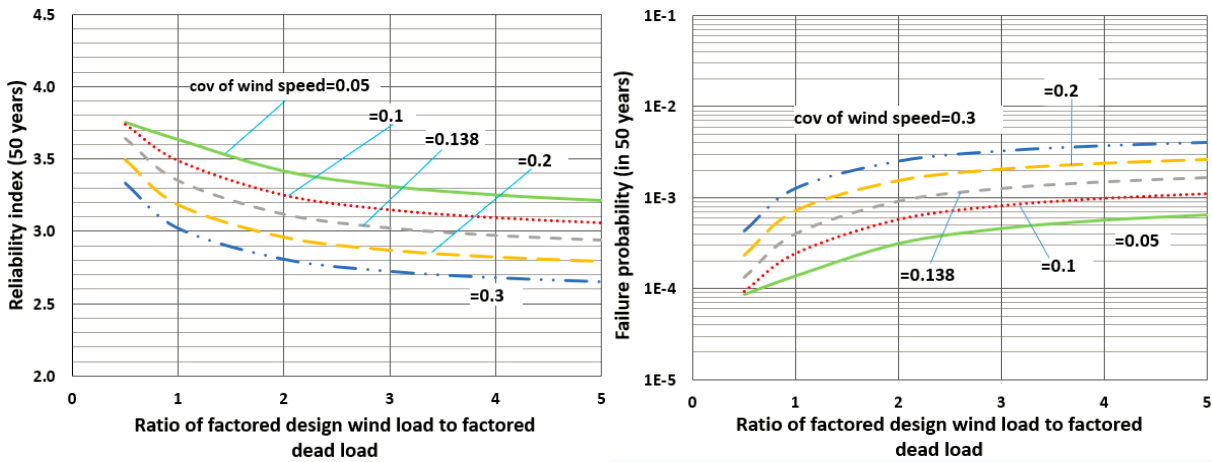
To illustrate this, analysis carried out for Figure 3-4 is repeated but using $T = 500$ years and $\alpha_W = 1.0$. The obtained results are shown in Figure 3-5.



a) Estimated β_{50} .

b) Estimated P_f .

Figure 3-4. Estimated β_{50} and P_f for $\alpha_W = 1.40$ and using $T = 50$ years to assigning the reference wind velocity pressure: a) Estimated β_{50} and b) Estimated P_f .



a) Estimated β_{50} .

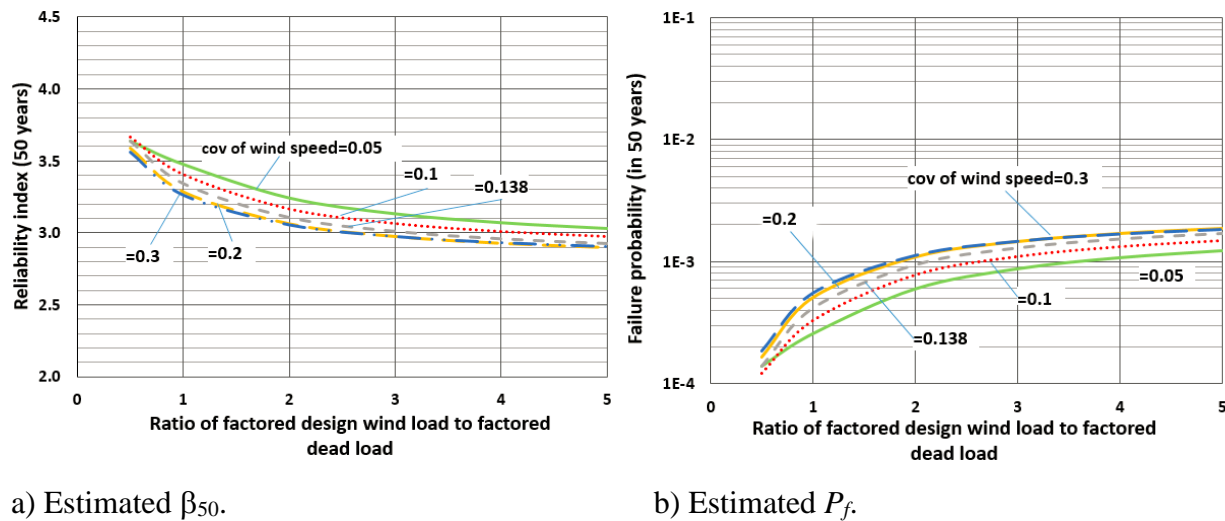
b) Estimated P_f .

Figure 3-5. Estimated β_{50} and P_f for $\alpha_W = 1.0$ and using $T = 500$ years to assigning the reference wind velocity pressure: a) Estimated β_{50} and b) Estimated P_f .

To further improve the reliability-consistency and ensure that the β_{50} values for sites with different v_V values are close to those for $v_V = 0.138$, the analysis of the required T is carried out by trial and error. The obtained T values are used to obtain the following empirical equation,

$$T = 75 + 3000 \times v_V \quad (3.5)$$

By using this suggested return period for assigning v_T , and $\alpha_W = 1.0$, the estimated β_{50} values for v_V ranging from 0.05 to 0.3 are shown in Figure 3-6. Comparison of the results presented in Figures 3-4 to 3-6 indicates that the use of the geographically (i.e., v_V) dependent return period to assign the reference wind speed or reference wind velocity pressure for the design under wind load, the reliability consistency is much improved.



a) Estimated β_{50} .

b) Estimated P_f .

Figure 3-6. Estimated β_{50} and P_f for $\alpha_W=1.0$ and using the return period given in Eq. (3.5) to assign v_T : a) Estimated β_{50} and b) Estimated P_f .

Therefore, if the use of T dictated by Eq. (3.5) is adopted for code making, by using the statistics of the annual maximum hourly-mean wind speed shown Figure 3-3, a wind speed map for

reliability consistent design is developed and shown in Figure 3-7. For the developed design wind load, the lower bound value of $\sqrt{1.4} \times 77.55$ ($= 91.8$ km/hr) that is consistent with that employed to develop the wind load criterion in NBCC (2010) is adopted. Note that by using Eq. (3.5) the calculated T equals 432 years for $v_V = 0.119$ and 930 years for $v_V = 0.285$ (for the range of v_V see Figure 3-3).

To see the differences between the suggested factored design wind load and those suggested in NBCC (2005, 2010), ratios of the factored design wind load in the code to that suggested by using Figure 3-7 with $\alpha_W = 1.0$ is calculated and shown in Figure 3-8. The results presented in the figure indicates that the ratio ranges from 0.8 to 1.5 if the NBCC-2005 is considered and from 0.8 to 0.14 if the NBCC-2010 is considered. However, for majority of locations the ratio is close to unity and within 0.9 to 1.1. Therefore, if the suggested design wind load is considered, significant change occurs only at localized sites.

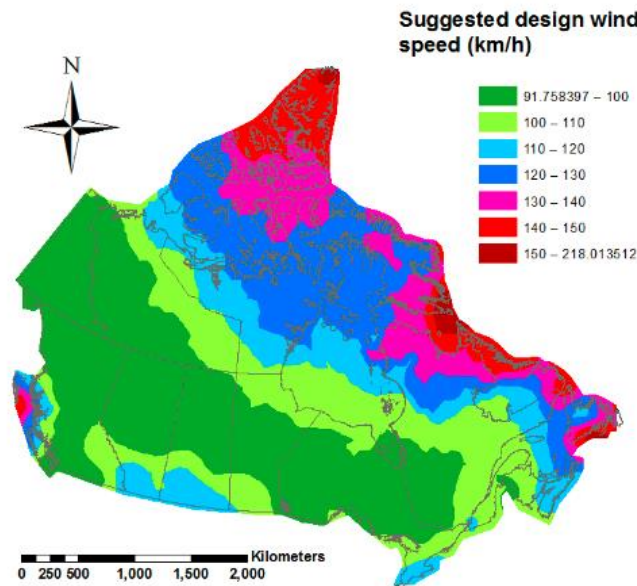


Figure 3-7. Suggested design wind speed considering the return period shown in Eq. (3.5).

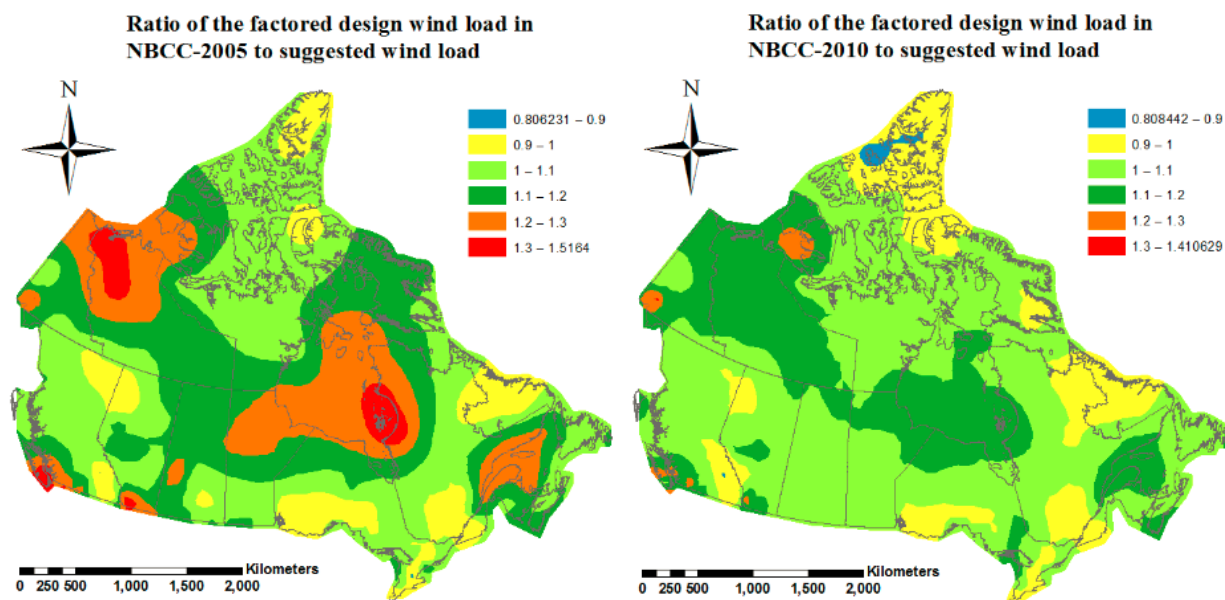


Figure 3-8. Ratio of factored design wind load to the suggested factored design wind load

3.4 Conclusions

We summarized newly developed probabilistic characteristics of wind hazard. One of the essential observation is that there is significant geographic variation of the coefficient of variation (cov) of the annual maximum wind speed. This variation results in the inconsistency in the reliability indices of structures placed at different sites and designed according to current structural design code.

To improve reliability-consistency, it is suggested that the use of 50-year return period value of the wind velocity pressure and a wind load factor of 1.4 is to be replaced by 500-year return period value of the wind velocity pressure and a wind load factor of 1.0.

To further improve the reliability-consistency, a somewhat bolder step is to implement the wind load based on the geographical location (or cov) dependent return period suggested in this study

(see Eq. (3.5)). Ready to use design wind speed based on such an approach is provided (Figure 3-6).

References

- Akaike, H. 1974. A new look at the statistical model identification. *IEEE Transactions on Automatic Control*, 19 (6), 716–723.
- Aurenhammer, F. 1991. A survey of a fundamental geometric data structure.
- Bartlett, F.M., Hong, H.P. and Zhou, W. 2003. Load factor calibration for the proposed 2005 edition of the National Building Code of Canada: Companion-action load combinations, *Canadian Journal of Civil Engineering*, 30 (2) 440-448.
- Bartlett, F.M., Hong, H.P. and Zhou, W. 2003. Load factor calibration for the proposed 2005 edition of the National Building Code of Canada: Statistics of loads and load effects, *Canadian Journal of Civil Engineering*, 30 (2) 429-439.
- Burn D.H. 1990. Evaluation of regional flood frequency analysis with a region of influence approach. *Water Resources Research*; 26(10): 2257-2265.
- Canadian Standards Association. 2001. "CAN/CSA–S16. 1 Limit States Design of Steel Structures." Mississauga, Ontario.
- Cook R., Griffis L., Vickery P. and Stafford E. 2011. ASCE 7-10 wind loads. In *Proceedings of the 2011 Structures Congress*, ASCE, Las Vegas, NV.
- Ellingwood B., Galambos T.V., MacGregor J.G. and Cornell C.A. 1980. Development of a probability based load criterion for American national standard A58. *Nat. Bureau of Standards Special Pub. No. 577*.
- Frank, H. 2001. Extreme winds over Denmark from the NCEP/NCAR reanalysis. *Technical Report Risø-R-1238(EN)*, Risø National Laboratory.
- Holmes, J.D. and Moriarty, W.W. 1999. Application of the generalized Pareto distribution to extreme value analysis in wind engineering. *Journal of Wind Engineering and Industrial Aerodynamics*, **83**: 1-10.
- Hong H.P., Mara T.G., Morris R., Li S.H. and Ye, W. 2014. Basis for recommending an update of wind velocity pressures in the 2010 National Building Code of Canada, *Canadian Journal of Civil Engineering*, March, Vol. 41, No.3: 206-221.
- Hong, H. P. and Ye, W. 2014. Estimating extreme wind speed based on regional frequency analysis. *Structural Safety*, 47, 67-77.
- Hong, H. P., Ye, W. and Li, S. H. 2016. Sample size effect on the reliability and calibration of design wind load. *Structure and Infrastructure Engineering*, 12(6), 752-764.

- Jenkinson, A. F. 1955. The frequency distribution of the annual maximum (or minimum) values of meteorological elements. *Quarterly Journal of the Royal Meteorological Society*, Volume 81, Issue 348, pages 158–171.
- Kasperski, M. 2002. A new wind zone map of Germany. *Journal of Wind Engineering and Industrial Aerodynamics*, **90**: 1271–1287.
- Madsen H.O., Krenk S. and Lind N.C. 2006. *Methods of structural safety*. Courier Corporation.
- Miller, C.A. 2003. A once in 50-year wind speed map for Europe derived from mean sea level pressure measurements, *Journal of Wind Engineering and Industrial Aerodynamics*, 91, 1813-1826.
- NRCC. 2005. *National Building Code of Canada*. Institute for Research in Construction, (NRCC) National Research Council of Canada, Ottawa, Ontario.
- NRCC. 2010. *National Building Code of Canada*. Institute for Research in Construction, National Research Council of Canada, Ottawa, Ontario.
- Peterka, J. and Shahid, S. 1998. Design gust wind speeds in the United States. *Journal of Structural Engineering*, **124**: 207–214.
- Pickands III, J. 1975. Statistical inference using extreme order statistics. *The Annals of Statistics* Vol. 3, No. 1 (Jan., 1975), pp. 119-131
- Vickery P.J., Wadhera D. Galsworthy J., Peterka, J.A., Irwin, P.A. and Griffis, L.A. 2010. Ultimate wind load design gust wind speeds in the United States for use in ASCE-7. *Journal of Structural Engineering*, ASCE, 136(5), 613-625.
- Yip, T., Auld, H. and Dnes, W. 1995. Recommendations for updating the 1995 National building code of Canada wind pressures. In *Proceedings of the 9th International Conference on Wind Engineering*. International Association for Wind Engineering, New Delhi, India.

Chapter 4 Conclusions and Recommendations for future work

4.1 Summary and conclusions

The summary and main conclusions are already included at the end of Chapters 2 and 3.

They are repeated below:

- (1) The spatial trends of the estimated mean values of annual maximum wind speed, V_{AH} , for the two cases (i.e., $n_A \geq 20$ and $n_A \geq 10$) are similar except there are three patches of low mean values within the region where the mean is less than 50 km/h for the case with $n_A \geq 10$. There are differences in the spatial trends of the cov values for the two cases. This shows that the small sample size effect could be significant for the estimated cov, which is expected.
- (2) For the case with $n_A \geq 10$, the cov of V_{AH} varies from 0.05 to 0.30 with an average of 0.125. For the case with $n_A \geq 20$, the cov varies from 0.05 to 0.3 with an average of 0.138. This showed that the range of cov of V_{AH} for the case with $n_A \geq 10$ is similar to that for the case with $n_A \geq 20$. The smaller mean of cov value for the former is attributed to that there are many more stations with smaller cov values for the former than for the latter.
- (3) Based on the at-site analysis, the overall spatial trends of v_{AH} are similar for the cases with $n_A \geq 20$ and $n_A \geq 10$, except that the contours obtained for the case with $n_A \geq 20$ is smoother. However, the mapped wind hazard differs from those recommended in NBCC-2005 and NBCC-2010. This is partly attributed to the use of constant cov or constant ratio of the standard deviation to the 30-year return period value of V_{AH} employed in developing the wind hazard in these editions of code.

- (4) Distribution fitting and the use of AIC criterion indicates that the Gumbel distribution for V_{AH} is preferable than the GEV distribution for approximately 70% of stations whether data from stations with $n_A \geq 10$ or $n_A \geq 20$ are considered. The estimated ratio of v_{AH-50} inferred from code to v_{AH-50} estimated based on the at-site analysis using the Gumbel distribution indicates that the ratio is within 0.95 to 1.05 for only 30% of the locations, and within 0.9 to 1.1 for 60% of the locations, quantifying the discrepancy.
- (5) The mapped wind hazard based on v_{AH-50} estimated using the ROI approach is not very sensitive to whether the Gumbel distribution or the GEVD distribution is employed, but is sensitive to whether the case with $n_A \geq 10$ or the case with $n_A \geq 20$ is considered. Therefore, to avoid possible small sample size effect, it is suggested the case with $n_A \geq 20$ to be employed for wind hazard mapping.
- (6) There is significant geographic variation of the coefficient of variation (cov) of the annual maximum wind speed. This variation results in the inconsistency in the reliability indices of structures placed at different sites and designed according to current structural design code.
- (7) To improve reliability-consistency, it is suggested that the use of 50-year return period value of the wind velocity pressure and a wind load factor of 1.4 is to be replaced by 500-year return period value of the wind velocity pressure and a wind load factor of 1.0.
- (8) To further improve the reliability-consistency, a somewhat bolder step is to implement the wind load based on the geographical location (or cov) dependent return period suggested in this study (see Eq. (3.5)). Ready to use design wind speed based on such an approach is provided (Figure 3-6).

4.2 Recommendations for future work

Several tasks can be carried out to enhance and support the conclusions drawn from this investigations. These include:

- 1) The use of the region of influence approach depends on the subjectively selected parameters. Therefore, it would be desirable to explore potential improvement of the approach, although how exact this can be done is not clear at present.
- 2) The calibration carried out considered only the dead and wind load. The analysis by also including the live load can strengthen the findings of this study.
- 3) Only synoptic winds are considered, and the wind directionality effect is ignored. How to consider wind directionality as well as high intensity winds (downburst and tornado) in the codified design could be important and should be investigated.

Appendix A. Spatially Interpolated Statistics of Annual Maximum Wind Based on Ordinary Kriging with Nugget Equal to Zero

The maps shown in this appendix is similar to those shown in the main text, except that they are obtained based on ordinary kriging with nugget equal to zero. In general, the spatial trends of the maps shown in the appendix are similar to those shown in the main text, except that more localized features are exhibited in the figures presented in this appendix.

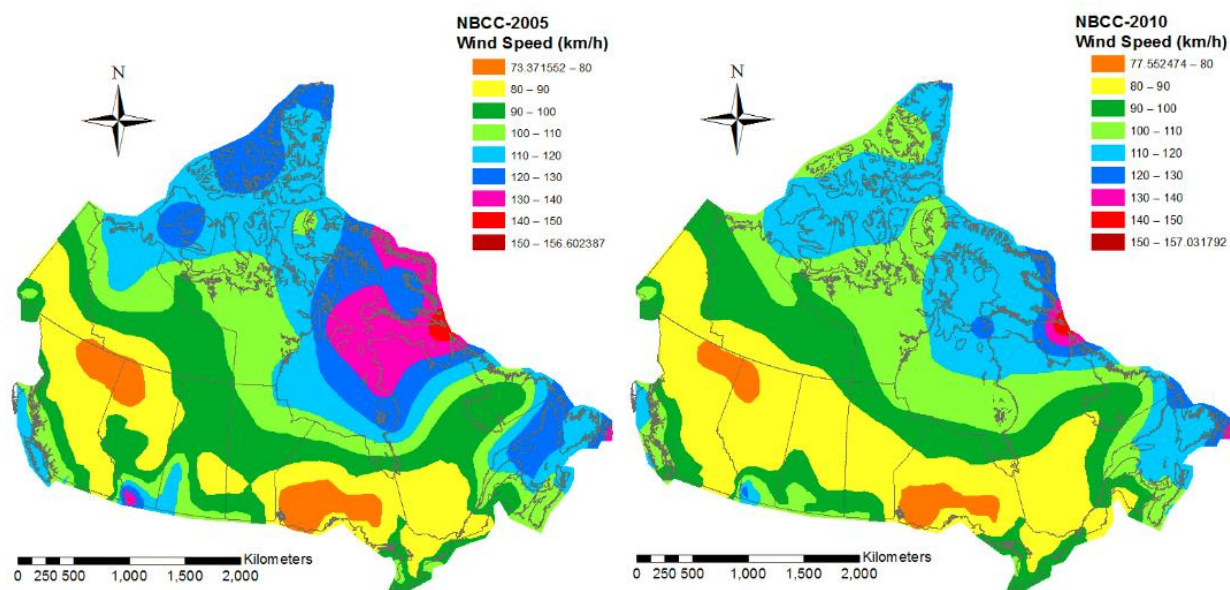


Figure A1. Wind hazard maps inferred from the reference velocity wind pressures given in the NBCC-2005 and NBCC-2010.

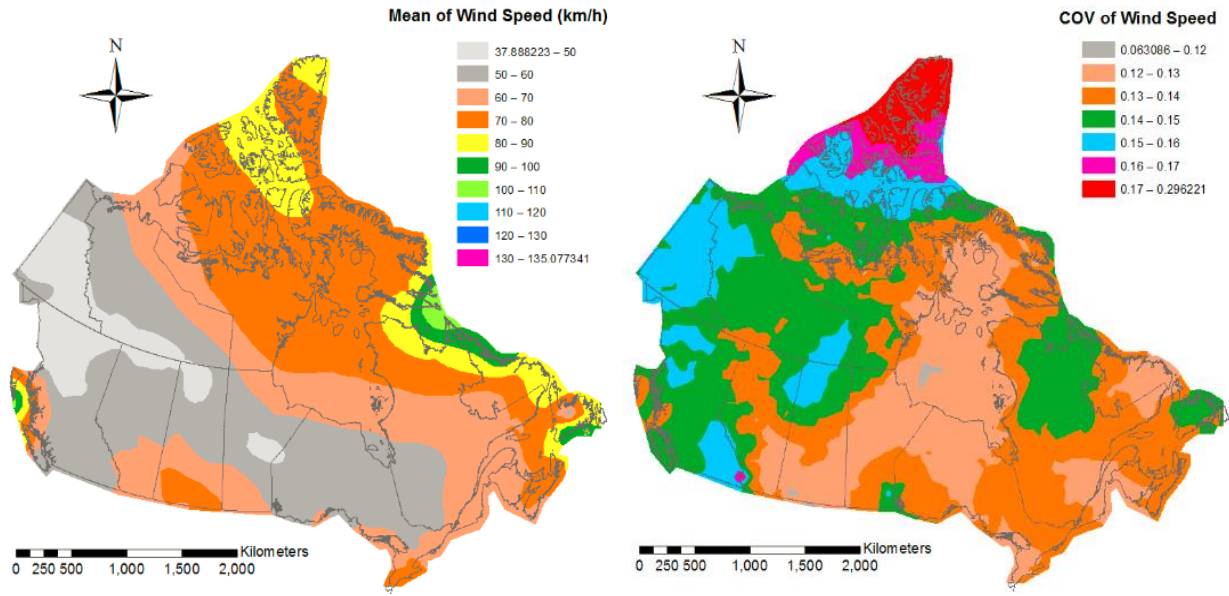


Figure A2. Mean and coefficient of variation of V_{AH} for the case with $n_A \geq 20$.

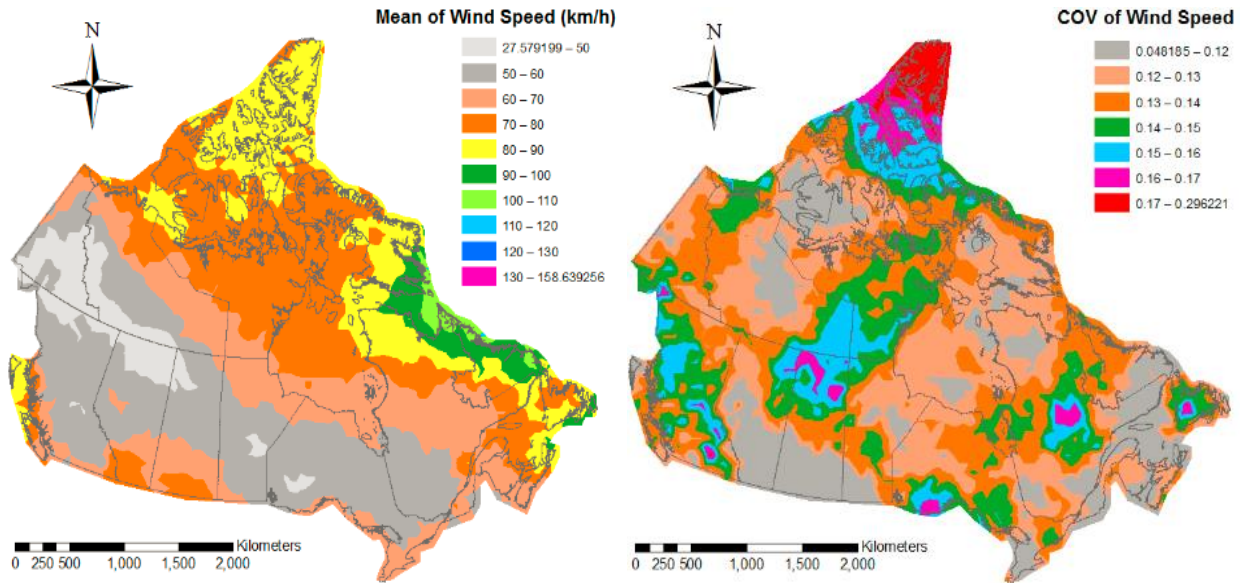


Figure A3. Mean and coefficient of variation of V_{AH} for the case with $n_A \geq 10$.

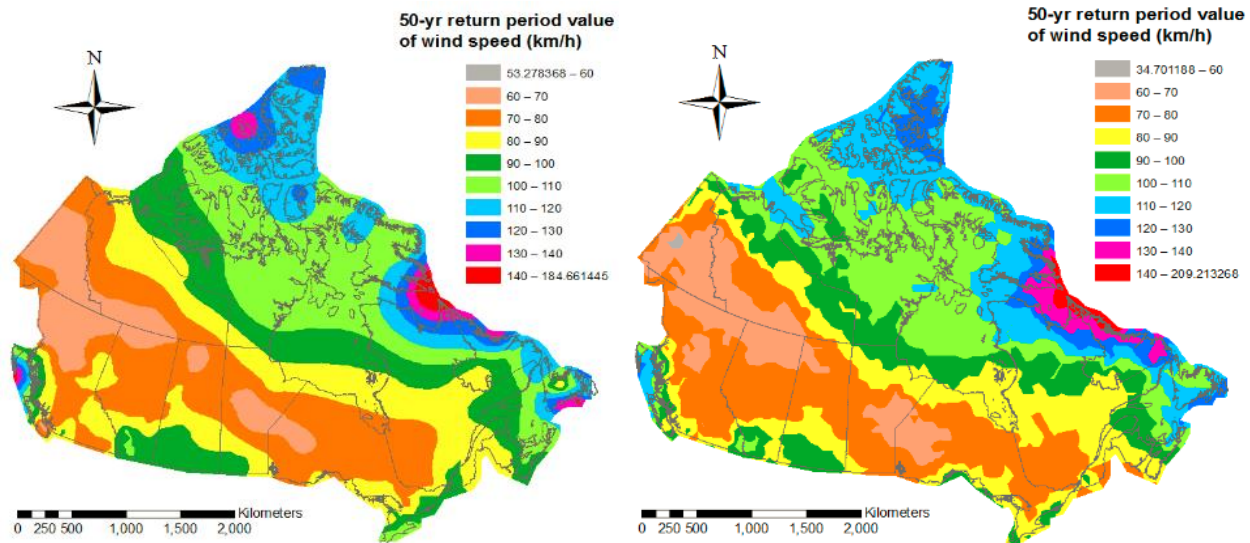
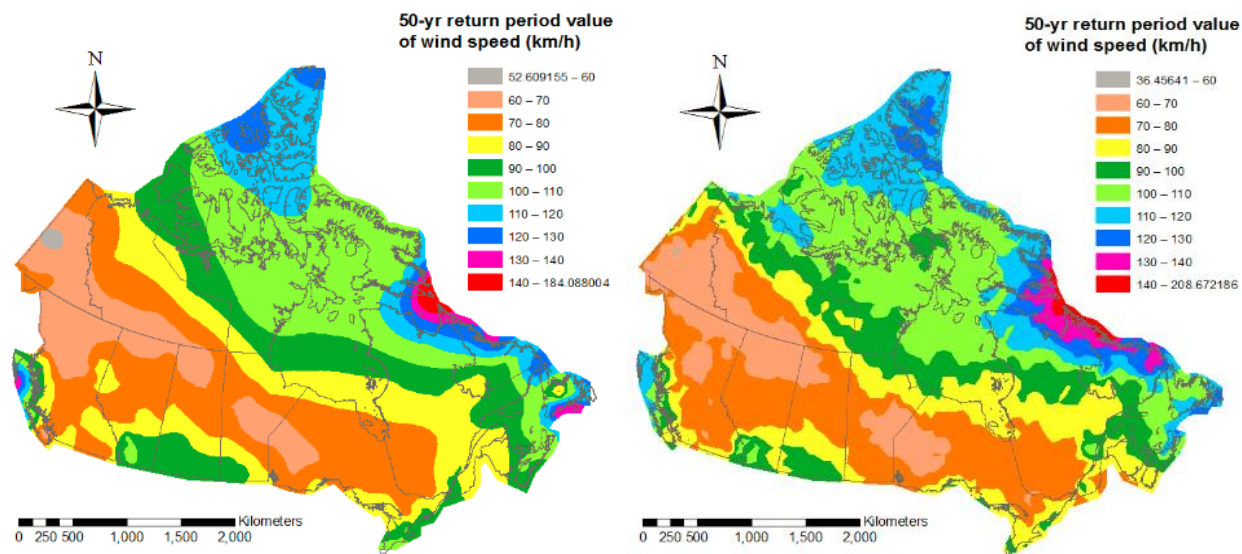


Figure A4. Estimated v_{AH-50} using the GLM for the selected meteorological stations shown in Figure 2-2: a) Contour map of v_{AH-50} for the case with $n_A \geq 20$, b) Contour map of v_{AH-50} for the case with $n_A \geq 10$.



a) Gumbel distribution and $n_A \geq 20$

b) Gumbel distribution and $n_A \geq 10$

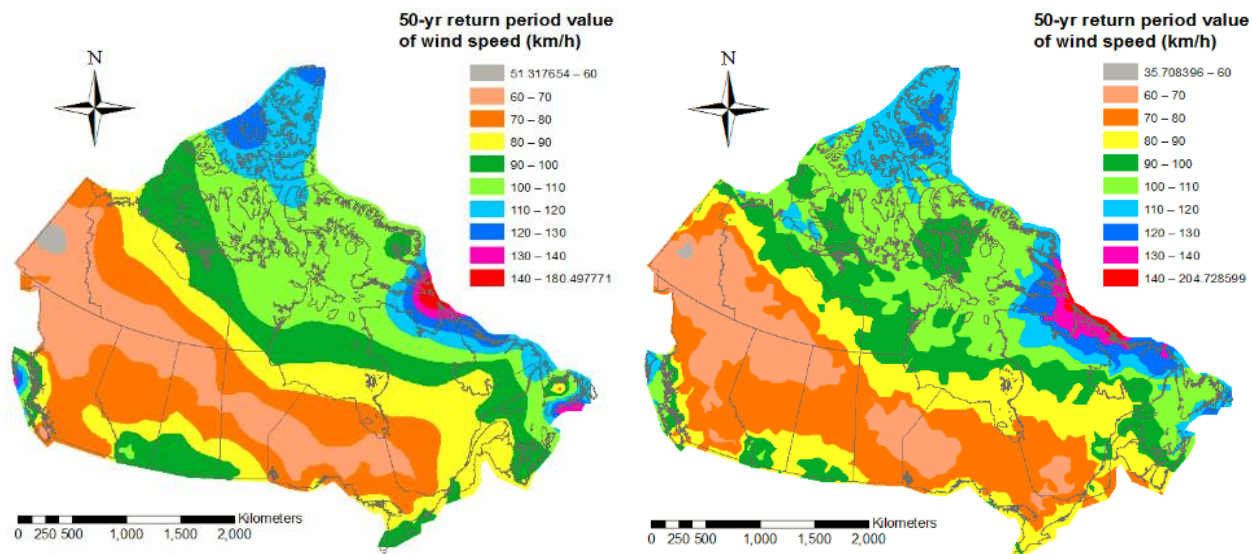
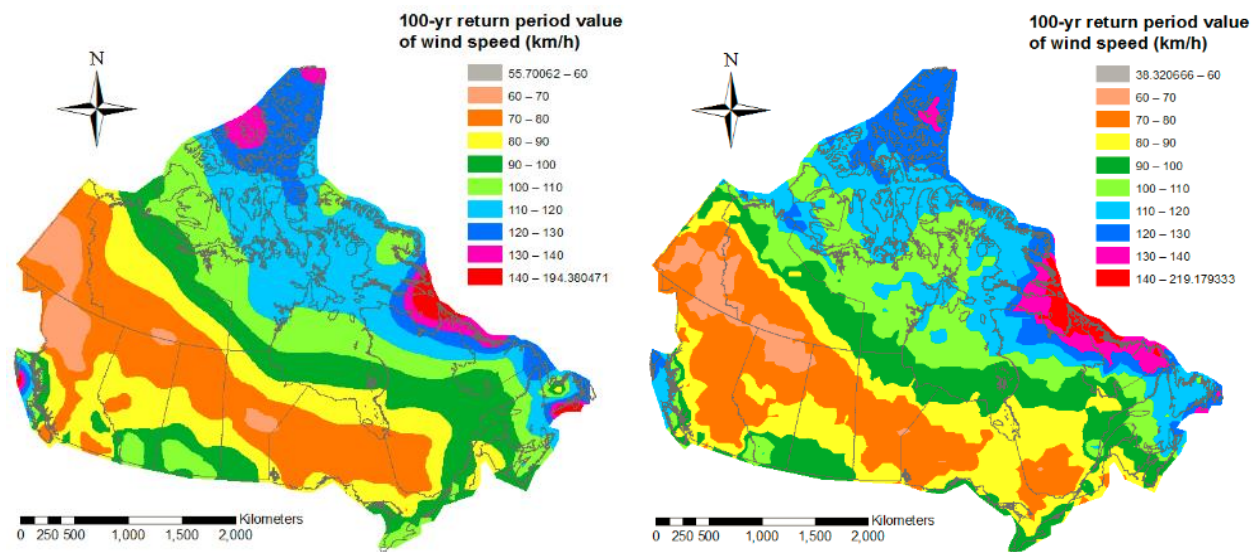
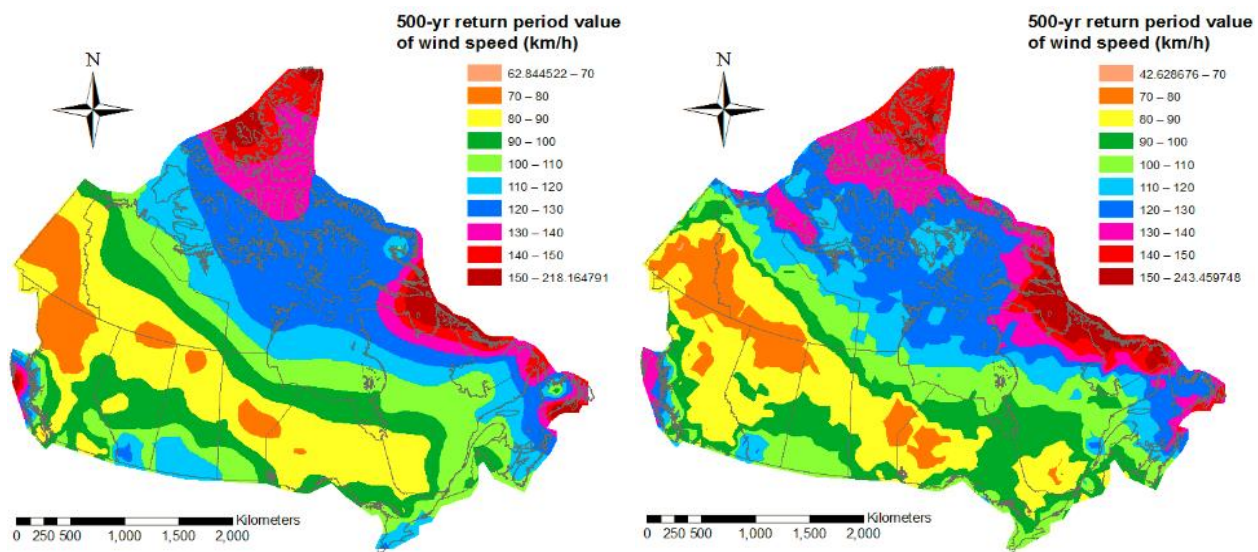
c) GEVD and $n_A \geq 20$ d) GEVD and $n_A \geq 10$

Figure A5. Wind hazard maps developed based on the ROI approach: a) Gumbel distribution and $n_A \geq 20$, b) Gumbel distribution and $n_A \geq 10$, c) GEVD and $n_A \geq 20$, d) GEVD and $n_A \geq 10$.

a) v_{AH-100} for $n_A \geq 20$ b) v_{AH-100} for $n_A \geq 10$



c) v_{AH-500} for $n_A \geq 20$

d) v_{AH-500} for $n_A \geq 10$

Figure A6. Wind hazard maps developed based on the ROI approach and considering the Gumbel model: a) v_{AH-100} for $n_A \geq 20$, b) v_{AH-100} for $n_A \geq 10$, c) v_{AH-500} for $n_A \geq 20$, and d) v_{AH-500} for $n_A \geq 10$.

Appendix B. Interpolated 50-year Return Period Values for Specified Locations in NBCC Based on At-site Analysis and ROI

Table B1. Comparison of NBCC-2005, NBCC-2010 and interpolated 50-year return period values (km/h) based on at-site analysis and ROI.

Location	NBCC-2005 (km/h)	NBCC-2010 (km/h)	Method			
			At-site analysis with $n_A \geq 20$ (km/h)	At-site analysis with $n_A \geq 10$ (km/h)	ROI with $n_A \geq 20$ (km/h)	ROI with $n_A \geq 10$ (km/h)
100 Mile House	88.18	83.77	79.92	71.51	78.53	70.80
Abbotsford	111.18	93.92	78.47	84.83	76.64	81.26
Agassiz	122.29	97.07	78.72	87.71	76.75	87.38
Alberni	112.08	80.10	86.01	68.04	83.96	68.04
Ashcroft	87.04	87.28	79.73	74.74	77.88	73.31
Beatton River	77.34	77.55	75.88	74.96	75.42	74.03
Burns Lake	88.18	88.42	81.99	66.96	79.31	66.19
Cache Creek	88.18	88.42	79.55	74.74	78.11	73.31
Campbell River	112.96	102.10	91.25	96.61	89.45	95.79
Carmi	87.04	87.28	83.99	81.10	81.19	80.56
Castlegar	82.34	82.56	84.39	75.57	82.00	73.46
Chetwend	89.31	89.55	75.52	82.67	74.77	79.11
Chilliwack	119.82	97.07	77.81	85.41	75.96	83.59
Comox	113.84	102.10	90.35	84.92	87.47	86.01
Courtenay	113.84	102.10	90.58	86.39	87.73	87.04
Cranbrook	81.12	81.34	86.66	99.80	85.78	99.14
Crescent Valley	81.12	81.34	86.55	80.46	84.41	79.09
Crofton	112.08	89.55	81.68	81.26	79.65	79.43
Dawson Creek	89.31	89.55	75.71	81.26	75.28	79.79
Dog Creek	89.31	83.77	77.44	71.23	76.32	71.95
Duncan	112.08	88.42	81.71	88.40	79.69	86.36
Elko	91.51	89.55	88.40	87.00	87.81	85.96
Fernie	97.83	89.55	86.97	88.69	86.75	88.24
Fort Nelson	74.72	77.55	71.14	69.20	69.61	68.79

Fort St. John	88.18	88.42	75.74	80.54	75.09	79.01
Glacier	79.88	80.10	82.28	78.73	81.37	77.68
Golden	83.54	83.77	82.83	80.20	82.13	78.32
Grand Forks	90.41	89.55	84.14	84.83	81.48	84.78
Greenwood	93.66	89.55	84.01	84.83	81.30	84.78
Hope	112.08	112.38	79.50	85.06	77.17	84.93
Kamloops	89.31	89.55	80.57	72.47	78.61	71.71
Kaslo	78.62	78.83	85.35	77.52	84.19	74.54
Kelowna	96.80	89.55	81.47	70.05	79.15	69.87
Kimberley	81.12	81.34	86.97	93.14	85.84	91.87
Kitimat Plant	97.83	98.10	89.59	79.75	87.29	80.98
Kitimat Townsite	97.83	98.10	89.77	90.89	87.63	91.55
Lillooet	93.66	93.92	78.54	74.60	77.20	73.84
Lytton	92.59	92.85	79.64	93.24	77.55	93.47
Mackenzie	79.88	80.10	75.70	64.43	74.37	62.95
Masset	111.18	110.59	99.07	113.88	96.99	114.81
McBride	83.54	83.77	78.49	75.80	77.19	73.68
McLeod Lake	79.88	80.10	76.94	73.86	75.40	71.96
Merritt	93.66	93.92	80.55	71.29	78.18	71.40
Mission City	115.58	92.85	78.82	85.01	77.18	82.11
Montrose	83.54	83.77	86.18	87.07	83.84	85.70
Nakusp	81.12	81.34	83.54	63.80	81.94	62.69
Nanaimo	112.08	100.12	85.26	82.02	82.76	80.63
Nelson	81.12	81.34	86.30	79.50	84.59	75.84
Ocean Falls	108.46	108.76	96.46	102.89	95.09	104.40
Osoyoos	99.85	89.55	83.01	68.49	80.43	67.82
Penticton	108.46	94.98	82.35	76.11	79.92	75.71
Port Alberni	112.08	80.10	86.00	68.10	83.94	68.01
Port Hardy	111.18	102.10	101.20	106.10	100.35	106.54
Port McNeill	111.18	102.10	99.29	106.79	98.19	107.13
Powell River	111.18	101.12	88.19	90.98	85.44	89.68
Prince George	85.89	86.13	77.86	74.53	76.45	72.40
Prince Rupert	103.76	104.05	93.04	96.69	90.74	96.93
Princeton	84.72	84.95	79.49	67.12	77.29	67.90
Qualicum Beach	112.96	103.08	86.58	83.47	84.05	83.16
Quesnel	78.62	78.83	77.09	69.34	75.90	68.09
Revelstoke	79.88	80.10	83.27	80.50	81.95	80.55
Salmon Arm	88.18	88.42	81.13	69.77	79.12	68.19
Sandspit	116.44	125.05	103.12	115.11	101.89	110.13

Sidney	109.38	91.76	82.61	85.80	80.87	82.64
Smith River	74.72	77.55	68.91	65.37	67.35	64.93
Smithers	89.31	89.55	84.05	70.80	80.74	69.37
Squamish	105.67	100.12	78.81	85.03	77.10	83.01
Stewart	92.59	84.95	83.63	73.76	79.81	72.60
Taylor	89.31	89.55	75.66	76.89	75.16	75.57
Terrace	84.72	84.95	87.09	87.09	84.37	86.52
Tofino	116.44	116.76	91.91	88.92	90.25	88.55
Trail	83.54	83.77	86.03	85.19	83.64	83.87
Ucluelet	116.44	116.76	86.41	84.17	85.65	84.97
Burnaby	97.83	97.07	78.84	86.24	77.12	83.55
Cloverdale	96.80	93.92	80.14	87.35	78.27	84.86
Haney	96.80	93.92	78.82	75.57	77.16	73.58
Ladner	98.84	96.03	81.68	84.14	79.48	81.80
Langley	96.80	93.92	80.16	88.38	78.31	85.80
New Westminister	96.80	93.92	79.24	89.11	77.42	86.32
North Vancouver	97.83	94.98	79.41	80.33	77.53	78.71
Richmond	97.83	94.98	83.74	85.24	81.45	82.30
Surrey (88 Ave & 156 St)	96.80	93.92	81.62	87.86	79.44	85.42
Vancouver	97.83	94.98	80.55	85.16	78.65	82.63
West Vancouver	97.83	98.10	80.58	58.82	78.66	57.96
Vernon	93.66	89.55	82.68	70.07	80.39	69.43
Victoria (Gonzales Heights)	112.08	106.90	79.89	121.05	77.62	120.10
Victoria (Mt Tolmie)	112.08	112.38	79.89	81.64	77.63	79.17
Victoria	112.08	106.90	79.87	120.79	77.59	120.40
Williams Lake	87.04	83.77	77.88	69.57	76.61	68.89
Youbou	109.38	80.10	85.51	84.31	83.10	82.52
Athabasca	89.31	84.95	77.64	75.99	77.64	75.27
Banff	97.83	80.10	84.89	66.37	84.77	66.18
Barrhead	93.66	93.92	80.37	73.66	80.10	73.85
Beaverlodge	84.72	84.95	77.65	73.32	77.18	73.02
Brooks	101.82	102.10	91.45	87.50	92.20	87.09
Calgary	99.85	98.10	87.48	101.28	87.93	99.34
Campsie	93.66	93.92	80.45	74.81	80.07	74.75
Camrose	89.31	88.42	83.48	79.97	83.30	79.40

Cardston	142.61	120.14	89.35	84.82	89.81	86.92
Claresholm	131.71	107.83	88.80	102.43	89.39	101.75
Cold Lake	89.31	87.28	80.11	76.85	79.70	76.03
Coleman	123.10	112.38	87.83	89.77	87.89	93.76
Coronation	85.89	86.13	88.03	79.02	88.47	82.29
Cowley	141.20	142.30	88.44	108.10	88.69	108.36
Drumheller	93.66	93.92	88.39	72.57	89.03	73.14
Edmonton	94.72	94.98	81.69	78.44	81.62	78.57
Edson	95.77	96.03	83.04	73.17	81.74	72.35
Embarras Portage	90.41	86.13	73.65	65.82	71.60	63.53
Fairview	83.54	83.77	77.02	73.67	76.28	73.39
Fort MacLeod	133.96	116.76	89.62	107.64	90.03	108.98
Fort McMurray	83.54	83.77	74.15	74.74	73.22	73.09
Fort Saskatchewan	92.59	92.85	81.10	79.07	81.24	79.12
Fort Vermillion	76.04	77.55	82.75	72.35	81.05	71.41
Grande Prairie	96.80	92.85	78.07	83.24	77.36	83.02
Habay	74.72	77.55	73.63	69.36	72.22	68.79
Hardisty	84.72	84.95	86.36	75.72	86.51	76.74
High River	113.84	114.15	87.95	108.37	88.53	108.84
Hinton	95.77	96.03	82.40	71.68	80.74	70.03
Jasper	95.77	80.10	81.70	71.36	80.31	67.24
Keg River	74.72	77.55	74.09	68.49	73.24	67.83
Lac la Biche	89.31	84.95	77.82	79.00	77.73	77.94
Lacombe	89.31	89.55	85.19	71.66	85.04	72.57
Lethbridge	127.87	115.03	89.97	101.23	90.52	104.48
Manning	74.72	77.55	75.78	69.44	74.89	69.48
Medicine Hat	103.76	98.10	94.81	83.01	95.29	83.34
Peace River	79.88	80.10	77.18	69.38	76.35	68.67
Pincher Creek	139.07	138.73	88.61	109.96	88.88	110.89
Ranfurly	79.88	84.95	83.53	78.73	83.65	79.19
Red Deer	89.31	89.55	85.35	76.92	85.19	76.85
Rocky Mountain House	92.59	84.95	83.41	70.61	83.36	69.63
Slave Lake	85.89	86.13	77.81	92.88	77.34	92.54
Stettler	84.72	84.95	85.31	79.14	85.63	79.39
Stony Plain	94.72	94.98	81.27	75.58	81.17	75.98
Suffield	106.61	99.11	91.50	83.89	92.32	85.36
Taber	122.29	112.38	91.30	90.94	91.76	93.07

Turner Valley	113.84	114.15	87.87	107.30	88.25	106.84
Valleyview	96.80	91.76	78.24	81.66	77.55	81.36
Begreville	83.54	84.95	82.85	81.93	82.97	82.85
Vermillion	78.62	84.95	82.75	72.35	81.05	71.41
Wagner	85.89	86.13	77.25	90.68	76.60	88.65
Wainwright	84.72	84.95	86.06	76.23	86.10	76.93
Wetaskiwin	89.31	88.42	83.50	75.78	83.25	75.59
Whitecourt	92.59	86.13	81.31	74.00	80.38	74.51
Wimborne	89.31	89.55	86.25	79.76	86.44	79.27
Assiniboia	106.61	99.11	95.51	97.39	95.29	94.45
Batrum	114.71	104.05	93.38	95.76	93.85	95.09
Biggar	115.58	94.98	87.04	84.42	87.26	83.23
Broadview	91.51	96.03	91.44	92.49	91.18	91.32
Dafoe	85.89	86.13	88.63	82.10	87.96	81.78
Dundurn	101.82	96.03	89.45	88.55	89.37	87.44
Estevan	105.67	102.10	93.56	91.72	93.40	90.01
Hudson Bay	85.89	86.13	81.53	82.24	80.60	77.93
Humboldt	88.18	88.42	87.39	82.22	86.52	81.63
Island Falls	93.66	83.77	74.75	70.33	73.33	69.11
Kamsack	89.31	89.55	85.96	77.16	85.69	78.03
Kindersley	112.96	96.03	90.93	99.09	91.51	96.80
Lloydminster	90.41	89.55	85.17	76.45	84.84	77.83
Maple Creek	112.08	94.98	95.29	84.13	95.60	83.56
Meadow Lake	98.84	89.55	81.05	74.87	80.40	74.41
Melfort	84.72	84.95	84.89	77.12	83.79	76.42
Melville	89.31	89.55	90.59	85.36	89.98	85.53
Moose Jaw	95.77	102.10	93.03	92.72	92.93	91.59
Nipawin	87.04	87.28	80.42	82.59	79.93	78.65
North Battleford	118.98	96.03	86.69	84.66	86.55	84.56
Prince Albert	87.04	87.28	83.77	82.21	82.85	80.79
Qu'Appelle	91.51	91.76	93.21	89.22	92.27	88.63
Regina	91.51	99.11	92.95	90.06	92.36	89.82
Rosetown	112.08	99.11	89.18	87.78	89.61	87.17
Saskatoon	97.83	92.85	87.59	89.03	87.48	86.87
Scott	113.84	94.98	87.85	72.83	87.85	71.66
Strasbourg	91.51	91.76	91.71	85.75	91.30	85.44
Swift Current	111.18	104.05	94.45	94.69	94.53	93.98
Uranium City	93.66	84.95	75.11	69.83	72.50	68.67
Weyburn	97.83	98.10	94.04	94.11	93.65	92.55

Yorkton	89.31	89.55	89.17	83.31	88.62	84.06
Beausejour	90.41	90.66	81.89	78.53	80.92	78.90
Boissevain	106.61	102.10	90.34	82.45	90.07	82.75
Brandon	98.84	99.11	89.54	85.31	89.19	84.73
Churchill	112.96	105.01	85.93	91.33	86.17	91.82
Dauphin	89.31	89.55	85.04	80.63	84.77	81.29
Flin Flon	93.66	83.77	75.02	72.62	73.65	71.05
Gimli	89.31	89.55	80.56	69.15	80.18	68.74
Island Lake	93.66	86.13	73.46	65.45	72.26	63.75
Lac du Bonnet	85.89	86.13	80.15	74.64	79.37	73.89
Lynn Lake	93.66	86.13	76.05	73.15	74.53	73.04
Morden	101.82	102.10	86.92	64.89	86.36	65.05
Neepawa	93.66	93.92	87.54	72.82	87.34	73.08
Pine Falls	88.18	88.42	79.19	75.78	78.60	75.39
Portage la Prairie	95.77	96.03	85.98	82.13	85.67	82.36
Rivers	95.77	96.03	89.84	80.78	89.54	80.76
Sandilands	89.31	89.55	82.51	80.49	81.78	79.56
Selkirk	92.59	90.66	82.19	78.36	81.40	79.52
Split Lake	98.84	88.42	77.15	78.35	76.49	77.08
Steinbach	89.31	89.55	82.22	77.01	81.87	77.28
Swan River	87.04	83.77	82.60	75.49	82.12	77.78
The Pas	93.66	86.13	77.03	76.33	75.89	74.67
Thompson	98.84	84.95	75.96	69.08	74.96	69.02
Virden	95.77	96.03	90.71	80.78	90.45	80.76
Winnipeg	94.72	94.98	83.23	76.62	82.41	75.68
Ailsa Craig	104.72	100.12	95.82	91.72	95.21	90.19
Ajax	106.61	98.10	94.91	88.32	92.73	87.15
Alexandria	89.31	89.55	91.36	76.03	89.13	74.76
Alliston	81.12	84.95	90.74	84.42	89.50	85.80
Almonte	90.41	90.66	88.10	80.88	86.12	79.66
Armstrong	73.37	77.55	74.54	68.60	72.98	66.01
Arnprior	85.89	86.13	86.51	80.80	84.37	79.26
Atikokan	73.37	77.55	77.79	71.21	76.14	70.65
Aurora	93.66	93.92	91.80	79.29	90.49	80.19
Bancroft	79.88	80.10	87.65	64.19	85.24	60.48
Barrie	81.12	84.95	90.17	78.89	88.75	80.09
Barriefield	96.80	97.07	87.80	86.75	85.63	84.94
Beaverton	84.72	84.95	90.06	79.05	88.48	78.84
Belleville	92.59	92.85	92.66	88.66	90.50	85.91

Belmont	100.84	97.07	98.76	91.67	97.09	89.54
Big Trout Lake	91.51	91.76	74.63	74.20	73.92	73.67
CFB Borden	81.12	84.95	90.43	79.99	89.13	81.32
Bracebridge	83.54	83.77	87.34	73.96	85.29	73.28
Bradford	84.72	84.95	91.50	74.38	90.17	76.33
Brampton	93.66	93.92	93.65	85.19	92.36	84.99
Brantford	89.31	91.76	97.97	85.59	96.33	85.67
Brighton	103.76	98.10	93.75	94.91	91.64	91.59
Brockville	93.66	93.92	87.88	85.93	85.74	84.24
Burk's Falls	83.54	83.77	84.21	69.13	82.12	68.39
Burlington	95.77	96.03	95.04	88.61	93.88	87.05
Cambridge	83.54	84.95	96.53	86.70	94.90	85.90
Campbellford	90.41	90.66	73.84	76.72	72.47	75.01
Cannington	84.72	84.95	90.76	80.38	89.15	79.53
Carleton Place	90.41	90.66	87.36	74.14	85.26	73.51
Cavan	93.66	93.92	91.63	83.66	90.00	82.43
Centralia	102.80	99.11	95.52	86.56	94.74	85.26
Chapleau	74.72	77.55	78.83	87.09	77.05	85.46
Chatham	92.59	92.85	98.31	92.83	96.75	90.49
Chesley	97.83	98.10	90.79	80.66	89.62	80.99
Clinton	102.80	99.11	95.01	87.47	93.67	86.51
Coboconk	83.54	83.77	88.72	80.86	86.90	80.47
Cobourg	108.46	99.11	94.05	80.41	91.82	79.00
Cochrane	83.54	83.77	75.89	77.10	73.59	76.67
Colborne	105.67	99.11	93.11	90.21	91.22	86.78
Collingwood	88.18	88.42	88.16	76.37	87.60	81.91
Cornwall	90.41	90.66	89.67	79.05	87.86	78.31
Cornunna	96.80	97.07	96.92	91.50	96.21	90.66
Deep River	83.54	83.77	83.43	71.40	80.83	69.77
Deseronto	92.59	92.85	89.77	95.93	87.88	93.05
Dorchester	97.83	97.07	98.79	87.08	97.05	85.97
Dorion	88.18	88.42	76.21	91.29	75.10	87.77
Dresden	92.59	92.85	97.91	90.08	96.78	88.90
Dryden	73.37	77.55	76.63	70.25	75.29	69.14
Dunnville	91.51	96.03	97.02	96.12	95.13	94.22
Durham	93.66	93.92	91.67	85.32	90.42	86.57
Dutton	96.80	97.07	98.64	88.88	97.22	87.73
Earlton	94.72	94.98	76.83	79.77	74.45	77.97
Edison	78.62	78.83	96.91	94.69	96.21	93.43

Elmvale	84.72	84.95	89.00	78.73	87.83	79.44
Embro	97.83	98.10	95.66	87.07	94.62	86.12
Englehart	90.41	90.66	76.79	75.73	74.43	75.58
Espanola	91.51	91.76	80.99	85.02	80.09	83.11
Exeter	102.80	99.11	95.37	91.20	94.58	89.66
Fenelon Falls	84.72	84.95	89.07	83.60	87.32	81.90
Fergus	84.72	84.95	94.85	75.19	93.29	77.31
Forest	101.82	98.10	95.81	91.72	95.24	90.19
Fort Erie	95.77	96.03	97.10	100.99	95.11	100.15
Fort Erie (Ridgeway)	95.77	96.03	96.90	100.99	94.95	100.16
Fort Frances	78.62	78.83	79.34	75.18	77.97	74.23
Gananoque	96.80	97.07	85.73	91.59	83.94	91.18
Geraldton	73.37	77.55	74.16	83.00	73.00	81.72
Glencoe	92.59	92.85	98.67	87.62	97.20	86.44
Goderich	104.72	105.01	94.25	79.27	93.24	82.59
Gore Bay	88.18	93.92	83.87	83.81	82.88	82.42
Graham	73.37	77.55	74.65	79.18	73.46	78.28
Gravenhurst (Muskoka Airport)	83.54	84.95	88.72	74.27	86.67	74.37
Grimsby	95.77	96.03	95.28	90.68	94.04	89.57
Guelph	81.12	84.95	95.40	84.72	93.93	85.57
Guthrie	81.12	84.95	89.94	79.30	88.42	80.55
Haileybury	93.66	93.92	77.72	73.22	75.31	72.60
Haldimand (Caledonia)	89.31	93.92	95.46	88.32	94.47	86.72
Haldimand (Hagersville)	91.51	96.03	97.05	88.35	95.81	87.00
Haliburton	83.54	83.77	86.77	76.50	84.95	75.06
Halton Hills (Georgetown)	85.89	86.13	93.79	84.41	92.56	84.34
Hamilton	95.77	96.03	96.53	77.34	95.10	77.35
Hanover	97.83	98.10	92.93	81.38	91.57	81.84
Hastings	90.41	90.66	92.45	88.02	90.29	85.02
Hawkesbury	90.41	90.66	90.72	78.91	88.40	77.60
Hearst	74.72	77.55	75.92	76.82	73.83	75.63
Honey Harbour	88.18	88.42	89.06	62.54	86.90	64.06
Hornepayne	74.72	77.55	76.36	78.09	74.44	77.13
Huntsville	83.54	83.77	85.16	72.80	83.33	71.47
Ingersoll	97.83	98.10	97.84	83.84	96.28	83.02

Iroquois Falls	89.31	86.13	76.81	75.85	74.31	75.01
Jellicoe	73.37	77.55	74.09	75.04	73.10	71.45
Kapuskasing	78.62	78.83	76.14	74.85	73.73	73.62
Kemptville	90.41	90.66	89.67	80.56	87.49	79.72
Kenora	78.62	78.83	77.70	77.25	76.75	75.33
Killaloe	83.54	83.77	86.07	90.88	83.48	87.83
Kincardine	104.72	105.01	93.34	84.87	92.27	85.52
Kingston	96.80	97.07	90.48	74.38	89.09	76.33
Kinmount	83.54	83.77	87.96	80.36	86.32	78.67
Kirkland Lake	90.41	88.42	77.08	76.39	74.60	76.40
Kitchener	85.89	86.13	94.17	84.08	93.23	83.86
Lakefield	87.04	87.28	89.23	85.64	87.89	83.34
Lansdowne House	79.88	80.10	73.65	68.62	72.57	68.83
Leamington	96.80	97.07	98.42	87.12	96.89	85.40
Lindsay	87.04	87.28	89.61	83.60	87.99	81.90
Lion's Head	97.83	98.10	86.18	80.95	85.32	80.14
Listowel	96.80	97.07	93.40	78.09	92.45	78.73
London	103.76	97.07	97.09	91.31	95.95	88.93
Lucan	104.72	100.12	95.75	86.56	95.01	85.26
Maitland	93.66	93.92	87.83	85.93	85.70	84.24
Markdale	90.41	90.66	89.97	78.77	88.99	78.93
Markham	102.80	93.92	93.32	81.20	91.94	81.26
Martin	73.37	77.55	75.73	68.87	74.47	68.74
Matheson	90.41	88.42	76.96	76.39	74.50	76.40
Mattawa	79.88	80.10	81.34	72.43	79.31	71.15
Midland	88.18	88.42	89.14	73.87	87.11	75.68
Milton	92.59	92.85	94.13	87.32	93.03	85.94
Milverton	92.59	92.85	94.77	79.73	93.61	80.14
Minden	83.54	83.77	86.95	76.50	85.31	75.06
Mississauga	98.84	93.92	94.16	87.37	92.96	85.98
Mississauga (Port Credit)	98.84	93.92	94.17	87.38	92.95	85.99
Mitchell	99.85	98.10	95.11	83.03	93.98	83.69
Moosonee	83.54	83.77	75.36	78.16	73.86	75.67
Morrisburg	90.41	90.66	92.06	78.67	89.82	78.40
Mount Forest	90.41	90.66	94.01	90.75	92.40	87.90
Nakina	73.37	77.55	73.87	74.88	72.49	74.08
Nanticoke (Jarvis)	92.59	98.10	96.78	86.95	95.67	85.94

Nanticoke (Port Dover)	95.77	98.10	96.91	89.26	95.81	87.38
Napanee	92.59	92.85	91.94	95.93	89.69	93.05
New Liskeard	92.59	92.85	78.08	72.23	75.71	72.32
Newcastle	108.46	98.10	94.72	94.02	92.55	91.64
Newcastle (Bowmanville)	109.38	98.10	94.84	91.19	92.61	89.24
Newmarket	87.04	87.28	91.67	79.29	90.34	80.19
Niagara Falls	92.59	92.85	96.00	90.30	94.04	88.99
North Bay	82.34	82.56	81.88	71.61	79.65	71.58
Norwood	90.41	90.66	92.58	88.96	90.34	87.04
Oakville	98.84	97.07	94.94	87.32	93.72	85.94
Orangeville	84.72	84.95	93.62	83.28	92.10	83.03
Orillia	83.54	84.95	88.84	79.33	87.61	80.56
Oshawa	106.61	98.10	94.85	88.32	92.64	87.15
Ottawa	90.41	90.66	87.83	82.35	86.30	82.26
Owen Sound	97.83	98.10	89.02	77.88	88.01	78.51
Pagwa River	74.72	77.55	75.69	74.09	73.84	73.59
Paris	90.41	91.76	97.41	85.59	95.84	85.67
Parkhill	104.72	100.12	95.75	91.72	95.15	90.19
Parry Sound	88.18	88.42	84.55	75.95	83.53	76.76
Pelham (Fonthill)	91.51	91.76	96.64	90.32	94.72	89.49
Pembroke	83.54	83.77	84.45	73.40	82.22	72.04
Penetanguishene	88.18	88.42	87.49	72.00	86.51	74.04
Perth	90.41	90.66	89.79	82.66	87.38	80.57
Petawawa	83.54	83.77	83.67	70.54	81.14	69.53
Peterborough	90.41	90.66	90.25	85.07	88.70	83.04
Petrolia	96.80	97.07	96.23	91.72	95.68	90.20
Pickering (Dunbarton)	106.61	98.10	94.93	88.32	92.77	87.15
Picton	98.84	99.11	89.60	88.56	87.86	86.99
Plattsville	90.41	91.76	96.38	86.94	94.93	86.15
Point Alexander	83.54	83.77	83.34	71.40	80.72	69.77
Port Burwell	96.80	97.07	98.50	90.94	97.11	90.10
Port Colborne	95.77	96.03	97.01	98.57	95.07	101.61
Port Elgin	104.72	105.01	91.44	84.87	90.27	85.52
Port Hope	108.46	98.10	94.07	92.73	91.84	90.70
Port Perry	93.66	93.92	91.33	78.93	89.91	78.76
Port Stanley	96.80	97.07	98.88	91.66	97.37	89.53

Prescott	93.66	93.92	88.91	86.75	86.82	84.94
Princeton	90.41	91.76	97.46	84.73	95.90	84.14
Raith	73.37	77.55	75.39	78.70	74.27	78.05
Rayside-Balfour (Chelmsford)	94.72	94.98	80.52	81.50	79.32	80.01
Red Lake	74.72	77.55	75.92	72.92	74.50	70.00
Renfrew	83.54	83.77	86.21	84.59	83.96	82.49
Richmond Hill	102.80	93.92	92.34	79.29	91.11	80.19
Rockland	89.31	89.55	88.46	78.10	86.84	76.35
Sarnia	96.80	97.07	95.72	99.88	94.95	97.81
Sault Ste. Marie	89.31	93.92	83.98	93.49	82.51	89.80
Schreiber	88.18	88.42	76.57	95.79	75.22	91.33
Seaforth	102.80	98.10	95.22	87.47	93.88	86.51
Simcoe	92.59	94.98	96.56	99.51	95.47	95.66
Sioux Lookout	73.37	77.55	75.04	70.13	73.62	67.20
Smiths Falls	90.41	90.66	89.97	83.79	87.64	82.79
Smithville	91.51	91.76	96.85	93.92	94.71	92.16
Smooth Rock Falls	79.88	80.10	75.77	76.62	73.48	76.10
South River	79.88	83.77	83.53	69.13	81.34	68.39
Southampton	102.80	103.08	91.44	84.28	90.24	84.83
St. Catherines	95.77	96.03	96.52	96.97	94.34	93.73
St. Mary's	100.84	97.07	95.72	82.32	94.63	82.51
St. Thomas	97.83	97.07	98.74	91.66	97.24	89.53
Stirling	89.31	89.55	92.37	90.70	90.10	87.35
Stratford	97.83	94.98	95.37	82.32	94.25	82.51
Strathroy	99.85	97.07	96.21	91.72	95.62	90.19
Sturgeon Falls	83.54	83.77	81.85	69.33	79.69	69.46
Sudbury	95.77	96.03	80.44	81.09	79.26	80.35
Sundridge	79.88	83.77	83.74	69.13	81.58	68.39
Tavistock	96.80	94.98	95.48	86.65	94.37	86.17
Temagami	85.89	86.13	78.65	75.50	76.66	74.37
Thamesford	97.83	98.10	97.77	84.12	96.22	83.19
Theford	104.72	100.12	95.71	91.72	95.12	90.19
Thunder Bay	88.18	88.42	76.99	88.77	75.82	85.60
Tillsonburg	93.66	93.92	98.14	78.75	96.58	78.80
Timmins	83.54	83.77	77.50	77.91	74.95	75.90
Timmins (Porcupine)	85.89	86.13	77.67	80.25	75.11	78.11
Etobicoke	102.80	93.92	95.32	90.43	93.30	89.37

North York	102.80	93.92	95.02	85.44	92.94	84.53
Scarborough	102.80	97.07	95.04	88.32	92.94	87.15
Toronto	101.82	93.92	95.33	87.65	93.29	86.61
Trenton	96.80	97.07	93.61	103.76	91.50	98.92
Trout Creek	79.88	83.77	83.09	69.13	80.83	68.39
Uxbridge	91.51	91.76	91.71	82.69	90.29	83.21
Vaughan (Woodbridge)	102.80	93.92	93.11	81.30	91.79	82.08
Vittoria	96.80	97.07	97.79	90.45	96.49	88.73
Walkerton	99.85	100.12	92.87	81.98	91.54	82.53
Wallaceburg	92.59	94.98	96.81	94.69	96.25	93.43
Waterloo	85.89	86.13	94.05	82.80	93.11	82.99
Watford	96.80	97.07	96.16	91.72	95.59	90.19
Wawa	88.18	88.42	78.36	81.76	76.93	82.22
Welland	92.59	92.85	96.65	90.93	94.74	89.72
West Lorne	96.80	97.07	98.64	88.88	97.24	87.73
Whitby	106.61	98.10	94.80	88.32	92.60	87.15
Whitby (Brooklin)	102.80	94.98	94.64	88.32	92.42	87.15
White River	73.37	77.55	76.74	71.75	75.30	66.32
Warton	97.83	98.10	87.38	93.09	86.67	91.33
Windsor	96.80	97.07	97.05	97.11	96.01	94.25
Wingham	99.85	100.12	93.26	90.20	92.38	89.84
Woodstock	93.66	93.92	97.72	87.30	96.12	86.51
Wyoming	96.80	97.07	96.08	91.75	95.53	90.21
Acton-Vale	79.88	83.77	90.33	94.23	89.60	94.86
Alma	79.88	83.77	86.29	80.51	85.38	79.84
Amos	79.88	80.10	77.08	73.27	74.75	73.71
Asbestos	83.54	83.77	90.06	84.25	89.33	85.14
Alymer	90.41	90.66	87.98	81.02	86.03	79.99
Baie-Comeau	109.38	100.12	88.56	89.89	87.66	90.56
Beauport	102.80	91.76	88.09	89.29	87.14	89.99
Bedford	90.41	90.66	90.16	85.65	89.52	85.73
Beloeil	85.89	86.13	90.72	86.48	89.53	86.36
Brome	85.89	86.13	90.46	91.17	89.73	91.04
Brossard	89.31	91.76	91.38	84.33	90.18	83.78
Buckingham	89.31	89.55	87.30	78.12	85.74	76.06
Campbell's Bay	79.88	80.10	85.46	74.96	83.20	73.21
Chambly	89.31	89.55	90.90	85.88	89.68	86.03
Coaticook	87.04	83.77	91.09	81.68	90.49	82.77

Contrecoeur	92.59	92.85	90.02	90.55	88.69	90.61
Cowansville	90.41	90.66	90.51	92.57	89.78	93.48
Deux-Montagnes	85.89	86.13	91.03	82.90	89.31	82.32
Dolbeau	83.54	83.77	85.12	78.25	84.44	77.41
Drummondville	79.88	83.77	89.13	93.93	88.16	93.83
Farnham	90.41	86.13	90.03	88.31	89.40	89.24
Fort-Coulonge	79.88	80.10	84.55	73.40	82.45	72.04
Gagnon	95.77	88.42	90.44	85.25	90.12	86.22
Gaspe	124.71	98.10	95.77	100.85	93.37	100.53
Gatineau	90.41	90.66	87.74	81.01	86.20	79.19
Gracefield	79.88	80.10	85.23	70.49	83.35	69.65
Granby	83.54	83.77	90.45	90.10	89.72	91.08
Harrington-Harbour	135.44	120.14	105.49	101.66	105.06	101.51
Havre-St-Pierre	124.71	112.38	97.38	93.65	96.12	94.59
Hemmingford	89.31	89.55	89.28	86.17	88.56	87.06
Hull	90.41	90.66	87.78	81.95	86.24	81.44
Iberville	90.41	90.66	90.01	88.48	89.35	89.04
Inukjuak	133.96	109.68	98.88	94.80	98.12	95.81
Joliette	84.72	84.95	88.45	80.96	87.53	80.05
Kuujuuaq	119.82	109.68	114.99	120.43	114.26	115.20
Kuujuarapik	128.64	105.01	86.97	84.27	86.68	82.22
La-Malbaie	104.72	98.10	88.33	99.21	87.47	99.04
La-Tuque	83.54	83.77	85.97	68.52	85.60	69.55
Lac-Megantic	83.54	83.77	91.54	74.67	91.25	76.29
Lachute	89.31	89.55	90.55	76.71	88.40	75.68
Lennoxville	79.88	80.10	91.10	80.26	90.23	83.19
Lery	89.31	91.76	89.30	82.37	88.20	82.09
Loretteville	102.80	90.66	87.57	86.38	86.81	86.84
Louiseville	92.59	92.85	88.08	78.48	87.35	77.57
Magog	83.54	83.77	91.14	87.70	90.29	88.17
Malartic	79.88	80.10	77.46	73.14	75.07	73.61
Maniwaki	78.62	78.83	84.13	75.25	82.06	73.24
Masson	89.31	89.55	88.37	78.12	86.69	76.33
Matane	109.38	109.68	88.50	94.42	87.89	94.50
Mont-Joli	109.38	102.10	88.41	84.89	87.12	85.45
Mont-Laurier	77.34	77.55	85.07	75.19	83.19	73.55
Montmagny	104.72	97.07	89.09	88.56	87.92	89.16
Beaconsfield	89.31	91.76	89.59	73.95	88.29	75.31

Dorval	89.31	91.76	90.02	96.00	88.70	95.07
Laval	89.31	91.76	90.78	83.40	89.37	82.63
Montreal	89.31	91.76	90.85	57.83	89.78	57.66
Montreal-Est	89.31	91.76	90.52	85.44	89.16	85.16
Montreal-Nord	89.31	91.76	90.65	82.10	89.22	82.01
Outremont	89.31	91.76	90.88	56.75	89.78	56.77
Pierrefonds	89.31	91.76	89.98	75.17	88.43	76.24
St-Lambert	89.31	91.76	91.83	78.38	90.42	78.56
St-Laurent	89.31	91.76	89.89	88.35	88.63	87.63
Ste-Anne-de-Bellevue	89.31	91.76	89.61	70.34	88.10	72.69
Verdun	89.31	91.76	91.42	72.23	90.18	72.81
Nicolet (Gentilly)	91.51	91.76	88.35	86.01	87.52	82.49
Nitchequon	85.89	86.13	90.16	88.14	89.42	89.96
Noranda	83.54	83.77	76.43	76.97	73.90	80.42
Perce	130.18	120.14	96.85	100.02	94.40	100.29
Pincourt	89.31	91.76	89.68	76.36	88.28	76.91
Plessisville	83.54	83.77	89.61	80.91	88.57	81.12
Port-Cartier	116.44	104.05	89.37	90.79	88.07	91.82
Povungnituk	134.70	109.68	110.71	114.17	109.53	112.17
Ancienne-Lorette	102.80	90.66	88.19	92.94	87.32	92.98
Levis	102.80	90.66	88.24	93.65	87.37	96.41
Quebec	102.80	90.66	88.22	96.62	87.35	97.77
Sillery	102.80	90.66	89.11	96.61	88.07	98.68
Ste-Foy	102.80	90.66	88.22	98.19	87.36	100.77
Richmond	79.88	80.10	90.17	91.68	89.44	91.66
Rimouski	109.38	102.10	88.07	96.29	86.87	95.77
Riveiere-du-Loup	107.54	100.12	88.37	86.96	87.12	86.21
Roberval	83.54	83.77	85.86	87.53	84.89	87.22
Rock-Island	90.41	83.77	91.16	80.93	90.52	81.78
Rosemere	89.31	89.55	90.72	83.37	89.25	82.30
Rouyn	83.54	83.77	76.43	76.89	73.90	80.06
Salaberry-de-Valleyfield	89.31	91.76	89.62	77.46	88.16	77.08
Schefferville	91.51	91.76	104.64	97.90	103.19	98.18
Senneterre	79.88	80.10	79.38	64.00	77.16	64.67
Sept-Iles	116.44	104.05	90.10	74.47	88.99	75.87
Shawinigan	83.54	83.77	86.64	65.73	86.16	68.50

Shawville	83.54	83.77	85.91	75.92	83.71	74.57
Sherbrooke	79.88	80.10	90.15	83.73	89.43	84.84
Sorel	92.59	92.85	88.61	85.22	87.68	84.78
St-Felicien	83.54	83.77	84.72	80.00	84.04	79.06
St-Georges-de-Cacouna	107.54	100.12	88.32	106.45	87.07	106.34
St-Hubert	89.31	91.76	91.35	98.90	90.16	99.15
St-Hubert-de-Temiscouata	107.54	89.55	88.62	100.57	87.26	99.58
St-Hyacinthe	83.54	83.77	90.58	87.17	89.44	87.40
St-Jerome	85.89	86.13	89.37	77.35	87.88	76.17
St-Jovite	81.12	81.34	87.00	61.96	85.67	59.84
St-Nicolas	98.84	91.76	88.02	83.68	87.24	85.52
Ste-Agathe-des-Monts	83.54	83.77	87.81	88.24	86.51	85.71
Sutton	90.41	90.66	91.19	81.22	90.38	82.62
Tadoussac	105.67	102.10	88.47	156.66	87.24	153.36
Temiscaming	79.88	80.10	80.00	62.34	77.65	64.78
Theford Mines	85.89	83.77	90.19	76.54	89.27	77.73
Thurso	89.31	89.55	88.41	78.10	86.79	76.35
Trois-Rivieres	92.59	92.85	87.91	84.75	87.30	86.40
Val-d'Or	79.88	80.10	78.07	71.33	75.67	71.78
Varennes	89.31	89.55	90.29	95.87	89.08	94.56
Vercheres	92.59	92.85	90.08	90.89	88.90	89.76
Victoriaville	83.54	83.77	89.30	78.92	88.41	78.86
Ville-Marie	89.31	89.55	78.52	75.84	76.21	75.41
Waterloo	83.54	83.77	90.40	90.94	89.68	91.42
Windsor	79.88	80.10	90.15	86.05	89.42	86.65
Alma	105.67	98.10	95.14	87.41	94.03	89.24
Bathurst	97.83	98.10	93.31	96.07	91.53	93.82
Campbellton	102.80	94.98	90.31	92.48	88.64	92.24
Edmundston	93.66	87.28	89.27	79.21	87.75	78.72
Fredericton	90.41	87.28	91.36	80.41	90.12	79.93
Gagetown	103.76	89.55	93.87	82.01	92.70	81.46
Grand Falls	91.51	87.28	90.32	78.57	88.31	77.12
Moncton	112.96	100.12	95.30	92.01	94.11	91.70
Oromocto	99.85	88.42	91.30	79.75	89.96	80.89
Sackville	107.54	99.11	96.92	96.29	95.50	96.93
Saint John	102.80	103.08	92.81	81.42	92.09	82.46
Shippagan	117.29	112.38	94.38	94.58	92.81	93.48

St. Stephen	109.38	91.76	94.14	65.80	92.63	67.35
Woodstock	85.89	86.13	91.26	85.77	90.69	85.30
Amherst	107.54	98.10	97.34	94.76	95.99	96.57
Antigonish	103.76	104.05	105.45	113.76	104.45	113.46
Bridgewater	108.46	105.01	95.16	86.04	94.83	85.40
Canso	111.18	110.59	106.79	105.74	105.75	105.97
Debert	104.72	98.10	97.39	94.47	96.78	93.55
Digby	104.72	105.01	93.16	82.96	92.98	83.41
Greenwood	103.76	104.05	92.12	84.23	92.59	84.12
Dartmouth	107.54	107.83	96.64	92.87	96.23	93.26
Halifax	107.54	107.83	96.63	92.70	96.22	93.11
Kentville	103.76	104.05	95.18	77.31	94.44	78.81
Liverpool	110.28	110.59	94.07	87.22	94.82	85.77
Lockeport	109.38	109.68	93.20	84.23	93.66	84.12
Louisburg	113.84	114.15	96.67	92.57	96.26	93.00
Lunenburg	110.28	110.59	94.37	86.04	95.19	85.40
New Glasgow	104.72	105.01	104.12	113.37	102.55	114.05
North Sydney	108.46	108.76	111.60	113.20	110.31	112.72
Pictou	104.72	105.01	103.61	106.52	102.12	105.53
Port Hawkesbury	121.47	121.80	107.22	110.69	106.08	110.39
Springhill	105.67	98.10	97.93	93.54	96.78	94.21
Stewiacke	104.72	100.12	97.75	100.32	97.26	100.13
Sydney	108.46	108.76	113.61	113.90	112.11	114.05
Tatamagouche	104.72	105.01	101.00	97.73	99.35	95.96
Truro	102.80	98.10	97.61	93.65	97.12	95.19
Wolfville	103.76	104.05	95.40	89.90	94.62	90.07
Yarmouth	105.67	105.96	92.93	90.26	93.31	90.78
Charlottetown	109.38	105.96	103.04	101.82	101.36	102.53
Souris	103.76	107.83	105.72	107.80	104.05	106.67
Summerside	116.44	109.68	98.37	98.30	97.09	95.31
Tignish	123.91	115.03	97.98	97.54	96.79	94.87
Argentia	122.29	122.62	114.04	116.93	114.64	111.51
Bonavista	117.29	129.77	114.10	126.53	113.83	121.27
Buchans	109.38	109.68	112.92	116.60	111.50	114.97
Cape Harrison	109.38	109.68	119.09	124.85	119.66	124.43
Cape Race	144.69	145.09	112.81	150.44	113.14	146.17
Channel-Port aux Basques	115.58	125.05	109.11	114.40	108.43	111.40
Corner Brook	121.47	105.01	110.08	125.45	109.06	98.13

Gander	109.38	109.68	112.93	105.06	111.90	106.82
Grand Bank	121.47	121.80	114.21	124.64	114.61	121.32
Grand Falls	109.38	109.68	114.14	106.67	112.55	105.74
Happy Valley - Goose Bay	85.89	91.76	111.96	99.56	111.33	97.27
Labrador City	89.31	89.55	94.73	81.77	94.04	82.83
St. Anthony	131.71	132.07	113.07	120.91	112.98	121.14
St. John's	126.30	125.05	113.12	112.43	113.23	113.14
Stephenville	123.91	107.83	108.96	123.91	108.14	112.95
Twin Falls	89.31	89.55	102.22	101.86	100.98	102.70
Wabana	122.29	122.62	114.56	113.03	114.86	111.61
Wabush	89.31	89.55	93.86	81.96	93.60	82.98
Aishihik	87.04	87.28	65.08	66.08	63.74	65.33
Dawson	78.62	78.83	66.75	60.74	65.15	62.00
Destruction Bay	109.38	109.68	64.58	65.75	63.30	64.95
Snag	78.62	78.83	64.58	71.08	63.27	69.00
Teslin	76.04	82.56	67.67	67.76	65.73	66.63
Watson Lake	83.54	83.77	67.66	62.92	66.12	62.04
Whitehorse	87.04	87.28	67.14	77.08	65.48	75.04
Aklavik	109.38	98.10	76.81	87.70	75.84	85.30
Echo Bay/Port Radium	102.80	103.08	84.11	90.89	83.55	90.27
Fort Good Hope	112.08	93.92	77.34	67.34	76.22	68.57
Fort Providence	83.54	83.77	73.83	73.03	72.13	73.54
Fort Resolution	88.18	88.42	74.03	68.31	71.85	68.16
Fort Simpson	90.41	88.42	72.48	69.91	71.12	70.26
Fort Smith	90.41	88.42	73.42	66.79	71.08	65.64
Hay River	83.54	83.77	73.39	65.84	71.26	66.36
Holman	130.18	131.31	95.48	113.96	95.27	113.63
Inuvik	112.96	98.10	78.29	84.35	77.20	83.79
Mould Bay	115.58	107.83	109.74	105.53	107.29	103.10
Norman Wells	115.58	93.92	76.16	78.20	75.10	75.60
Rae-Edzo	96.80	97.07	76.87	72.33	75.44	73.95
Tungsten	93.66	93.92	68.51	66.64	67.40	66.39
Yellowknife	96.80	97.07	76.82	70.73	74.92	70.62
Alert	123.10	122.62	122.50	128.19	121.23	128.50
Arctic Bay	104.72	105.01	112.16	112.29	109.98	110.21
Arviat/Eskimo Point	112.96	107.83	94.72	119.50	94.65	114.31
Baker Lake	103.76	104.05	101.41	111.52	101.46	109.33

Cambridge Bay	103.76	104.05	100.63	101.53	100.88	102.84
Chesterfield Inlet	105.67	105.96	102.17	105.04	102.80	103.60
Clyde River	133.96	120.14	108.19	111.23	105.46	109.25
Coppermine	95.77	96.03	90.76	91.34	90.58	89.34
Coral Harbour	140.50	117.61	105.24	105.62	104.99	104.82
Eureka	115.58	105.01	122.43	114.53	119.80	114.36
Iqaluit	122.29	107.83	121.32	121.05	118.72	113.64
Isachsen	133.96	109.68	120.45	140.97	119.04	138.26
Nottingham Island	140.50	125.05	108.77	130.75	107.41	125.53
Rankin Inlet	109.38	109.68	100.23	109.56	100.83	106.61
Resolute	117.29	117.61	113.97	111.07	112.46	110.98
Resolution Island	156.60	157.03	128.70	141.41	128.79	139.73

Curriculum Vitae

Name: Qian Tang

Post-secondary Education and Degrees: Department of Computer Science and Technology. East China Normal University
2009-2013 B.E.

Department of Civil and Environmental Engineering. The University of Western Ontario
2014-2016 M.ESc.

Related word Experience: Teaching Assistant
Department of Civil and Environmental Engineering. The University of Western Ontario
2014-2016

Research Assistant
Department of Civil and Environmental Engineering. The University of Western Ontario
2014-2016